STUDIES ON SOME ASPECTS OF LIGHT BEAM

PROPAGATION THROUGH CERTAIN

NONLINEAR MEDIA

Thesis submitted to

Cochin University of Science and Technology

in partial fulfillment of the requirements
for the award of the degree of

DOCTOR OF PHILOSOPHY

by

Jisha C P
Theory Division
Department of Physics
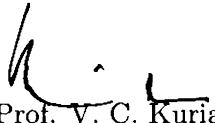Cochin University of Science and Technology
Kochi - 682022

March 2008

CERTIFICATE

Certified that the work presented in this thesis is a bonafide research work done by Ms. Jisha C P under my guidance in the Department of Physics, Cochin University of Science and Technology, Kochi, India - 682022, and has not been included in any other thesis submitted previously for the award of any degree.

Kochi-22

March 06, 2008

Prof. V. C. Kuriakose

(Supervising Guide)

DECLARATION

I hereby declare that the work presented in this thesis is based on the original research work done by me under the guidance of Prof. V. C. Kuriakose, Department of Physics, Cochin University of Science and Technology, Kochi, India - 682022, and has not been included in any other thesis submitted previously for the award of any degree.

Kochi-22
March 06, 2008

Jisha C P

Contents

IN certain materials, the spreading of a laser beam owing to diffraction can be compensated by the material nonlinearity and as a result the beam propagates without any change in its shape. Such non-diffracting beams are known as spatial solitons. These solitons have been observed in various nonlinear media including Kerr, photorefractive, quadratic and liquid crystals. Solitons are ubiquitous in nature and have been studied in many branches of science. In the field of optics, temporal solitons, short temporal pulses that do not change shape as they propagate in a dispersive material such as an optical fiber, has been studied widely. It was first proposed in the year 1973 by Hasegawa and Tappert and observed experimentally in 1980 by Mollenauer et al.

In this thesis, we have studied the propagation of light beam through various nonlinear media like the cubic-quintic medium, the photorefractive medium and the photopolymer system. The fundamental mechanism responsible for the refractive index modulation in each of the three media are different.

Chapter 1 gives a basic introduction to the concept of solitons. Different terms and concepts associated with soliton theory are introduced. Its historical development and current status are also given. A comprehensive review in the area of spatial solitons is presented. An introduction to the basic analytical and numerical methods used in this thesis is given.

In **Chapter 2**, we have studied two kinds of solitons, the $(2+1)$ D spatial solitons and the $(3+1)$ D spatio-temporal solitons in a cubic-quintic medium. The change in refractive index in such a medium occurs due to two competing effects, focusing due to the third order nonlinearity and defocusing due to the fifth order nonlinearity. We have studied the propagation of an optical high power cylindrically symmetric beam in such a medium both analytically and numerically. In this case, we have to consider the self-defocusing effect caused by the presence of free electrons produced due to plasma formation. Multiphoton absorption is a nonlinear process, in contrast with the one-photon absorption process. It has a self defocusing effect on the material. The counteracting self-defocusing effect of both photoionized free electrons and the quintic nonlinearity restricts the unbounded growth of the Kerr nonlinearity. Variational method is used to study the system analytically. Finite Difference Beam Propagation Method is used for the numerical analysis. In the second part of this chapter, we have studied the propagation of spatio-temporal solitons (Light Bullets) through a cubic-quintic medium. The same approach is used to study the propagation of a pulsed high power beam through

a cubic-quintic medium with the effect of nonlinear multiphoton ionization. When a pulsed optical beam propagates through a bulk nonlinear medium, it is affected by diffraction and dispersion simultaneously and at the same time the two effects become coupled through the nonlinearity of the medium. Such a space-time coupling leads to various nonlinear effects like the possibility of spatio-temporal collapse or pulse splitting and the formation of light bullets. We could show the existence of stable light bullets in this medium using both analytical and numerical studies. Self-focusing in a plasma can balance the natural diffraction and channel a laser beam. Such effect is beneficial for many applications, since it helps increasing the length of the interaction between laser and medium. This is crucial, for example, in laser-driven particle acceleration, laser-fusion schemes and high harmonic generation.

In **Chapter 3**, we have studied the evolution of light beam through a different kind of nonlinear media, the photorefractive polymer. When illuminated, a space-charge field is formed in the photorefractive material which induces nonlinear changes in the refractive index of the material by the electro-optic (Pockels) effect. This change in refractive index can counter the effect of beam diffraction forming a PR soliton. The light beam effectively traps itself in a self-written waveguide. As compared to the Kerr-type solitons, these solitons exist in two dimensions and can be generated at low power levels of the order of several microwatts. We study modulational instability and beam propagation through a photorefractive polymer in the presence of absorption losses. The one dimensional beam propagation through the nonlinear medium is studied using variational and numerical methods. Stable soliton propagation is observed both analytically and numerically.

Chapter 4 deals with the study of modulational instability in a photorefractive crystal in the presence of wave mixing effects. Modulational instability is a universal process in which tiny phase and amplitude perturbations that are always present in a wide input beam grow exponentially during propagation under the interplay between diffraction (in spatial domain) or dispersion (in temporal domain) and nonlinearity. Modulational instability in a photorefractive medium is studied in the presence of two wave mixing. We then propose and derive a model for forward four wave mixing in the photorefractive medium and investigate the modulational instability induced by four wave mixing effects. By using the standard linear stability analysis the instability gain is obtained. Such instabilities will be useful for pattern formation. Photorefractive materials are attractive for the studies of pattern formation as their slow time constant gives the

possibility of observing the spatiotemporal dynamics of the system in real time. This also reduces the demands on experimental equipment where speed is often a crucial parameter. Another advantage of photorefractive pattern formation is that patterns can be observed using optical powers of tens of mW. In contrast, pattern formation using other nonlinearities require optical powers of the order of 1W.

Chapter 5 deals with the study of self-written waveguides. Besides the usual analytical analysis, basic experiments were done showing the formation of self-written waveguide in a photopolymer system. Light induced or self-written waveguide formation is a recognized technology by which we can form an optical waveguide as a result of the self-trapping action of a laser beam passed through a converging lens or a single mode fiber. We report the observation of self-writing in a bulk photopolymer (Methylene Blue sensitized poly (Vinyl Alcohol)/Acrylamide (MBPVA/Acrylamide)). We first present the model equation for the beam propagation through the photopolymer and analyze it using the variational method. A potential well formulation is developed. The results are further confirmed by doing experiments.

The formation of a directional coupler in a photopolymer system is studied theoretically in **Chapter 6**. Directional couplers are the basis of several guided wave devices and are mainly used for optical switching networks. It is a passive device which couples part of the transmission power by a known amount through two transmission lines which are very close to each other such that energy passing through one is coupled to the other. We propose and study, using the variational approximation as well as numerical simulation, the evolution of a probe beam through a directional coupler formed in a photopolymer system. The two waveguides of the coupler are formed by direct self-writing. The waveguides so formed are permanent and can be used to guide light. We show that probe beam launched into one of the core can efficiently couple into the other core and the efficiency of coupling increases with the reduction of distance between the two waveguides. The coupler is analyzed using the variational method and the results are compared with that from direct numerical simulation. Both the results are comparable. An analytical result describing the behavior of the coupler was obtained using the Lagrangian formulation. This result compares well with the results obtained for a standard linear directional coupler. A potential well formulation is also developed which gives a physical insight into the dynamics of the coupler.

The main results and conclusion of this thesis are given in **Chapter 7**. The future prospects are also presented.

Publications related to the work presented in the thesis
In referced journals

1. **C. P. Jisha**, V. C. Kuriakose, and K. Porsezian, "Variational approach to spatial optical solitons in bulk cubic-quintic media stabilized by self-induced multiphoton ionization," Phys. Rev. E **71**, 056615 (2005).

2. **C. P. Jisha**, V. C. Kuriakose, and K. Porsezian, " Spatio-temporal solitons in bulk cubic-quintic media stabilized by self-induced multiphoton ionization," Phys. Lett. A **352**, 496 (2006).

3. **C. P. Jisha**, V. C. Kuriakose, and K. Porsezian, "Dynamics of a light induced self-written waveguide directional coupler in a photopolymer," Opt. Commun. **281**, 1093 (2008).

4. **C. P. Jisha**, V. C. Kuriakose, and K. Porsezian, "Modulational instability and beam propagation in photorefractive polymer," (accepted for publication in J. Opt. Soc. Am. B).

5. Self-written waveguide in a methylene blue doped photopolymer **C. P. Jisha**, V. C. Kishore, Beena Mary John, V. C. Kuriakose, K. Porsezian and C. Sudha Kartha J. Mod. Opt. (under review).

6. Modulational instability of optical beams in photorefractive medium in the presence of two wave and four wave mixing effects **C. P. Jisha**, V. C. Kuriakose, K. Porsezian and B. Kalithasan, (to be submitted for publication).

In conferences/seminars

1. Spatial Solitons in bulk cubic-quintic media with multiphoton ionization effect **C. P. Jisha**, V. C. Kuriakose and K. Porsezian, National Conference on Nonlinear Systems and Dynamics, Aligarh Muslim University, Feb 2005.

2. Three- dimensional self -written optical waveguide in a photopolymer **C. P. Jisha**, Beena Mary John, V. C. Kishore, V. C. Kuriakose, K. Porsezian and C. Sudha Kartha. International Conference on Optoelectronic Materials and Thin films for Advanced Technology - 2005, Cochin (Best poster).

3. Light bullets in a PTS medium stabilized by multiphoton ionization **C. P. Jisha**, V. C. Kuriakose and K. Porsezian, International Conference on Optics & Optoelectronics - 2005, Dehradun.

4. Photorefractive polymeric solitons **C. P. Jisha**, V. C. Kuriakose and K. Porsezian, National Conference on Nonlinear Systems and Dynamics, Madras University, Jan 2006.

5. Directional coupler in a photopolymer - a theoretical study **C. P. Jisha**, V. C. Kuriakose and K. Porsezian, Photonics 2006, University of Hyderabad.

6. Four wave mixing induced modulational instability in photorefractive media **C. P. Jisha**, V. C. Kuriakose and K. Porsezian, International Conference on Optical, Optoelectronic and Photonic Materials and Applications, Queen Mary, London, July 31st to August 3, 2007.

Other publications to which author has contributed

1. P. A. Subha, **C. P. Jisha**, and V. C. Kuriakose, " Stable diffraction managed spatial soliton in bulk cubic-quintic media," J. Mod. Opt. **54**, 1827 (2007).

2. P. A. Subha, **C. P. Jisha**, and V. C. Kuriakose, " Nonlinearity management and diffraction management for the stabilization of two dimensional spatial solitons," Pramana J. Phys. **69**, 229 (2007).

3. Two dimensional diffraction managed soliton in cubic-quintic media P. A. Subha, **C. P. Jisha** and V. C. Kuriakose, National Conference on Nonlinear Systems and Dynamics, Madras University, Jan 2006.

4. Soliton switching in nonlinear directional coupler with varying dispersion and nonlinearity P. A. Subha, **C. P. Jisha** and V. C. Kuriakose, Photonics 2006, University of Hyderabad.

ACKNOWLEDGEMENTS

game which was monopolized by the boys but would come looking for us when they were short of a player. I especially thank Sreekumar, Asha, Jayakrishnan, Vimal, Joshy sir, Ajimsha, Reshmi, Anoop, Saji, Senoy, Rajesh C S, Deepa, Merril, Sajeesh and Srikanth for going out of their way to help me out when ever I needed them.

I especially remember the support I got from Vinu Namboory and Manu Punnen during a difficult time and for giving me the encouragement I needed.

I am also thankful to all my friends in the hostel who have made the stay there a wonderful experience. I am thankful to my roommate Gisha and my other friends Vasuja, Sheeba, Ragitha, Subhasree, Vijutha, Pramitha, Tina, Mangala, Gleeja and Angel for their love and care.

I would like to thank the most important people in my life, my parents for all the patience and support they gave me throughout this whole time. I am thankful to my brother and sister for all the wonderful time I have with them. Also, I thank my two good friends Vidya and Kishore, who were (and probably always will be) there for me.

Finally, I thank the Almighty for making me what I am.

Jisha C P

Optical Solitons : An Introduction

1.1 Basic concepts and terminology

S OLITONS have been the subject of intense studies in many different fields including hydrodynamics,[1] nonlinear optics,[2] plasma physics[3] and biology.[4] Electromagnetic waves have an innate tendency to spread as they evolve. Individual frequency components, which are superimposed to form the wavepacket, propagate with different velocities or in different directions resulting in the spreading of the wavepacket. An example is the spreading of light pulses as they propagate in a medium due to the group velocity dispersion. As a result each Fourier component of the pulse has a different velocity. The spreading of laser beam due to diffraction when passing through a medium is another example. Diffraction/dispersion of optical beams and pulses occurring in a medium is a linear effect. However, when nonlinear effects are present, it may compensate the linear effects and result in the formation of optical solitons, a localized pulse or beam which can propagate without decay. The word soliton is commonly used for pulses in exactly integrable nonlinear-wave models. However, most physical nonlinear systems are nonintegrable but support self-trapped solutions and exhibit important features and conserved quantities. Such self-trapped solutions were initially called "solitary waves". Solitons and solitary waves differ from each other as the former do not couple to radiation on collision and the number of solitons is conserved. But both of them still exhibit particle like properties. As a result, in todays literature this distinction is, in general, no longer used, and all self-trapped beams are loosely called solitons.

Optical solitons can be broadly classified into two categories : Temporal solitons and spatial solitons, the distinction being that in the former dispersion effect counteracts nonlinearity and in the later it is the diffraction effect. There is a third category of solitons, the spatio-temporal solitons or

the commonly called "light bullets". Here both dispersion and diffraction effects are dominant. All the three kinds of solitons are briefly introduced in the following sections.

1.1.1   Temporal solitons

This is the prototypical soliton which occurs in single mode optical fibers. It was first proposed in the year 1973 by Hasegawa and Tappert[5] and observed experimentally in 1980 by Mollenauer et al.[6] The light wave in a fiber loses its energy as it propagates through the medium either due to absorption or due to scattering. The loss in the fiber originates from the imaginary part of the linear refractive index $n_0(\omega)$ and is given by

$$\alpha = \frac{\omega_0}{c} Im(n_0), \tag{1.1}$$

where c is the velocity of light and ω_0 is the frequency of light. The power loss can be expressed in terms of decibels per kilometer (dB/km) as $-20 \log(e^{-\alpha}) = 8.69\alpha$. The fiber loss depends upon the wavelength of light. Fig. 1.1 shows the loss spectrum for a typical low loss fiber.[7]
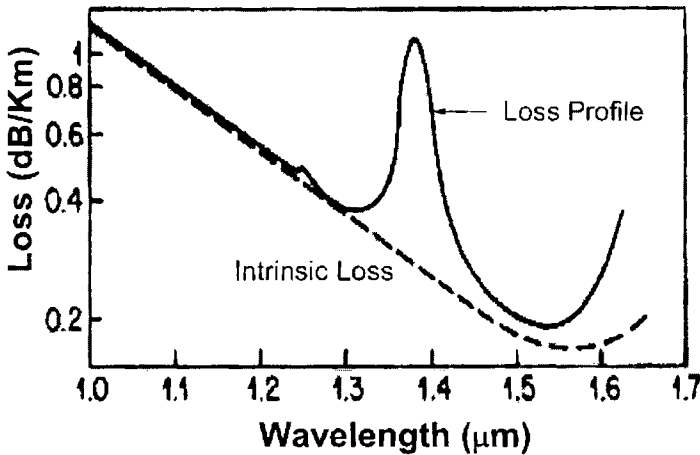
Figure 1.1: Measured loss spectrum of single mode silica fiber. Dashed curve shows the contribution from Rayleigh scattering.[7]

Another process in fibers which results in loss is due to Rayleigh scattering. It is a fundamental loss mechanism occurring because of random density fluctuations embedded in the fiber material. As a result there is a local fluctuation in the index of refraction which scatters light in all directions. The Rayleigh scattering loss is proportional to λ^{-4} and hence, it is dominant at short wavelength. This loss is intrinsic to any dielectric medium. The intrinsic loss level is

$$\alpha_R = C/\lambda^4 \mathrm{dB/km}, \tag{1.2}$$

where C is in the range $0.4-0.5\mathrm{dB/(km}\ \mu\mathrm{m}^4)$ depending on the constituent of the fiber core. Successful fabrication of low loss fibers has resulted in the wide use of fibers in optical communication. Data is sent using these fibers. But after some distance, the pulse begins to disperse and the input data is no longer available at the output. One needs to put repeaters through out the transmission line for an effective data transfer.

When an electromagnetic wave interacts with the bound electrons of a dielectric medium, the response of the medium depends upon the optical frequency ω. As a result, the refractive index depends upon the frequency of light. This is known as chromatic dispersion. The origin of chromatic dispersion is related to the characteristic resonance frequencies at which the medium absorbs the electromagnetic radiation through oscillation of bound electrons. The effect of fiber dispersion is accounted for by expanding the mode propagation constant β in a Taylor series about the frequency ω_0 at which the pulse spectrum is centered and is written as

$$\beta(\omega) = n(\omega)\frac{\omega}{c} = \beta_0 + \beta_1(\omega - \omega_0) + \frac{1}{2}\beta_2(\omega - \omega_0)^2 + \ldots, \tag{1.3}$$

where

$$\beta_n = \left(\frac{d^m\beta}{d\omega^n}\right)_{\omega=\omega_0} \qquad (m = 0, 1, 2, \ldots). \tag{1.4}$$

The parameters β_1 and β_2 are related to the refractive index n and its derivatives as

$$\beta_1 = \frac{1}{v_g} = \frac{n_g}{c} = \frac{1}{c}\left(n + \omega\frac{dn}{d\omega}\right), \tag{1.5}$$

$$\beta_2 = \frac{1}{c}\left(2\frac{dn}{d\omega} + \omega\frac{d^2n}{d\omega^2}\right), \tag{1.6}$$

where n_g is the group index and v_g is the group velocity. The parameter β_2 is responsible for pulse broadening and is known as the group-velocity dispersion parameter. The variation of β_2 with wavelength is such that

it decreases with increase in λ, becomes zero at a particular wavelength known as the zero dispersion wavelength λ_d (around $1.27\mu m$ for silica) and becomes negative for further increase in wavelength. For wavelengths $\lambda < \lambda_d$, the fiber is said to exhibit normal dispersion. In this regime, high frequency components of an optical pulse travels slower than low frequency components of the same pulse. The case when $\lambda > \lambda_d$, that is, $\beta_2 < 0$, is known as the anomalous dispersion regime. The high frequency components of the pulse travel faster than the low frequency components in this regime. It is in this regime of pulse propagation that optical fibers support solitons.

For large distances of pulse propagation, as in case of fiber optic communication, in addition to the pulse dispersion nonlinear effects also become appreciable. The properties of a dielectric medium when an electromagnetic wave propagates through it are completely described by the relation between the polarization and the electric field. When an intense light propagates through a dielectric medium, the response of the medium becomes nonlinear which is due to the anharmonic motion of bound electrons. As a result, the total polarization **P** induced by electric dipoles is no longer linear with the electric field **E**, but satisfies a relation of the form

$$\mathbf{P} = \epsilon_0(\chi^1.\mathbf{E} + \chi^2 : \mathbf{E}\ \mathbf{E} : +\chi^3 : \mathbf{EEE} : + \dots), \qquad (1.7)$$

where ϵ_0 is the vacuum permittivity, χ^1 is the linear susceptibility and χ^2, χ^3, ... are respectively the second, third and higher order nonlinear susceptibilities. In general χ^j $(j = 1, 2, \dots)$ is a tensor of rank $j+1$ if the medium is anisotropic. The physical processes that occur as a result of χ^2 are distinct from those that occur due to χ^3. Second order nonlinear optical interactions occur only in noncentrosymmetric crystals, that is, there is no inversion symmetry in the crystal. But third order nonlinear optical interactions can occur both for centrosymmetric and noncentrosymmetric media. However, in media in which there is an inversion symmetry, like silica, χ^2 and the other higher even powers of χ^j vanishes.

The third order susceptibility χ^3 is responsible for various nonlinear phenomena occurring in an optical fiber such as third harmonic generation, four wave mixing, intensity dependent refractive index etc. The intensity dependent refractive index can be written as

$$n(\omega, |E|^2) = n(\omega)_0 + n_2|E|^2, \qquad (1.8)$$

where $n(\omega)_0$ is the linear refractive index and $|E|^2$ is the optical intensity inside the medium. Such nonlinearity is known as the Kerr nonlinearity.

If the optical intensity is high enough, in addition to the third order term, the refractive index will depend upon the fifth order nonlinear susceptibility. Such materials are known as cubic-quintic nonlinear materials. In the case of fibers, the intensity dependent refractive index leads to a number of interesting nonlinear effects like self-phase modulation and cross-phase modulation. When an optical field propagates through a fiber, it experiences a self-induced phase shift and is known as self-phase modulation. The magnitude of the phase shift is given by

$$\Phi = (n_0 + n_2|E|^2)k_0L, \tag{1.9}$$

where $k_0 = 2\pi/\lambda$ and L is the fiber length. The second term is due to self-phase modulation. This is responsible for the spectral broadening of ultrashort pulses and the formation of optical solitons in the anomalous dispersion regime. A temporal optical soliton is formed in the anomalous dispersion regime ($\beta_2 < 0$) when the effect of group velocity dispersion is completely compensated by the self-phase modulation. In the normal dispersion regime ($\beta_2 > 0$), the combined effects of group velocity dispersion and self-phase modulation can be used for pulse compression. In the context of pulse propagation through a nonlinear media, a characteristic length known as the dispersion length is defined as

$$L_{dis} = \frac{T^2}{|\beta_2|^2}, \tag{1.10}$$

where T is the measure of the pulse duration. This length signifies the distance in which the pulse broadens significantly when propagating through the fiber. The envelope of a light wave in a fiber can be described by the nonlinear Schrödinger (NLS) equation which has the form[8]

$$i\frac{\partial u}{\partial z} + \frac{1}{2}\frac{\partial^2 u}{\partial t^2} + |u|^2u = 0. \tag{1.11}$$

Here z represents the direction of propagation, t represents the time in the group velocity frame and the third term originates from the Kerr effect.

1.1.2 Spatial solitons

In the field of optics, even though the temporal solitons have been studied extensively, it was the spatial soliton which was observed first by Bjorkholm and Ashkin[9] in the early 1970s. Spatial solitons are self trapped beams of light which propagate through a nonlinear medium without any diffraction.

It is the natural property of a beam of light to diverge when propagating through a medium. A collimated beam of light with a diameter d will spread with an angle λ/d owing to diffraction. Such divergence is compensated and the beam propagates with out any change in its shape when propagating through a suitable nonlinear media.

The intense beam of light modifies the optical properties of the medium through which it propagates such that it is focused inside the medium. This effect is known as self-focusing. Such effects are known as self-action effects in which a beam of light modifies its own propagation by means of the nonlinear response of the medium. If the effect is such that there is an exact balance between self-focusing and diffraction so that the beam of light propagates with a constant diameter, this is known as the self-trapping of light. There is a possibility of another effect which can occur. If the power of the beam is such that it is much greater than a critical power, then the beam can breakup into many components each having a power approximately equal to the critical power. This critical power in case of a Kerr type nonlinear media is obtained to be[10]

$$P_{cr} = \frac{\pi(0.61)^2\lambda_0^2}{8n_0n_2}. \tag{1.12}$$

The beam can self-trap only if the power of the beam is exactly equal to the critical power. The schematic illustration of the self-focusing effect and the self trapping effect is shown in Fig. 1.2.

In one transverse dimension, diffraction can be formally considered as representing the anomalous dispersion in case of temporal solitons. We can define a characteristic length known as the diffraction length for the propagation of the soliton. This is the distance at which the beam broadens appreciably in space if the propagation is linear and is given by

$$L_{diff} = \frac{1}{2}k_0w_0^2 = \frac{\pi}{\lambda}w_0^2, \tag{1.13}$$

where w_0 is the radius of the beam.

The idea of controlling light with light by taking advantages of nonlinear optical effects, has become a topic of interest to many researchers and scientists. The fundamental benefit is in the possibility of avoiding any opto-electronic conversion process, and hence increasing the device speed and efficiency. It is in this scenario that these self-guided beams called "spatial solitons" find importance. The areas of application include all optical switching devices,[11] optical computing, all optical polarization
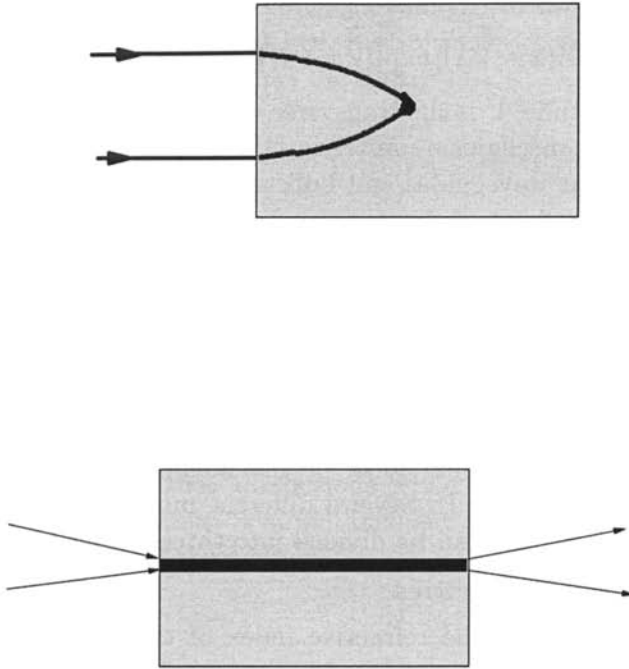
Figure 1.2: Schematic diagram of self-focusing (top) and self-trapping (bottom) effects occurring in a Kerr media.

modulators,[12] logic gates[13] etc. The prospect of forming all-optical switches and logic gates presents promise for generations of novel optical interconnects for computing and communications.

From a mathematical point of view, continuous wave beam propagation in planar waveguides is identical to the phenomenon of pulse propagation in fibers because of the spatiotemporal analogy[14] and is described by the NLS equation of the form

$$i\frac{\partial u}{\partial z} + \frac{1}{2}\frac{\partial^2 u}{\partial x^2} + |u|^2 u = 0, \qquad (1.14)$$

where x represents the transverse dimension. This can be integrated exactly using the inverse scattering transform method. The one soliton solution of Eq. (1.14) has the following general form

$$u(x, z) = A\mathrm{sech}[A(x - Vz)]\exp[iVx + i(V^2 - A^2)z/2 + i\phi], \qquad (1.15)$$

where A is the amplitude, V is the transverse velocity of soliton and ϕ is an arbitrary phase. The mechanism underlying the propagation of continuous wave beams in planar waveguides and bulk media is quite different. The spreading of the beam due to diffraction has to be completely compensated by the nonlinearity. Much larger nonlinearities are required for observing spatial solitons and often such nonlinearities are not of the Kerr type. As a result the NLS equation can be generalized as

$$i\frac{\partial u}{\partial z} + \frac{1}{2}\left(\frac{\partial^2 u}{\partial x^2} + \frac{\partial^2 u}{\partial y^2}\right) + F(|u|^2)u = 0, \qquad (1.16)$$

where $F(|u|^2)$ is the functional form of the nonlinear refractive index change $n_{nl}(I)$ with intensity I. Several different models have been used for the functional form and can be divided into three classes.[15]

- **Competing nonlinearities**

  For large intensities, the refractive index of the material deviates from the Kerr dependence and we have to include higher order terms. Such deviations have been observed for many nonlinear materials including PTS, AlGaAs, CdS and the nonlinear refractive index is modeled by a cubic-quintic form of nonlinearity

  $$n_{nl}(I) = n_2 I + n_4 I^2, \qquad (1.17)$$

  where n_2 and n_4 have opposite signs. We have used this kind of nonlinearity to study spatial solitons in chapter 2.

- **Saturable nonlinearities**

  This results from the saturation of the nonlinearity at high powers. This has been observed in many materials including two-level atomic systems, photorefractive materials etc. The nonlinearity is characterized by three parameters, the saturation intensity I_{sat}, the maximum change in the refractive index n_∞ and the Kerr coefficient n_2 for small I. A phenomenological model of the form

  $$n_{nl}(I) = n_\infty\left[1 - \frac{1}{(1 + I/I_{sat})^p}\right], \qquad (1.18)$$

  can be used for describing the nonlinearity. Here p is a constant.

- **Transitive nonlinearities**

  In this kind of nonlinearity, the refractive index transits from one functional form to another as intensity increases. Such nonlinearity was used in the case of bistable solitons. A simple model for the transitive nonlinearity has the form

  $$n_{nl}(I) = \left\{ \begin{array}{ll} n_{21}I & I < I_{cr}, \\ n_{22}I & I > I_{cr}. \end{array} \right. \tag{1.19}$$

1.1.3   Spatio-temporal solitons

When both the spatial and temporal effects are present together, we get a different entity called the spatio-temporal solitons or the "light bullets". The word was first coined by Silberberg.[16] Spatio-temporal solitons are packets of wave which are confined in all three dimensions (two transverse dimensions and one time dimension) while propagating. The effect of dispersion and diffraction is simultaneously present and is compensated by the nonlinearity of the medium.
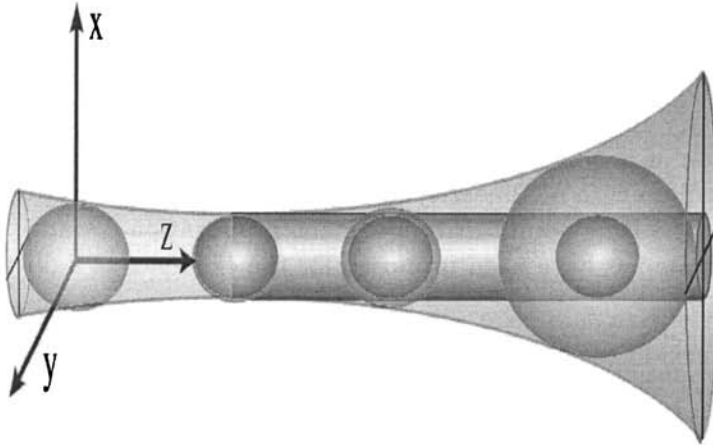
Figure 1.3: Schematic diagram of formation of a spatiotemporal soliton due to the simultaneous balance of diffraction and dispersion by nonlinear self-focusing.[17]

That is both L_{disp} and L_{diff} can not be neglected and their effects are canceled by the nonlinearity of the medium. Eq. 1.16 can be generalized to include both the temporal and spatial effects for describing the propagation of optical pulses in a bulk nonlinear medium as

$$i\frac{\partial u}{\partial z} + \frac{1}{2}\Big(\frac{\partial^2 u}{\partial x^2} + \frac{\partial^2 u}{\partial y^2}\Big) + \frac{1}{2}\frac{\partial^2 u}{\partial t^2} + F(|u|^2)u = 0. \qquad (1.20)$$

Formation of spatio-temporal solitons may be understood as the result of the simultaneous balance of diffraction and group velocity dispersion by the transverse self-focusing and nonlinear phase modulation in the longitudinal direction, respectively. A schematic diagram of the formation of the spatio-temporal soliton is shown in Fig. 1.3.

Since all solitary wave solutions of the cubic NLS equation in dimension $D \geq 2$ are unstable, it is believed that optical bullets are unstable in a pure Kerr medium. For the stable propagation of multidimensional solitons, a suitable nonlinear media is needed. The requisites for the generation of stable completely localized spatio-temporal solitons in homogeneous media are self-focusing nonlinearity, anomalous group velocity dispersion, and one or more processes that can prevent collapse of the pulse. Fibich and Ilan[18] showed that small negative fourth-order dispersion can arrest spatiotemporal collapse of ultrashort pulses with anomalous dispersion in a planar waveguide with pure Kerr nonlinearity, resulting in $(2 + 1)$ D optical bullets. In all previous theoretical and experimental investigations, spatio-temporal solitons were studied for nonlinearities different from Kerr nonlinearity. Towers and Malomed in 2002[19] had shown that complete stabilization of a cylindrical $(2 + 1)$D spatial soliton can be secured in a layered medium with nonlinearity management, i.e., periodic alternation of the sign of the Kerr nonlinearity along the propagation distance. Various theoretical models have been proposed for the existence of light bullets.[17]

Trapani et al.[20] reported the first evidence that the natural 3 D (temporal and spatial) spreading of a focused ultrashort wave packet can be balanced in transparent materials at high intensity. The underlying mechanism is the spontaneous formation of an X wave characterized by an intense (i.e., nonlinear) central hump self-trapped through mutual balance with (essentially linear) dispersive contributions associated with coexisting slowly decaying conical tails (see Fig. 1.4). The experiment was carried out by exploiting self-focusing nonlinearities arising from quadratic nonlinearity. They found that when a conventional laser pulse is launched into a lithium triborate crystal, the pulse spontaneously "reshapes" into
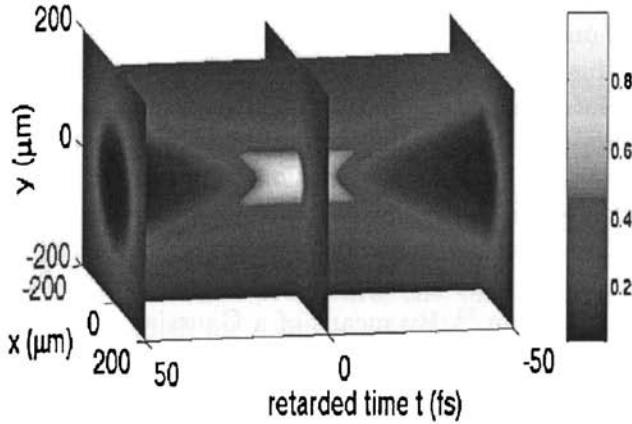
Figure 1.4: Intensity versus r and t of a nondiffracting nondispersive linear X wave in a normally dispersive media.[20]

a nonlinear X wave which maintains its shape using the non-linear principles of a soliton. The same idea was used by Xu and Zeng.[21] They also used the fact that in a quadratic nonlinear medium with normal dispersion and non-vanishing group velocity mismatch between fundamental wave and second-harmonic pulses, the wave packets of two harmonics can be locked together in propagation in the form of walking X-shaped light bullets. The output wave packets develops into X-shaped light bullets with significant group delay time due to mutual dragging and significant shifting in spatiotemporal spectrum due to delayed nonlinear phase shift. They also showed that spontaneously generated phase-front tilting could balance the dragging force induced by group velocity mismatch and lead to zero-velocity walking X-shaped light bullets. Although the nonlinear X-waves are not localized solutions and thus not light bullets in the usual sense, they do exhibit a kind of 3D spatiotemporal self-focusing and trapping.

1.2   Variational method

The pulse/beam propagation through a nonlinear media is described by nonlinear partial differential equations which in general can not be solved

exactly unless for certain idealized conditions. Approximate methods have been used to study general nonlinear partial differential equations. Variational method is one among them. Here we will describe the variational method used in this thesis for studying the different nonlinear systems. The method first introduced by Whitham.[22] It centres upon the use of an average Lagrangian density and the inevitable introduction of trial functions. Whitham points out that the variational approach is not a separate method and that it permits the development of quite general results but naturally the accuracy of any description must depend upon a judicious choice of trial functions. The variational method was applied to the NLS equation first by Anderson.[23] By means of a Gaussian trial function and a Ritz optimization procedure, approximate solutions are obtained for the evolution of pulse width, pulse amplitude and frequency chirp during propagation. The result so obtained was in good comparison with that from inverse scattering and numerical simulations. Since then the method has been used successively by various authors.[24–27]

The method proceeds by first writing the Lagrangian associated with the system under study. A suitable trial solution is assumed using which a reduced Lagrangian is obtained. A set of evolution equations called Euler-Lagrange equation is obtained by finding the variation of the various unknown parameters in the ansatz with respect to the reduced Lagrangian.

Lagrangian formulation

To illustrate the variational method, let us consider the nonlinear Schrödinger equation of the form

$$iu_z + u_{xx} + u_{yy} + s|u|^2 u = 0, \tag{1.21}$$

where u is the field, z is the propagation direction, x and y are the two transverse dimensions and s is a parameter signifying the strength of the nonlinearity. The NLS can be restated as a variational problem by casting it in the form of the Euler-Lagrange equation

$$\frac{\partial}{\partial z}\Big(\frac{\partial L}{\partial X_x}\Big) + \frac{\partial}{\partial y}\Big(\frac{\partial L}{\partial X_x}\Big) + \frac{\partial}{\partial z}\Big(\frac{\partial L}{\partial X_y}\Big) - \frac{\partial L}{\partial X} = 0, \tag{1.22}$$

where $X = u$ or u^* and the Lagrangian L is given by

$$L = \frac{i}{2}(uu_z^* - u^* u_z) + |u_x|^2 + |u_y|^2 - \frac{s}{2}|u|^4. \tag{1.23}$$

It can be easily verified that the evolution Eq. (1.21) can be reproduced from the Lagrangian L using the Euler-Lagrange equation. The action functional is defined as

$$I(u) = \int_0^\infty dz \int_{-\infty}^\infty L(u)dxdy, \qquad (1.24)$$

where

$$\langle L(u) \rangle = \int_{-\infty}^\infty L(u)dxdy, \qquad (1.25)$$

is known as the reduced Lagrangian.

In the Ritz optimization procedure, the variation of the action functional is made to vanish for a set of suitable chosen functions which are considered as the trial solution of the variational problem. Generally we choose a Gaussian trial function of the form

$$u(z,x,y) = A(z) \exp\left[-\frac{x^2}{2w(z)^2} + -\frac{y^2}{2w(z)^2} + ib(z)x^2 + ib(z)y^2 \right], \quad (1.26)$$

where $A(z)$ is the maximum amplitude, $b(z)$ is the curvature parameter, $w(z)$ is the beam radius. Such a trial function is simple and general enough to incorporate the exact solution in the linear limit and the essential features of the self phase modulation. So one expect that this particular trial function will produce a fairly good approximation to the solution of the NLS equation. The Euler-Lagrange equations for the reduced problem give four differential equations for the variational parameters A, A^*, b and w. The beam width $w(z)$ and the chirp parameter $b(z)$ are real parameter functions, whereas the amplitude $A(z)$ is complex to allow the possibility of a wave number shift. These equations can be reduced to one single differential equation for the beam width of the form

$$\frac{1}{2}\left(\frac{dw}{dz}\right)^2 + \Pi(w) = 0, \qquad (1.27)$$

where Π is the potential which is a function of $w(z)$. This implies that the evolution of the width can formally be seen as the motion of a particle with unit mass in a potential Π.

1.3 Finite difference beam propagation method

A numerical approach is often adopted for understanding the problem of pulse/beam propagation through a nonlinear media. The various numerical schemes can be classified into two broad categories as the finite-difference method and the pseudospectral method. Both the methods have

been extensively used for studying nonlinear systems.[28-31] We have used the finite difference method for studying the various systems considered in this thesis. In the finite difference method the derivatives at a point are approximated by difference quotients over a small interval. That is, $\partial\phi/\partial x$ is approximated as $\delta\phi/\delta x$ where δx is small.

Finite-difference approximation to derivatives

If a function u and its derivatives are single-valued, finite and continous functions of x, then using Taylor's theorem

$$u(x+h) = u(x) + hu'(x) + \frac{1}{2}h^2u''(x) + \frac{1}{6}h^3u'''(x) + \dots, \qquad (1.28)$$

and

$$u(x-h) = u(x) - hu'(x) + \frac{1}{2}h^2u''(x) - \frac{1}{6}h^3u'''(x) + \dots, \qquad (1.29)$$

Adding Eqs. (1.28) and (1.29) gives

$$u(x+h) + u(x-h) = 2u(x) + h^2u''(x) + O(h^4), \qquad (1.30)$$

where $O(h^4)$ denote terms containing fourth and higher powers of h and can be assumed to be negligible in comparison with lower powers of h. Hence we can write

$$u''(x) = \frac{d^2u}{dx^2} \simeq \frac{1}{h^2}(u(x+h) - 2u(x) + u(x-h)), \qquad (1.31)$$

with an error of order h^2.

Similarly, subtracting Eq. (1.29) from Eq. (1.28) and neglecting terms of order h^3 gives

$$u'(x) = \frac{du}{dx} \simeq \frac{1}{2h}(u(x+h) - u(x-h)), \qquad (1.32)$$

with an error of order h^2.

Now, if u is a function of the independent variables x and z, we can divide the $x - z$ plane into sets of equal rectangles such that

$$x = ih, \quad z = jk$$

where i and j are integers. Now the derivatives can be represented as

$$\left(\frac{\partial^2 u}{\partial x^2}\right)_{i,j} = \frac{u_{i+1}^j - 2u_i^j + u_{i-1}^j}{h^2}, \qquad (1.33)$$

and

$$\left(\frac{\partial u}{\partial z}\right)_{i,j} = \frac{u_i^{j+1} - u_i^j}{k}, \tag{1.34}$$

using a forward-difference approximation for $\partial u / \partial z$.

Crank-Nicolson implicit method

Crank and Nicolson proposed a method that is convergent and stable for all finite values of k/h^2. They replaced $\partial^2 u/\partial x^2$ by the mean of its finite-difference representations on the (j+1)th and jth rows such that

$$\left(\frac{\partial^2 u}{\partial x^2}\right)_{i,j} = \frac{1}{2}\left(\frac{u_{i+1}^{j+1} - 2u_i^{j+1} + u_{i-1}^{j+1}}{h^2} + \frac{u_{i+1}^j - 2u_i^j + u_{i-1}^j}{h^2}\right). \tag{1.35}$$

The method is illustrated by considering the NLS equation of the form

$$iu_z = u_{xx} + |u|^2 u. \tag{1.36}$$

We consider the propagation of a one dimensional beam through a non-linear medium. Knowing the input field at $z = 0$, we need to find out the output field at $z = L$. The material is divided into planes which are equally spaced by k along the propagation direction z. The governing equation is written in the finite difference form as

$$\begin{aligned} i\frac{u_i^{j+1} - u_i^j}{k} &= \frac{1}{2}\left(\frac{u_{i+1}^{j+1} - 2u_i^{j+1} + u_{i-1}^{j+1}}{h^2} + \frac{u_{i+1}^j - 2u_i^j + u_{i-1}^j}{h^2}\right) \\ &+ \frac{1}{2}\left(|u_i^{j+1}|^2 u_i^{j+1} + |u_i^j|^2 u_i^j\right). \end{aligned} \tag{1.37}$$

Rearranging, we can write as

$$C_i u_{i+1}^{j+1} + B_i u_i^{j+1} + A_i u_{i-1}^{j+1} = -C_i u_{i+1}^j + D_i u_i^j - A_i u_{i-1}^j, \tag{1.38}$$

where

$$A_i = -\frac{k}{2h^2} = C_i,$$

$$B_i = i + \frac{k}{h^2} - \frac{k}{2}|u_i^{j+1}|,$$

and

$$D_i = i - \frac{k}{h^2} + \frac{k}{2}|u_i^j|.$$

Eq. 1.38 is in the form of a tridiagonal matrix with Λ as the lower and upper diagonal element. If the initial condition, i.e $u(z = 0)$ is known,

then the right hand side consists of known quantity and can be expressed in the matrix form as

$$
\begin{bmatrix}
B_1 & C_1 & & & 0 \\
A_2 & B_2 & C_2 & & \\
& A_3 & B_3 & & \\
& & & \cdot & C_{n-1} \\
0 & & & B_n & C_n
\end{bmatrix}
\begin{bmatrix}
u_1 \\
u_2 \\
\cdot \\
u_n
\end{bmatrix}
=
\begin{bmatrix}
d_1 \\
d_2 \\
\cdot \\
d_n
\end{bmatrix}. \tag{1.39}
$$

Such a system can be solved using the Thomas algorithm which is a simplified form of Gaussian elimination.

Thomas Algorithm

The method is as follows. The coefficients of the matrix are modified as

$$ C_1' = C_1/B_1, \tag{1.40} $$

$$ A_1' = 0, \tag{1.41} $$

$$ d_1' = d_1/B_1. \tag{1.42} $$

For $i = 1$ to $n - 1$

$$ C_i' = \frac{C_i}{B_i - A_i'C_{i-1}'}, \tag{1.43} $$

$$ d_1' = \frac{d_i - A_i'd_{i-1}}{B_i - A_i'C_{i-1}'}. \tag{1.44} $$

Now the field u at the first step can be obtained as

$$ u_n = d_n', \tag{1.45} $$

and for $i = n - 1$ to 1

$$ u_i = d_i' - C_i'u_{i+1}. \tag{1.46} $$

The field at $z = k$ step is obtained. Knowing the field at $z = k$, we can find the field at $z = 2k$. Repeating this throughout the material, we can obtain the output field at $z = L$.

1.4 Historical developments and current status

The first scientifically documented report of a solitary wave came only in 1834 when John. S. Russell, a Scottish scientist observed a "rounded smooth and well defined heap of water" propagating in a narrow and shallow canal "without change of form and diminution of speed". The word solitary wave was coined by Scott-Russell himself. This phenomenon attracted attention of scientists including Stokes, Boussinesq and Rayleigh, but a theoretical confirmation had to wait until 1898 when two Dutch physicists, Korteweg and de Vries,[32] presented their famous equation now known as KdV equation.

In 1955, Fermi, Pasta and Ulam[33] investigated how the equilibrium state is approached in a one-dimensional nonlinear lattice. It was expected that the nonlinear interactions among the normal modes of the linear system would lead to the energy of the system being evenly distributed throughout all the modes, that is, the system would be ergodic. The results of numerical analysis contradicted this idea. The energy is not distributed equally into all the modes, but the system returns to the initial state after some period (the recurrence phenomena). In 1965, Zabusky and Kruskal solved the KdV equation numerically as a model for nonlinear lattice and observed the recurrence phenomena. Zabusky and Kruskal[3] coined the name "soliton" to represent a solitary wave showing particle property.

In 1964, Chiao, Garmire and Townes[34] showed that the spreading of an optical beam could be avoided in a nonlinear optical medium. They discussed conditions under which an electromagnetic beam could produce its own dielectric waveguide and propagate without spreading. They considered the case of a medium which possesses an intensity dependent index of refraction in which the beam could form its own waveguide such that the refractive index is greater at the center of the beam than its wings. This results in a non-spreading propagation of the beam inside the self-formed waveguide. The phenomenon of self-trapping of an optical beam was thereby predicted. Later on in 1974, Bjorkholm and Ashkin[9] reported steady-state self-focusing, self-trapping and self-defocusing of a continuous wave dye laser beam in sodium vapor. They used a circularly symmetric beam in a 2-D medium, namely, a cell filled with sodium vapor and operated their input laser near the sodium yellow line. At low powers, the laser beam diverged (diffracted) in the gas cell, whereas at higher powers, the beam diameter self-stabilized and propagated without diffraction. This is the classical signature of a spatial soliton. They concluded their report with the words "Our demonstration of self-trapping should simulate

further work to elucidate the general conditions under which self-trapping can occur". Ironically, this experiment did not arouse the interest of the scientific community. It was more than ten years later that this field was revisited by Barthelemy et al.[35] They performed the first 1-D soliton experiments in waveguides using the reorientational nonlinearity of liquid carbon disulphide.

It was only in the mid 1990s that the studies on spatial solitons gained momentum. It was during this time that the photorefractive solitons and the quadratic solitons were proposed and observed. The first experimental observation of the spatial photorefractive (PR) solitons was reported by Duree et al.[36] using a strontium barium niobate (SBN) PR crystal. By applying an external voltage (few hundred volts per centimeter), a clear focusing of the beam and soliton formation was observed. However, the solitons observed in this particular experiment were of transient nature (so called quasisteady state) and existed only within a narrow temporal window before the screening of the external field actually took place.

In 1994, Stepanovs group[37] reported the first observation of steady-state screening solitons in PR barium titanium oxide (BTO). This crystal possesses significantly weaker electrooptic properties than SBN and therefore a much higher electric field (a few kilovolts per centimeter) was used to create solitons. In the same year, Shih et al.[38] demonstrated the formation and propagation of steady-state screening bright spatial solitons in SBN crystal. Due to the extremely high value of electrooptic coefficient, the nonlinearity was high enough to allow for the creation of very narrow (less than 10 μm in diameter) solitons.

In 1995, Duree et al.[39] reported the first experimental observations of dark, planar, spatial photorefractive solitons, and photorefractive vortex solitons that are trapped in a bulk (three-dimensional) photorefractive media. Both the dark and vortex solitons possess the signatures of the photorefractive solitons: they are independent of absolute intensity, can afford significant absorption, and are inherently asymmetric with respect to the transverse dimensions of trapping. Since then a variety of such solitons, of both 1D and 2D types, have been discovered and explored. This includes landmark advances, such as self-trapping of incoherent light by Mitchel and Segev in 1997[40] and the generation of ordinary solitons (Fleischer et al 2003)[41] and vortex (Fleischer et al 2004,[42] Neshev et al 2004[43]) solitons in optically induced photonic lattices, as well as robust necklace shaped soliton clusters (Yang et al. 2005[44]).

Stepken et al.[45] investigated theoretically and experimentally the three dimensional propagation and interaction of mutually incoherent screening

spatial solitons in an SBN crystal. They showed that the interaction of solitons results in complex trajectories which typically show partial mutual spiraling, followed by damped oscillations and the fusion of solitons. This nontrivial behavior is caused by the anisotropy of the nonlinear refractive index change in the crystal.
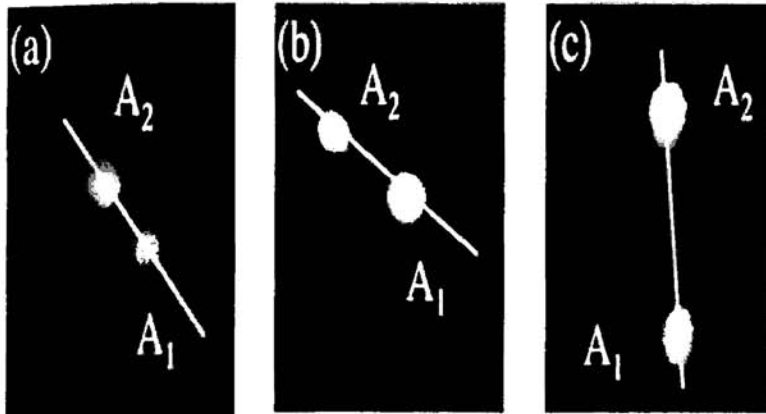
Figure 1.5: Mutual rotation of initially coplanar solitons. (a) Initial positions of the beams; (b) relative position of the solitons at the exit face of the crystal for individual propagation; (c) exit position of the solitons for joint propagation. The propagation distance was 10 mm (from Ref[45]).

Two circular beams (2 mW each) derived from an argon ion laser with wavelength 514.5 nm were directed by a system of mirrors and beam splitters such that they were focused with Gaussian diameters of 15 μm on the entrance face of the crystal, and were polarized along the c axis, to make use of the r_{33} electro-optic coefficient, which had a measured value of 180 pM/V. A voltage of 2 kV was applied along the c axis and the beams were launched along the a axis. Both beams were made incoherent by reflecting one of them from a mirror mounted on a piezoelectric transducer driven by an ac voltage at several kHz. A white light source was used to control the degree of saturation. The input and output light intensity distributions were recorded with a CCD camera. Fig. 1.5 shows the experimental result.

The lattice solitons in photorefractive media were first predicted by Efremidis et al. in 2002.[46] Families of two-component spatial solitons

in a one-dimensional lattice with saturable on-site nonlinearity (focusing or defocusing) in a photorefractive crystal was constructed by Fitrakis et al.[47] They identified 14 species of vector solitons, depending on their type (bright/dark), phase (in-phase/staggered), and location on the lattice (on/off-site). Two species of the bright/bright type form entirely stable soliton families, four species are partially stable (depending on the value of the propagation constant), while the remaining eight species are completely unstable. Symbiotic soliton pairs (of the bright/dark type), which contain components that cannot exist in isolation in the same model, were also found.

The role of resonance and dark irradiance for infrared photorefractive self-focusing and solitons in bipolar InP:Fe is studied by Fressengeas et al.[48] They showed experimental evidence for photorefractive steady state self-focusing in InP:Fe for a wide range of intensities, at both 1.06 and 1.55 μm. To explain the results, it is shown that despite the bipolar nature of InP:Fe where one photocarrier and one thermal carrier are to be considered, the long standing one photocarrier model for photorefractive solitons can be usefully applied.

Existence of long distance gap solitons has been studied considering a self-focusing photorefractive nonlinearity by Ricter et al.[49] They numerically investigated the stability of one- and two-dimensional gap solitons for very long propagation distances both in self-focusing and in self-defocusing nonlinear photonic media and demonstrated that the existence of stable solitons in the first gap requires much stronger lattices in a self-focusing than in a self-defocusing medium. They further considered an anisotropic model[50] for the PR nonlinearity and numerically demonstrated that both focusing and defocusing gap vortex solitons existed in this system. They found that both kind of solitons could be dynamically stable under certain circumstances.

Quasi-Bragg-matched counter-propagating spatial solitons in a reflection grating in the presence of a longitudinally modulated Kerr nonlinearity was investigated by Ciattoni et al.[51] The physical interplay of linear reflection and Kerr self-focusing with the modulation in the nonlinearity yields a variety of elaborate self-action mechanisms. They analytically predicted the existence of symmetric soliton pairs supported by a pure Kerr-like effective nonlinearity and derived two families of solitons, associated with the linear grating eigenmodes, supported by an effective incoherent Kerr-like coupling arising from the exact balance between the modulation in the nonlinearity and the Kerr interaction due to beam interference.

In an another investigation,[52] the effects of diffusion on the evolution

of steady-state dark and gray spatial solitons in biased photorefractive media is studied. The system was studied numerically as well as using perturbative methods showing that the soliton beams experience a modification of their initial trajectory and that the center of the optical beam moves along a parabolic trajectory. Peccianti and Assanto[53] investigated total internal reflection of nonlocal spatial optical solitons at the interface separating two liquid crystalline regions which, biased by unequal external voltages, exhibit different walk-offs and nonlinear responses. The solitons undergo nonspecular reflection, with an emerging angle differing appreciably from the incidence angle. The results can be used in tunable birefringent elements in soliton-based optical circuits and reconfigurable photonic interconnects.

Tiemann et al.[54] suggested photorefractive spatial solitons as optically induced information channels. They developed and demonstrated an experimental technique to measure the information throughput of photorefractive spatial solitons in accordance with Shannon's definition. They experimentally demonstrated that in the wavelength range of 1520-1630 nm, it could be estimated as large as $\sim$ 90 Tbits/s. They also experimentally demonstrated a measurement of the group-velocity dispersion and showed the limitation of the pulse transfer rate of the induced waveguides to $\sim$ 6.2 THz.

Recently, Fanjoux et al.[55] reported the observation of slow-light spatial solitons in a Kerr medium owing to light amplification by stimulated Raman scattering. This was achieved in a CS_2 nonlinear planar waveguide possessesing a strong self-focusing nonlinearity to generate the spatial Raman soliton and a Raman susceptibility sharp enough to induce the slow-light process simultaneously. They showed that the Raman Stokes component is optically delayed by more than 120 ps for a 140 ps Raman pulse duration and only 3 cm of propagation length, while propagating as a spatial soliton beam.

1.5   Outline of the thesis

This thesis deals with the study of light beam propagation through different nonlinear media. Analytical and numerical methods are used to show the formation of solitons in these media. Basic experiments have also been performed to show the formation of a self-written waveguide in a photopolymer. The variational method is used for the analytical analysis throughout the thesis. Numerical method based on the finite-difference

forms of the original partial differential equation is used for the numerical analysis.

In **Chapter 2**, we have studied two kinds of solitons, the $(2 + 1)$ D spatial solitons and the $(3 + 1)$D spatio-temporal solitons in a cubic-quintic medium in the presence of multiphoton ionization.

In **Chapter 3**, we have studied the evolution of light beam through a different kind of nonlinear media, the photorefractive polymer. We study modulational instability and beam propagation through a photorefractive polymer in the presence of absorption losses. The one dimensional beam propagation through the nonlinear medium is studied using variational and numerical methods. Stable soliton propagation is observed both analytically and numerically.

Chapter 4 deals with the study of modulational instability in a photorefractive crystal in the presence of wave mixing effects. Modulational instability in a photorefractive medium is studied in the presence of two wave mixing. We then propose and derive a model for forward four wave mixing in the photorefractive medium and investigate the modulational instability induced by four wave mixing effects. By using the standard linear stability analysis the instability gain is obtained.

Chapter 5 deals with the study of self-written waveguides. Besides the usual analytical analysis, basic experiments were done showing the formation of self-written waveguide in a photopolymer system.

The formation of a directional coupler in a photopolymer system is studied theoretically in **Chapter 6**. We propose and study, using the variational approximation as well as numerical simulation, the evolution of a probe beam through a directional coupler formed in a photopolymer system.

The main results and conclusion of this thesis are given in **Chapter 7**. The future prospects are also presented.

References

[1] B. A. Dubrovin and S. P. Novikov, "Hydrodynamics of weakly deformed soliton lattices. differential geometry and hamiltonian theory," Russ Math Surv **44**, 35–124 (1989).

[2] G. P. Agrawal, *Nonlinear Fiber Optics* (Academic Press, San Diego, California, 2001).

[3] N. J. Zabusky and M. D. Kruskal, "Interaction of "solitons" in a collisionless plasma and the recurrence of initial states," Phys. Rev. Lett. **15**, 240 – 243 (1965).

[4] A. S. Davydov, *Solitons in Molecular Systems* (Kluwer Academic Publishers, Dordrecht, Holland, 1991).

[5] A. Hasegawa and F. D. Tappert, "Transmission of stationary nonlinear optical pulses in dispersive dielectric fibers. i. anomalous dispersion," Appl. Phys. Lett. **23**, 142–144 (1973).

[6] L. F. Mollenauer, R. H. Stolen, and J. P. Gordon, "Experimental observation of picosecond pulse narrowing and solitons in optical fibers," Phys. Rev. Lett. **45**, 1095–1098 (1980).

[7] T. Li, *Optical Fiber Communications: Fiber Fabrication*, vol. 1 (Academic Press, San Diego, 1985).

[8] A. Hasegawa, *Optical Solitons in Fibers* (Springer-Verlag, berlin, 1989).

[9] J. E. Bjorkholm and A. A. Ashkin, "cw self-focusing and self-trapping of light in sodium vapor," Phys. Rev. Lett. **32**, 129 – 132 (1974).

[10] R. Boyd, *Nonlinear Optics* (Wiley, New York, 1998), 3rd ed.

[11] V. Van, T. A. Ibrahim, P. P. Absil, F. G. Johnson, R. Grover, and P.-T. Ho, "Optical signal processing using nonlinear semiconductor microring resonators," IEEE J. Sel. Top. Quantum Electron **8**, 705–713 (2002).

[12] G. Cancellieri, F. Chiaraluce, E. Gambi, and P. Pierleoni, "All-optical polarization modulator based on spatial soliton coupling," J. Lightwave Technol. **14**, 513–523 (1996).

[13] S. Blair and K. Wagner, "Cascadable spatial-soliton logic gates," Appl. Opt. **39**, 6006–6018 (2000).

[14] L. Bergé, "Wave collapse in physics: principles and applications to light and plasma waves," Phys. Rep. **303**, 259–370 (1998).

[15] Y. S. Kivshar and G. P. Agrawal, *Optical Solitons - From Fibers to Phtonic Crystals* (Academic Press, San Diego, California, 2003).

[16] Y. Silberberg, "Collapse of optical pulses," Opt. Lett. **15**, 1282–1284 (1990).

[17] B. A. Malomed, D. Mihalache, F. Wise, and L. Torner, "Spatiotemporal optical solitons," J. Opt. B **7**, R53–R72 (2005).

[18] G. Fibich and B. Ilan, "Optical light bullets in a pure kerr medium," Opt. Lett. **29**, 887–889 (2004).

[19] I. Towers and B. A. Malomed, "Stable (2+1)-dimensional solitons in a layered medium with sign-alternating kerr nonlinearity," J. Opt. Soc. Am. B **19**, 537–543 (2002).

[20] P. D. Trapani, G. Valiulis, A. Piskarskas, O. Jedrkiewicz, J. Trull, C. Conti, and S. Trillo, "Spontaneously generated x-shaped light bullets," Phys. Rev. Lett. **91**, 093904 (2003).

[21] H. Xu and H. Zeng, "Spontaneously generated walking x-shaped light bullets," Opt. Lett. **32**, 1944–1946 (2007).

[22] G. B. Whitham, *Linear and Nonlinear Waves* (John Wiley & Sons, New York, 1974).

[23] D. Anderson, "Variational approach to nonlinear pulse propagation in optical fibers," Phys. Rev. A **27**, 3135–3145 (1983).

[24] M. Karlsson, D. Anderson, A. Höök, and M. Lisak, "A variational approach to optical soliton collisions," Phys. Scr. **50**, 265–270 (1994).

[25] N. F. Smyth and A. L. Worthy, "Dispersive radiation and nonlinear twin-core fibers," J. Opt. Soc. Am. B **14**, 2610–2617 (1997).

[26] M. Chen, D. J. Kaup, and B. A. Malomed, "Three-wave solitons and continuous waves in media with competing quadratic and cubic nonlinearities," Phys. Rev. E **69**, 056605 (2004).

[27] J.-K. Xue, G.-Q. Li, A.-X. Zhang, and P. Peng, "Nonlinear mode coupling and resonant excitations in two-component bose-einstein condensates," Phys. Rev. E **77**, 016606 (2008).

[28] M. Margalit and M. Orenstein, "Simulation of passively mode locked lasers, using natural boundary conditions: multi pulse evolution and ordering," Opt. Commun. **124**, 475–480 (1996).

[29] G. P. Agrawal, "Optical pulse propagation in doped fiber amplifiers," Phys. Rev. A **44**, 7493–7501 (1991).

[30] D. Yevick and M. Glassner, "Forward wide-angle light propagation in semiconductor rib waveguides," Opt. Lett. **15**, 174–176 (1990).

[31] R. Ratowsky and J. A. Fleck, "Accurate numerical solution of the helmholtz equation by iterative Lanczos reduction," Opt. Lett. **16**, 787–789 (1991).

[32] D. J. Korteweg and F. de Vries, "On the change of form of long waves advancing in a rectangular canal, and on a new type of long stationary waves," Philos. Mag. **39**, 422–443 (1895).

[33] E. Fermi, J. Pasta, and S. Ulam, "Studies of nonlinear problems," Technical Report LA-1940 pp. 977–988 (1955).

[34] R. Y. Chiao, E. Garmire, and C. H. Townes, "Self-trapping of optical beams," Phys. Rev. Lett. **13**, 479–482 (1964).

[35] A. Barthelemy, S. Maneuf, and C. Froehly, "Soliton propagation and self-confinement of laser-beams by Kerr optical nonlinearity," Opt. Commun. **55**, 201–206 (1985).

[36] G. C. Duree, J. L. Shultz, G. J. Salamo, M. Segev, A. Yariv, E. J. Sharp, and R. R. Neurgaonkar, "Observation of self-trapping of an optical beam due to the photorefractive effect," Phys. Rev. Lett. **71**, 533–536 (1993).

[37] M. D. Castillo, A. Aguilar, J. J. Mondragon, S. Stepanov, and V. Vysloukh, "Spatial solitons in photorefractive $Bi_{12}TiO_{20}$ with drift mechanism of non-linearity," Appl. Phys. Lett. **64**, 408–410 (1994).

[38] M. F. Shih, M. Segev, G. C. Valley, G. Salamo, B. Crosignani, and P. D. Potto, "Observation of two-dimensional steady state photorefractive screening solitons," Electron. Lett. **31**, 826–827 (1995).

[39] G. Duree, M. Morin, G. Salamo, M. Segev, B. Crosignani, P. D. Porto, E. Sharp, and A. Yariv, "Dark photorefractive spatial solitons and photorefractive vortex solitons," Phys. Rev. Lett. **74**, 1978–1981 (1995).

[40] M. Mitchel and M. Segev, "Self-trapping of incoherent white light," Nature **387**, 880–883 (1997).

[41] J. W. Fleischer, M. Segev, N. K. Efremidis, and D. N. Christodoulides, "Observation of two-dimensional discrete solitons in optically induced nonlinear photonic lattices," Nature **422**, 147–150 (2003).

[42] J. W. Fleischer, G. Bartal, O. Cohen, O. Manela, M. Segev, J. Hudock, and D. N. Christodoulides, "Observation of vortex-ring "discrete" solitons in 2 D photonic lattices," Phys. Rev. Lett. **92**, 123904 (2004).

[43] D. N. Neshev, T. J. Alexander, E. A. Ostrovskaya, Y. S. Kivshar, H. Martin, I. Makasyuk, and Z. Chen, "Observation of discrete vortex solitons in optically induced photonic lattices," Phys. Rev. Lett. **92**, 123903 (2004).

[44] J. Yang, I. Makasyuk, H. Martin, P. G. Kevrekidis, B. A. Malomed, D. J. Frantzeskakis, and Z. Chen, "Necklace-like solitons in optically induced photonic lattices," Phys. Rev. Lett. **94**, 113902 (2005).

[45] A. Stepken, M. R. Belić, F. Kaiser, W. Królikowski, and B. Luther-Davies, "Three dimensional trajectories of interacting incoherent photorefractive solitons," Phys. Rev. Lett. **82**, 540–543 (1999).

[46] N. K. Efremidis, S. Sears, D. N. Christodoulides, J. W. Fleischer, and M. Segev, "Discrete solitons in photorefractive optically induced photonic lattices," Phys. Rev. E **66**, 046602 (2002).

[47] E. P. Fitrakis, P. G. Kevrekidis, B. A. Malomed, and D. J. Frantzeskakis, "Discrete vector solitons in one-dimensional lattices in photorefractive media," Phys. Rev. E **74**, 026605 (2006).

[48] N. Fressengeas, N. Khelfaoui, C. Dan, D. Wolfersberger, G. Montemezzani, H. Leblond, and M. Chauvet, "Roles of resonance and dark irradiance for infrared photorefractive self-focusing and solitons in bipolar InP:Fe," Phys. Rev. A **75**, 063834 (2007).

[49] R. Richter, K. Motzek, and F. Kaiser, "Long distance stability of gap solitons," Phys. Rev. E **75**, 016601 (207).

[50] T. Richter and F. Kaiser, "Anisotropic gap vortices in photorefractive media," Phys. Rev. A **76**, 033818 (2007).

[51] A. Ciattoni, C. Rizza, E. DelRe, and E. Palange, "Counterpropagating spatial solitons in reflection gratings with a longitudinally modulated kerr nonlinearity," Phys. Rev. Lett. **98**, 043901 (2007).

[52] M. I. Carvalho, M. Facao, and D. N. Christodoulides, "Self-bending of dark and gray photorefractive solitons," Phys. Rev. E **76**, 016602 (2007).

[53] M. Peccianti and G. Assanto, "Nonspecular total internal reflection of spatial solitons at the interface between highly birefringent media," Phys. Rev. Lett. **98**, 113902 (2007).

[54] M. Tiemann, J. Schmidt, V. M. Petrov, J. Petter, and T. Tschudi, "Information throughput of photorefractive spatial solitons in the telecommunication range," Appl. Opt. **46**, 2683–2687 (2007).

[55] G. Fanjoux, J. Michaud, H. Maillotte, and T. Sylvestre, "Slow-light spatial solitons," Phys. Rev. Lett. **100**, 013908 (2008).

2

Solitons in Bulk Cubic-Quintic Media

2.1 Introduction

A spatial soliton results from the balance between linear diffraction and nonlinear self-focusing, usually with a Kerr-type ultrafast nonlinearity. This effect was discovered in 1964.[1] It was Askaryan in 1962[2] who first suggested the idea that an optical beam can induce a waveguide and guide itself in it. A light beam traveling either in vacuum or in a medium always broadens because of the light's natural wave property of diffraction. But if the beam is incident into a bulk nonlinear material, such as silica glass, it changes the refractive index of the material. The consequent variation of the velocity of light across the wavefront of the beam focuses the beam as if it were passing through a lens. The earliest experimental observation of the self-focusing of optical beams was made in 1964.[3] If the diffraction of the beam can be compensated by the self-focusing of the beam, we get the so called *spatial solitons*. The perfect balance between diffraction and self-focusing which results in spatial solitons has been found to occur in one and two transverse dimensions, and the solitons are named $(1+1)$D or $(2+1)$D accordingly. When time is also included in the evolution equation, we get the so called spatio-temporal solitons. These spatial solitons have been found to occur in a variety of materials like Kerr materials, photorefractive materials, liquid crystals etc. Peccianti et al.[4] set up an experiment to demonstrate all-optical switching and logic gate blocks using spatial solitons in liquid crystals.

In this chapter, we study the propagation of an optical high-power cylindrically symmetric beam and a pulsed optical high-power beam in a material characterized by cubic-quintic nonlinearity using both analytical and numerical methods taking into consideration of the self-defocusing

effect caused by the presence of free electrons produced due to plasma formation. In section 2.2, a detailed study of two dimensional spatial solitons in a bulk cubic-quintic medium is presented. Spatio-temporal solitons in such a medium stabilized by multiphoton ionization is studied in section 2.3. Both kinds of solitons are studied analytically and numerically. We use the variational method[35] with a Gaussian ansatz for the analytical analysis. Approximate solutions can be found using this method. The Finite Difference Beam Propagation Method (FD-BPM) is used for the numerical analysis.[36]

The $(1+1)$D spatial solitons, a continuous wave beam linearly confined in one transverse dimension and self-guided in the other transverse dimension, are stable to perturbations and have been observed experimentally. A $(2+1)$D soliton that is self-guided in both transverse dimensions is not stable with a Kerr-type nonlinearity. Additional mechanisms such as index saturation or inclusion of higher-order nonlinearity helps to stabilize the propagation of such beams. A simple model for the stable propagation of $(2+1)$D solitons may be based on the cubic-quintic nonlinearity.[5,6] This model has attracted considerable attention. It has been shown that the cubic-quintic nonlinearity correctly describes the dielectric response of the polydiacetylene p-toluene sulfonate (PTS) crystal.[7] This type of nonlinear response is known for semiconductor-doped glasses[8] and various π conjugated polymers.[9-11] In these types of materials the refractive index, n, is of the form

$$n = n_0 + n_2 I + n_4 I^2, \qquad (2.1)$$

where I is the beam intensity n_0 is the linear refractive index and n_2 and n_4 are nonlinear coefficients with $n_2 > 0$ and $n_4 < 0$, i.e., the higher order nonlinearity is of the saturating kind. The propagation of spatial solitons in a PTS like medium has been studied by various groups.[12-14]

Now, if we are using a high power laser beam we have to consider the phenomenon of plasma generation through multiphoton absorption. For an extreme high power laser pulse of the order of 10 TW relativistic self-channeling in an underdense plasma has been predicted and experimentally observed over a plasma length of 3 mm. In this regime nearly all molecules of the medium are ionized and relativistic self-focusing develops from an increase of electron inertia under the influence of the intense electromagnetic wave. When such pulses are propagated through air, they can propagate over considerable distances because of the formation of filaments after the plasma has been generated through multiphoton ionization of air.[15] The

dispersive effects are less important in this case. The main mechanism behind the filament formation is related to a dynamic balance between the Kerr self-focusing and the defocusing induced by the plasma.[16]

We study the propagation of an optical high power beam through a PTS like medium. In this high energy regime, we have to consider the phenomenon of plasma generation through multiphoton absorption.[17] Multiphoton absorption is a nonlinear process, in contrast with the one-photon absorption process. It has a self defocusing effect on the material. The counteracting self-defocusing effect of both photoionized free electrons and the quintic nonlinearity restricts the unbounded growth of the Kerr nonlinearity. The study of spatial solitons in a bulk Kerr medium with multiphoton ionization has been carried out by Herrmann et al.[18] Couairon[19] has studied the dynamics of light filaments formed when a femtosecond laser pulse propagates in air taking into consideration the plasma generated using photoionization and has given an extensive review[20] on the main aspects of ultrashort laser pulse filamentation in various transparent media such as air (gases), transparent solids and liquids. The refractive index now takes the form

$$n = n_0 + n_2 I + n_4 I^2 - \frac{N_e}{2 n_0 N_{cr}}, \qquad (2.2)$$

where N_e is the number density of free electrons and N_{cr} is the critical plasma density. The beam evolution is studied using the cubic-quintic nonlinear Schrödinger equation with the effect of multiphoton ionization.

Now, when a pulsed optical beam propagates through a bulk nonlinear medium, it is affected by diffraction and dispersion simultaneously and at the same time the two effects become coupled through the nonlinearity of the medium. Such a space-time coupling leads to various nonlinear effects like the possibility of spatio-temporal collapse or pulse splitting and the formation of light bullets. The idea of "light bullets" was first proposed by Silberberg.[21] Optical spatiotemporal solitons, or the so called "light bullets", have attracted growing interest because of their potential applications in ultra fast all-optical switching in a bulk medium. The binary information once brought by temporal solitons has to be retreated in all-optical systems. Therefore, there is a growing interest in spatio-temporal solitons.[22] In a medium with purely cubic nonlinear response light bullets (LB) formally exist. But in the higher dimensions (2D and 3D) they are unstable against the spatiotemporal collapse induced by the combined effects of nonlinearity and anomalous dispersion. They are not stable in the uniform self-focusing Kerr medium[23] but stability can be

achieved in saturable,[16, 24] quadratically nonlinear,[25-27] and graded-index Kerr media.[28] Spatio-temporal solitons can also be found in self-induced-transparency media,[29] in off-resonance two-level systems,[30] as well as in engineered tandem structures made with quadratically nonlinear pieces.[31] A fully localized "light bullet" in all the three dimensions of space and time has not yet been found in an experiment but two-dimensional (2D) spatio-temporal solitons in bulk χ^2 media, such as lithium iodate ($LiIO_3$) and barium metaborate (BBO) has been observed.[32] This was the first experimental observation of a 2D spatio-temporal solitons in a second harmonic generation setting. This experiment was performed using tilted-pulse technique using highly elliptical beams. As a result diffraction is minimal in the remaining spatial transverse dimensions. Stable spinning solitons have also been predicted to exist in χ^2 media combined with the self-defocusing Kerr nonlinearity.[33] Stable spinning solitons of the same kind have also been found in an optical model based on the cubic-quintic nonlinear Schrödinger equation.[34]

2.2   Spatial solitons stabilized by multiphoton ionization

2.2.1   Model equation and analysis

An electric field $E(r, t)$ in a dielectric medium satisfies Maxwell's equation in the form

$$\nabla^2 E - \frac{1}{c^2}\frac{\partial^2 D}{\partial t^2} = \nabla(\nabla.E), \qquad (2.3)$$

where $D = \epsilon E$ is the displacement vector in the dielectric medium, with ϵ being the dielectric constant relative to vacuum and it is approximately equal to n^2; n being the refractive index. For a medium characterized by cubic nonlinearity, D can be written as, $D = (n_0(\omega) + n_2(\omega) |E|^2)^2 E$ where, $E = \frac{1}{2}[A(r, t) \exp i(wt - kz) + c.c]$. Using this, we can reduce the Maxwell's equation to

$$2ik\frac{\partial A}{\partial z} + \nabla^2 A + 2kk_0 n_2 |A|^2 A = 0, \qquad (2.4)$$

for a cubic medium where, $k = \omega/c$, $k_0 = n_0 k$, and A is the amplitude of the beam. This is the cubic nonlinear Schrödinger equation.

There are many materials which show quintic nonlinear effect in addition to the cubic one. In this case, the Maxwell's equation can be sim-

plified to obtain the cubic-quintic nonlinear Schrödinger equation. Hence the dynamics of the amplitude A of a laser beam in a PTS like medium is governed by the cubic-quintic nonlinear Schrödinger equation of the form

$$2ik\frac{\partial A}{\partial z} + \nabla^2 A + 2kk_0n_2 |A|^2 A + 2kk_0n_4 |A|^4 A = 0. \qquad (2.5)$$

Since we are using a very high power laser beam we have to consider the effect of multiphoton ionization as well. The reduced Maxwell's equation for the slowly varying amplitude A now takes the form

$$2ik\frac{\partial A}{\partial z} + \nabla^2 A + 2kk_0n_2 |A|^2 A + 2kk_0n_4 |A|^4 A$$
$$-\rho a A \int_{-\infty}^{\eta} |A(t')|^{2N} dt' = 0, \qquad (2.6)$$

where N is the number of quanta necessary to ionize the molecules, $\eta = t - z/v$ is the time of the moving frame of the pulse maximum and ρ and a are constants.

Here, we are considering the propagation of the beam along the z direction and variation along the radial direction. So we will use cylindrical coordinates for our analysis. Hence Eq. (2.6) takes the form

$$2ik\frac{\partial A}{\partial z} = -\frac{1}{r}\frac{\partial}{\partial r}\left(r\frac{\partial A}{\partial r}\right) + 2k\lambda_1 |A|^2 A$$
$$+2k\lambda_2 |A|^4 A + \rho a A \int_{-\infty}^{\eta} |A(t')|^{2N} dt, \qquad (2.7)$$

where $\lambda_1 = -k_0n_2$ and $\lambda_2 = -k_0n_4$.

The time dependence of the beam is taken into account by the ansatz, $A(z,r,\eta) = B(z,r)T(\eta)$. $T(\eta)$ is the normalized input shape.

Eq. (2.7) can be obtained from the Lagrangian

$$L = i\frac{r}{2}\left(B\frac{\partial B^*}{\partial z} - B^*\frac{\partial B}{\partial z}\right)T + \frac{r}{2k}\frac{\partial B}{\partial r}\frac{\partial B^*}{\partial r}T$$
$$+r\frac{\lambda_1}{2} |B|^4 T^3 + r\frac{\lambda_2}{3} |B|^6 T^4 + r\frac{\rho a}{2k}\frac{|B|^{2N+2}}{N+1}Tg(\eta), \qquad (2.8)$$

where

$$g(\eta) = \int_{-\infty}^{\eta} T^{2N} dt.$$

For a solution of this problem, let us assume a trial solution of the form

$$B(z,r) = C(z)\exp[-\frac{r^2}{2w(z)^2} + ib(z)r^2], \qquad (2.9)$$

where $C(z)$ is the maximum amplitude, $b(z)$ is the curvature parameter, $w(z)$ is the beam radius. Ideally, the trial function should include a possibility to model the dynamically varying radial shape function of the beam. But that will make the variational analysis more complicated.

The reduced Lagrangian is then given by

$$\langle L \rangle = \int_0^\infty Lr \, dr, \qquad (2.10)$$

$$\langle L \rangle = i\frac{T}{2}\left(C\frac{\partial C^*}{\partial z} - C^*\frac{\partial C}{\partial z}\right)w^3\frac{\sqrt{\pi}}{4} + b_z|C|^2 Tw^5\frac{\sqrt{\pi}}{8}$$

$$+\frac{|C|^2 T}{2k}\left\{\frac{1}{w^4} + 4b^2\right\}w^5\frac{\sqrt{\pi}}{8} + \frac{\lambda_1}{2}|C|^4 T^3 w^3\frac{\sqrt{\pi}}{8\sqrt{2}}$$

$$+\frac{\lambda_2}{3}|C|^6 T^4 w^3\frac{\sqrt{\pi}}{12\sqrt{3}} + \frac{\rho a}{2k}\frac{|C|^{2N+2}}{(N+1)^{5/2}}Tg(\eta)w^3\frac{\sqrt{\pi}}{4}. \qquad (2.11)$$

Now we can find the variation of $\langle L \rangle$ with respect to the various Gaussian parameters $C(z)$, $C(z)^*$, $w(z)$ and $b(z)$. We have

$$\frac{\partial}{\partial z}\left(\frac{\partial\langle L\rangle}{\partial C_z}\right) - \frac{\partial\langle L\rangle}{\partial C_z} = 0. \qquad (2.12)$$

Thus the variation with $C(z)$ and $C(z)^*$ gives

$$C\frac{\partial\langle L\rangle}{\partial C} = i\frac{T}{2}CC_z^* w^3 + b_z|C|^2 T\frac{w^5}{2}$$

$$+\frac{|C|^2 T}{2k}\left\{\frac{1}{w^4} + 4b^2\right\}\frac{w^5}{2} + \frac{\lambda_1}{2\sqrt{2}}|C|^4 T^3 w^3$$

$$+\frac{\lambda_2}{3\sqrt{3}}|C|^6 T^4 w^3 + \frac{\rho a}{2k}\frac{|C|^{2N+2}}{(N+1)^{5/2}}Tg(\eta)w^3, \qquad (2.13)$$

and

$$C^* \frac{\partial \langle L \rangle}{\partial C^*} = -i \frac{T}{2} C^* C_z w^3 + b_z |C|^2 T \frac{w^5}{2}$$

$$+ \frac{|C|^2 T}{2k} \left\{ \frac{1}{w^4} + 4b^2 \right\} \frac{w^5}{2} + \frac{\lambda_1}{2\sqrt{2}} |C|^4 T^3 w^3$$

$$+ \frac{\lambda_2}{3\sqrt{3}} |C|^6 T^4 w^3 + \frac{\rho a}{2k} \frac{|C|^{2N+2}}{(N+1)^{5/2}} T g(\eta) w^3. \tag{2.14}$$

Subtracting Eq. (2.14) from Eq. (2.13) and using Eq. (2.12), we get

$$\frac{\partial}{\partial z}(w^2 C C^*) = 0.$$

$$\Rightarrow w(0)^2 |C(0)|^2 = w(z)^2 |C(z)|^2 = E_0. \tag{2.15}$$

Adding Eq. (2.13) and Eq. (2.14) we obtain

$$i(CC_z^* - C^* C_z) = -2b_z |C|^2 w^2 - \frac{2|C|^2}{2k} \left\{ \frac{1}{w^4} + 4b^2 \right\} w^2$$

$$- \frac{2\lambda_1}{\sqrt{2}} |C|^4 T^2 - \frac{4\lambda_2}{3\sqrt{3}} |C|^6 T^3 + \frac{4\rho a}{2k} \frac{g(\eta) |C|^{2N+2}}{(N+1)^{5/2}}. \tag{2.16}$$

Now, the variation of $\langle L \rangle$ with respect to $w(z)$ and b gives

$$\frac{\partial \langle L \rangle}{\partial w} = \frac{3}{2} iT(CC_z^* - C^* C_z) + 5b_z |C|^2 T \frac{w^4}{2} + \frac{|C|^2 T}{4k}$$

$$+ 10 |C|^2 Tb^2 \frac{w^4}{2k} + \frac{3\lambda_1}{4\sqrt{2}} |C|^4 T^3 w^2 + \frac{\lambda_2}{3\sqrt{3}} |C|^6 T^4 w^2$$

$$+ \frac{3\rho a}{2k} \frac{|C|^{2N+2}}{(N+1)^{5/2}} T g(\eta) w^2, \tag{2.17}$$

and

$$\frac{\partial \langle L \rangle}{\partial b} = 0 \Rightarrow \frac{d}{dz}(w^5 |C|^2) = \frac{6b}{k} |C|^2 w^5. \tag{2.18}$$

From this and considering the fact that $w^2 |C|^2$ is a constant, we can write

$$\frac{dw}{dz} = \frac{4bw}{2k}. \tag{2.19}$$

This implies

$$b(z) = \frac{k}{2} \frac{d(\ln w)}{dz}.$$ (2.20)

Comparing Eq. (2.16) and Eq. (2.17) we obtain

$$b_z w^2 + \frac{5}{2kw^2} + \frac{4b^2 w^2}{2k} + \frac{9\lambda_1}{2\sqrt{2}} |C|^2 T^2$$

$$+ \frac{10\lambda_2}{3\sqrt{3}} |C|^4 T^3 + \frac{6(2N+1)\rho a}{2k(N+1)} \frac{|C|^{2N}}{(N+1)^{5/2}} g(\eta) = 0.$$ (2.21)

Now, combining Eq. (2.21) with the derivative form of Eq. (2.19), we obtain

$$\frac{d^2 w}{dz^2} = -\frac{20}{(2k)^2 w^3} - \frac{36\lambda_1 T^2 E_0}{4k\sqrt{2}w^3} - \frac{40\lambda_2 T^3 E_0^2}{6k\sqrt{3}w^5}$$

$$- \frac{24(2N+1)\rho a g(\eta) E_0^N}{(2k)^2(N+1)^{5/2} w^{2N+1}}.$$ (2.22)

Here $|C|^2$ has been eliminated by using the fact that $w^2 |C|^2 = E_0$.

On integrating the above equation, we get an equation for the variation of $w(z)$ as

$$\frac{1}{2} \left(\frac{dw}{dz} \right)^2 + \Pi(w) = 0.$$ (2.23)

This is analogous to the equation of a particle moving in a potential well. The potential $\Pi(w)$ is given by

$$\Pi(w) = -\frac{10}{(2k)^2 w^2} - \frac{18\lambda_1 T^2 E_0}{4k\sqrt{2}w^2} - \frac{10\lambda_2 T^3 E_0^2}{6k\sqrt{3}w^4}$$

$$- \frac{24(2N+1)\rho a g(\eta) E_0^N}{2N(2k)^2(N+1)^{5/2} w^{2N}} + c.$$ (2.24)

The phase $\phi(z)$ of $C(z)$ $(C(z) = |C(z)| exp[i\phi(z)])$ is obtained from Eq. (2.16) and also using Eq. (2.21) as

$$\frac{d\phi}{dz} = \frac{4}{2kw^2} + \frac{7\lambda_1}{2\sqrt{2}} |C|^2 T^2 + \frac{8\lambda_2}{3\sqrt{3}} |C|^4 T^3$$

$$+ \frac{2(7N+4)\rho a}{(N+1)2k} \frac{g(\eta |C|^{2N}}{(N+1)^{5/2}}.$$ (2.25)

Introducing $w(z)/w_0 = y(z)$, Eq. (2.23) becomes

$$\frac{1}{2}\left(\frac{dy}{dz}\right)^2 + \Pi(y) = 0, \tag{2.26}$$

where

$$\Pi(y) = \frac{\mu}{y^2} + \frac{\nu}{y^4} + \frac{\xi}{y^{2N}} + K, \tag{2.27}$$

with

$$\mu = -\frac{10}{4k^2w_0^4} - \frac{18\lambda_1 T^2 E_0}{4k\sqrt{2}w_0^4},$$

$$\nu = -\frac{10\lambda_2 T^3 E_o^2}{6k\sqrt{3}w_0^6},$$

$$\xi = -\frac{24(2N+1)\rho a g(\eta) E_0^N}{2N(2k)^2(N+1)^{5/2}w_0^{2N+2}},$$

and

$$K = \frac{c}{w_0^2}.$$

Now, let us assume that the beam at $z = 0$ has $w(0) = w_0$ and $[dw(z)/dz]_{z=0} = 0$. This gives $K = -(\mu + \nu + \xi)$.

Depending on the values of μ, ν and ξ we can identify four different regimes for the propagation of the beam.
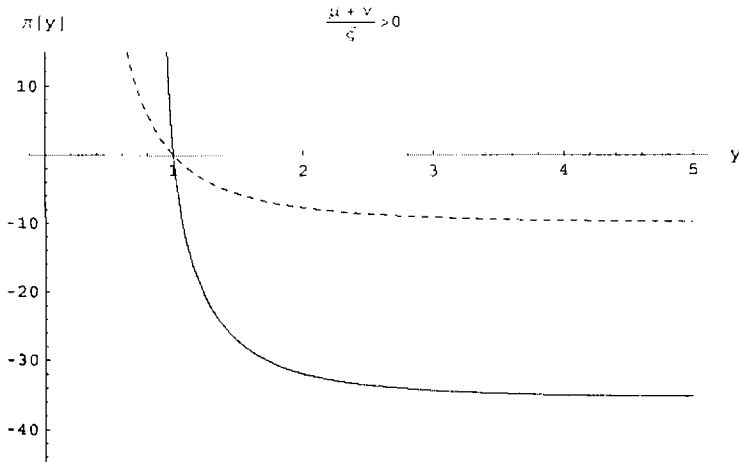

Figure 2.1: Qualitative plot of the potential function $\Pi(y)$ when all the nonlinearities are of defocusing nature ($\frac{\mu+\nu}{\xi} > 0$). Dotted line represents the linear case.

1) $\frac{\mu+\nu}{\xi} > 0$. This condition implies defocusing due to both third and fifth order nonlinearity as well as the nonlinearity due to the multiphoton effect. We can clearly see from Fig. 2.1 that the beam diffracts faster than in the purely linear case.

2) $-1 < \frac{\mu+\nu}{\xi} < 0$. This condition implies focusing due to the third order nonlinearity and defocusing due to a weak fifth order nonlinearity. The multiphoton effect is also of defocusing nature. We can see (Fig. 2.2) that the effect of nonlinearity is to focus the beam.
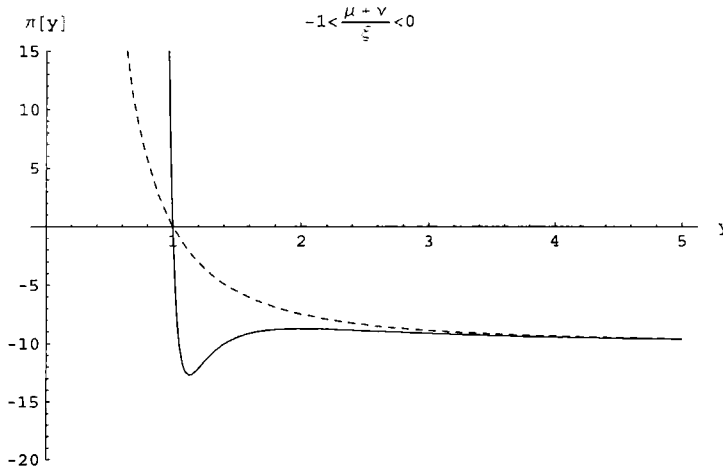

Figure 2.2: Qualitative plot of the potential function $\Pi(y)$ when third order nonlinearity is of focussing nature and all other nonlinearities are of defocusing nature (weak fifth order) ($-1 < \frac{\mu+\nu}{\xi} < 0$). Dotted line represents the linear case.

3) $-2.5 < \frac{\mu+\nu}{\xi} < -1$. In this case the third order nonlinearity is of focusing type and there is a strong fifth order nonlinearity. A potential well has been created. The spreading of the beam is stopped at the zeros of the potential function (Fig. 2.3).

4) $\frac{\mu+\nu}{\xi} = -2.5$. This is the limit case. The potential well has degenerated into a single point. The diffraction of the beam is exactly compensated by the focusing effect of the nonlinearity and beam propagates without any change in its shape (Fig. 2.4). The collapse of the beam has been arrested and we get a stable $(2+1)$D spatial soliton which propagates through the medium without any shape change.
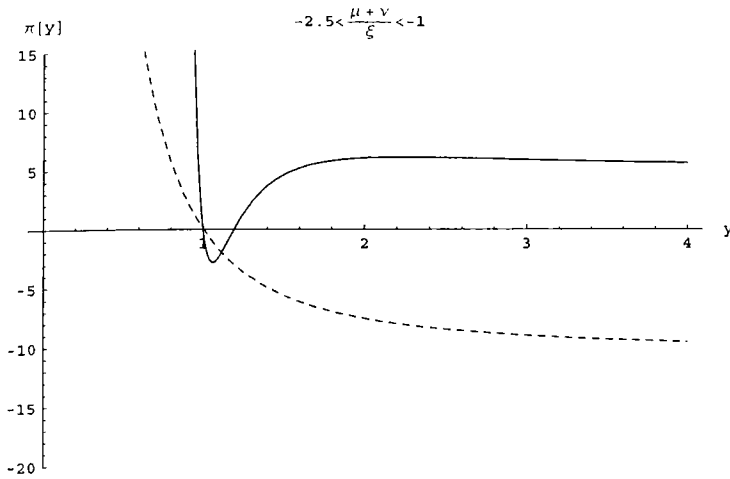
Figure 2.3: Qualitative plot of the potential function $\Pi(y)$ when third order nonlinearity is of focusing nature and all other nonlinearities are of defocusing nature (strong fifth order) $(-2.5 < \frac{\mu+\nu}{\xi} < -1)$. Dotted line represents the linear case.
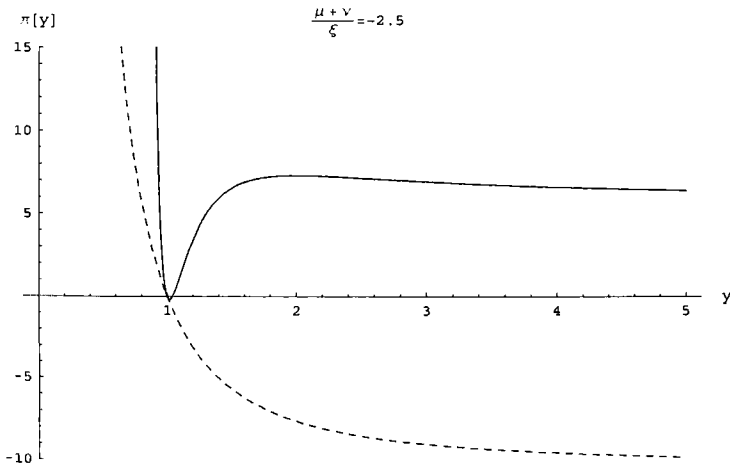

Figure 2.4: Qualitative plot of the potential function $\Pi(y)$ when focusing due to the third order nonlinearity is completely balanced by the defocusing due to the fifth order nonlinearity and multiphoton ionization $(\frac{\mu+\nu}{\xi} = -2.5)$. This is the limit case. Dotted line represents the linear case.

A three-dimensional plot of the normalized soliton intensity versus the

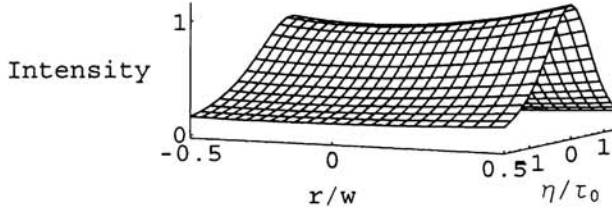time η and the radial variable r is plotted (Fig. 2.5).

Figure 2.5: Three-dimensional plot of the normalized soliton intensity versus the time η and the radial variable r.

2.2.2   Numerical analysis

Eq. 2.6 is numerically studied using the Finite Difference Beam Propagation Method (FD-BPM). It is a cylindrical partial differential equation that can be "integrated" forward in z by a number of standard techniques. In this approach, the field in the transverse plane is represented only at discrete points on a grid, and at discrete planes along the propagation direction z. Given the field at one z plane, we can find the field at the next z plane. This is then repeated to determine the field throughout the structure.

Let Ψ_i^{s+1} denote the field at transverse grid point i and longitudinal plane s_i, and assume that the grid points and planes are equally spaced by Δr and Δz apart, respectively. The radial and longitudinal dimensions are discretized by the values r_i and z_s according to the relations

$$r_i = i\Delta r, \tag{2.28}$$

and

$$z_s = s\Delta z. \tag{2.29}$$

Simplifying we get a tridiagonal matrix of the form

$$-c_1\Psi_{i+1}^{s+1} + d\Psi_i^{s+1} - c_3\Psi_{i-1}^{s+1} = c_1\Psi_{i+1}^s + c_2\Psi_i^s + c_3\Psi_{i-1}^s. \tag{2.30}$$

This can be easily solved using Thomas Algorithm[37] as discussed in section 1.3. Once the field at s is known, we can determine the field at $s + 1$ and so on.

We integrated Eq. (2.6) using the result obtained from the variational analysis as initial condition. The numerical parameters of the simulation has been chosen so as to fit the usual experimental configurations. Here, we have chosen $n_0 = 1.6755$, $n_2 = 2.2 \times 10^{-12}$ cm^2/W and $n_4 = -8 \times 10^{-22}$ cm^4/W^2 which are the nonlinear coefficients of PTS at wavelength 1600nm.[38] Similarly, for AlGaAs, with $n_0 = 3$, $n_2 = 1.5 \times 10^{-13}$ cm^2/W, $n_4 = -5 \times 10^{-23}$ cm^4/W^2 at wavelength 1550 nm.[38] The beam intensity is chosen as 1.1×10^9 W/m^2. The outcome of these simulations (see Fig. (2.6)) agrees very well with that obtained from the variational approach. The beam propagates without any change in shape.
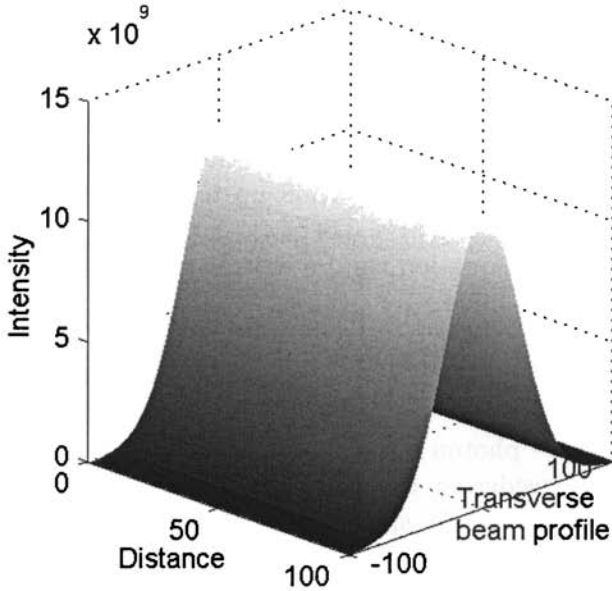
Figure 2.6: Numerically computed beam profile after it propagates a distance of 1 mm through the medium. Here Intensity is in W/m^2 and distance and transverse beam profile are in micrometers.

2.3 Spatio-temporal solitons stabilized by multiphoton ionization

2.3.1 Analytical and numerical analysis

We can generalize Eq. (2.5) to include both the temporal and spatial effects such that the new equation describes the propagation of an optical pulse

in a bulk medium whose transverse dimensions remain much larger than the beam size. In this case we have to include the effects of diffraction, dispersion and nonlinearity. Thus the general form of the (3+1)D nonlinear Schrödinger equation governing the evolution of the electromagnetic field A in a cubic-quintic isotropic dispersive medium can be written as

$$2ik\frac{\partial A}{\partial z} + \frac{\partial^2 A}{\partial \tau^2} + \frac{\partial^2 A}{\partial x^2} + \frac{\partial^2 A}{\partial y^2}$$
$$- \ 2k\lambda_1 |A|^2 A - 2k\lambda_2 |A|^4 A = 0. \qquad (2.31)$$

The change in the refractive index by the effect of Kerr nonlinearity, defocusing quintic nonlinearity and the self-induced ionization can be written as, $n = n_0 + n_2 I + n_4 I^2 - N_e/2n_0 N_{cr}$, where N_e is the number density of free electrons and N_{cr} is the critical plasma density. In this case, D takes the form $D = (n_0(\omega) + n_2(\omega) |E|^2 + n_4(\omega) |E|^4 - N_e/2n_0 N_{cr})^2 E$, where, $N_e = \int_{-\infty}^{\tau} |E|^{2n} d\tau'$. Using a simple integration rule, the electron density can be approximated for an integration up to the peak of the pulse, as $N_e = g(\tau) Na |E|^{2n}$, where $g(\tau) = 0.5(\tau_{min} + \tau)$.

Now the evolution equation can be written as

$$2ik\frac{\partial A}{\partial z} + \frac{\partial^2 A}{\partial \tau^2} + \frac{\partial^2 A}{\partial x^2} + \frac{\partial^2 A}{\partial y^2}$$
$$- \ 2k\lambda_1 |A|^2 A - 2k\lambda_2 |A|^4 A - \beta^{(N)} |A|^{2N} A = 0, \qquad (2.32)$$

where $\beta^{(N)}$ is the N- photon absorption coefficient.

Here we are considering the propagation of the pulsed beam along the z direction. We will take spherical coordinates for our analysis. The comoving coordinate τ can be treated on the same footing as a spatial coordinate. We can introduce the spatiotemporal radius[21] as, $r = (x^2 + y^2 + \tau^2)^{1/2}$. Now Eq. (2.32) takes the form

$$2ik\frac{\partial A}{\partial z} \ = \ -\frac{1}{r^2}\frac{\partial}{\partial r}\left(r^2\frac{\partial A}{\partial r}\right) - +2k\lambda_1 |A|^2 A$$
$$+ \ 2k\lambda_2 |A|^4 A + \beta^{(N)} |A|^{2N} A. \qquad (2.33)$$

We follow the standard variational method [35] for the analysis of this equation. For this we first write the Lagrangian of the above equation as

$$L \ = \ i\frac{r^2}{2}\left(A\frac{\partial A^*}{\partial z} - A^*\frac{\partial A}{\partial z}\right) + \frac{r^2}{2k}\frac{\partial A}{\partial r}\frac{\partial A^*}{\partial r}$$
$$+ \ \frac{r^2}{2}\lambda_1 |A|^4 + \frac{r^2}{3}\lambda_2 |A|^6 + \frac{r^2}{2k}\beta^{(N)} |A|^{2N+2}. \qquad (2.34)$$

We proceed by assuming a trial solution of the form

$$A(r, z) = C(z) \exp[-\frac{r^2}{2w(z)^2} + ib(z)r^2 + i\phi r^2], \qquad (2.35)$$

where $C(z)$ is the maximum amplitude, $w(z)$ is the beam width, $b(z)$ is the curvature parameter and ϕ is the phase.

Now the reduced Lagrangian for the system can be written as

$$
\begin{aligned}
\langle L \rangle = & \int_0^\infty Lr\,dr \\
= & \frac{i}{2}(CC_z^* - C^*C_z)w^4 + 3b_z\,|C|^2\,w^6 \\
+ & \frac{3\,|C|^2}{2k}\left(\frac{1}{w^4} + 4b^2\right)w^6 + \frac{\lambda_1}{8}\,|C|^4\,w^4 \\
+ & \frac{\lambda_2}{27}\,|C|^6\,w^4 + \frac{\beta^{(N)}}{kN^3}\,|C|^{2N+2}\,w^4. \qquad (2.36)
\end{aligned}
$$

Now we can find the variation of $\langle L \rangle$ with respect to the various Gaussian parameters $C(z)$, $C(z)^*$, $w(z)$ and $b(z)$:

$$C\frac{\partial \langle L \rangle}{\partial C} - C^*\frac{\partial \langle L \rangle}{\partial C^*} \Longrightarrow \frac{i}{2}CC_z^* w^4 + \frac{i}{2}C^*C_z w^4. \qquad (2.37)$$

This gives

$$\frac{\partial}{\partial z}(w^3 CC^*) = 0.$$

That is

$$w^3\,|C|^2 = E_0 = w_0^3\,|C_0|^2. \qquad (2.38)$$

$$
\begin{aligned}
& C\frac{\partial \langle L \rangle}{\partial C} + C^*\frac{\partial \langle L \rangle}{\partial C^*} = \frac{i}{2}w^4(CC_z^* - C^*C_z) \\
+ \;& 6b_z|C|^2 w^6 + \frac{6}{2k}|C|^2\{\frac{1}{w^4} + 4b^2\}w^6 \\
+ \;& \frac{\lambda_1}{2}|C|^4 w^4 + \frac{2}{9}\lambda_2|C|^6 w^4 + \frac{2\beta^{(N)}}{k^2}|C|^{2N}w^4 = 0. \qquad (2.39)
\end{aligned}
$$

The variation of $\langle L \rangle$ with w gives

$$\frac{\partial \langle L \rangle}{\partial w} = iw^3(CC_z^* - C^*C_z)$$

$$+ \quad 18b_z|C|^2w^5 + \frac{3}{k}|C|^2w + \frac{36}{k}|C|^2b^2w^5$$

$$+ \quad \frac{\lambda_1}{2}|C|^4w^3 + \frac{4}{27}\lambda_2|C|^6w^3 + \frac{4\beta^{(N)}}{k^2}|C|^{2N}w^3 = 0. \qquad (2.40)$$

Similarly, after some algebra, we get the following equations:

$$b = \frac{k}{2w}\frac{dw}{dz}, \qquad (2.41)$$

and

$$\frac{d^2w}{dz^2} = -\frac{3}{k^2w^3} - \frac{\lambda_1|C|^2}{2kw} - \frac{20}{81kw}\lambda_2|C|^4$$

$$- \quad \frac{4\beta^{(N)}}{3k^2N^2w}|C|^{2N+2}. \qquad (2.42)$$

Integration of Eq. (2.42) using Eq. (5.18) and introducing the normalized variables, $w(z)/w_0 = y(z)$, gives an equation of the form

$$\frac{1}{2}\left(\frac{dy}{dz}\right)^2 + \Pi(y) = 0, \qquad (2.43)$$

where

$$\Pi(y) = \frac{\mu}{y^2} + \frac{\nu}{y^3} + \frac{\xi}{y^6} + \frac{\alpha}{y^{3N-1}} + K, \qquad (2.44)$$
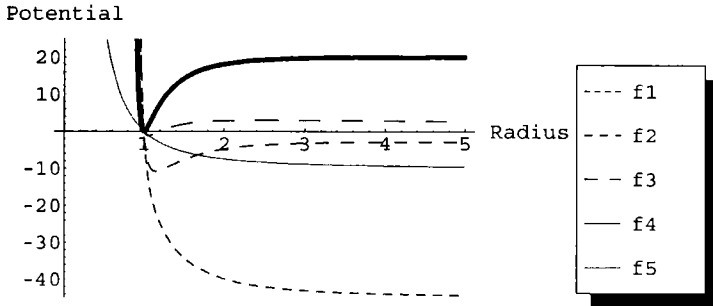
Figure 2.7: Qualitative plot of the potential function for different magnitudes and sign of nonlinearity.

with

$$\mu = -\frac{3}{(2k^2w_0^4)},$$

$$\nu = -\frac{\lambda_1 E_0}{6kw_0^5},$$

$$\xi = \frac{10\lambda_2 E_0^2}{243kw_0^8},$$

$$\alpha = -\frac{4\beta^{(N)} E_0^{(N)}}{3k^2 N^2 (3N-4) w_0^{(3N+1)}},$$

$$K = c/w_0^2,$$

and c is a constant of integration.

This represents a particle in a potential well. Based on the magnitude and sign of the nonlinearity we can identify four different regimes of propagation. Only when the focussing due to third order nonlinearity is compensated by the defocusing due to fifth order nonlinearity and the free electrons produced due to plasma formation, we get a stable light bullet. All the four regimes are plotted in Fig. 2.7. The linear case is also plotted for reference ($f5$). When all the nonlinearities are of defocusing kind the beam diffracts even faster than the purely linear case ($f1$).

Figure 2.8: Normalized beam profile at the input face of the medium. Inset: Two dimensional view of the beam profile.

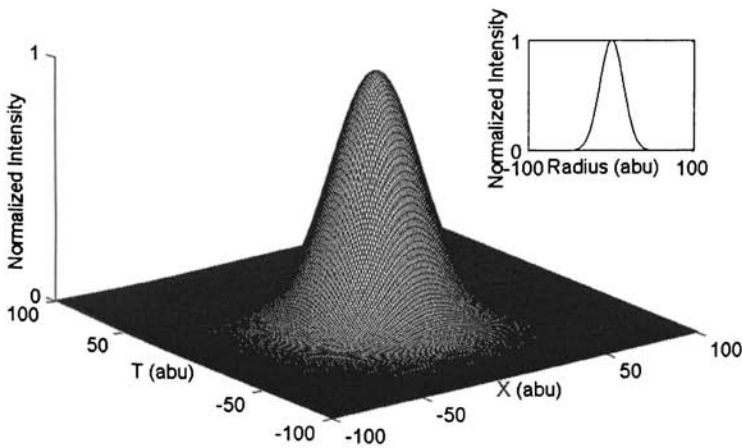A stable light bullet is formed when the focussing of the beam is completely compensated by the defocusing due to fifth order nonlinearity and the free electrons. This is the limit case ($f4$). The plots for intermediately high nonlinearity are shown in ($f2$) and ($f3$).

In order to verify the results from the variational approach, we studied the system numerically using the finite-difference beam propagation method (FD-BPM). The solution obtained using the variational method was used as the input for the numerical simulation. In our simulations we could observe a stable light bullet which propagated through the medium preserving its spatial and temporal radius. We propagated a 50 micrometer, 20 fs pulse through a medium with cubic-quintic nonlinearity. The nonlinear parameters of the medium are $n_0 = 3$, $n_2 = 1.5 \times 10^{-13} cm^2/W$, $n_4 = -5 \times 10^{-23} cm^4/W^2$ at wavelength 1550 nm.[38] The normalized initial profile of the beam is shown in Fig. 2.8 and the output profile after 5 diffraction lengths of travel through the medium is given in Fig. 2.9. From the figures we can clearly see that the beam propagated through the medium maintaining its spatio-temporal profile. This is the signature of the formation of light bullets.
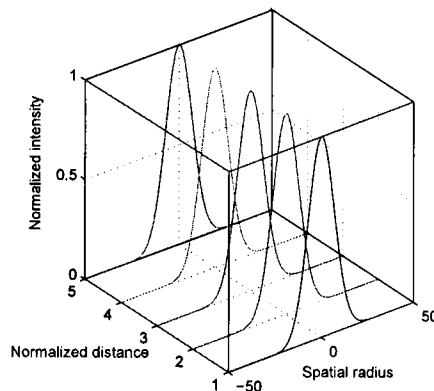

Figure 2.9: Numerically computed normalized beam profile using the solution of variational method as the input after it propagates 5 diffraction lengths through the medium.

2.4   Conclusions

In this chapter, first we have presented the studies on the propagation of a high energy laser beam through a PTS like medium characterized by both third and fifth order nonlinearities. We have employed both analytical and numerical methods. The energy of the beam considered in the present problem is sufficiently high enough to produce multiphoton ionization. Solutions are obtained using the variational formulation. It is found that multiphoton ionization helps in containing the catastrophic breakdown of the beam and helps in forming stable solitons. We could also show analytically the formation of stable solitons. This solution was taken as the initial condition for the numerical simulation. The soliton is found to propagate without any shape change.

We have further shown the existence of stable light bullets in a medium with cubic-quintic nonlinearity and self-defocusing effect of free electrons due to plasma formation. The system was studied both analytically and numerically and the results were found to be in good agreement. These LBs have potential application in all optical communication. It has been demonstrated numerically that the three-dimensional low energy spinning solitons are unstable in the CQ model.[39] The consideration of multiphoton ionization term in the evolution equation may stabilize the spinning light bullets in the cubic-quintic model. However, high-energy spinning solitons are stable in the cubic-quintic model.

References

[1] R. Y. Chiao, E. Garmire, and C. H. Townes, "Self-trapping of optical beams," Phys. Rev. Lett. **13**, 479–482 (1964).

[2] G. A. Askaryan, "Effects of the gradient of strong electromagnetic beam on electrons and atoms," Sov. Phys. JETP. **15**, 1088–1090 (1962).

[3] M. Hercher, "Laser-induced damage in transparent media," J. Opt. Soc. Amer. **54**, 563–569 (1964).

[4] M. Peccianti, C. Conti, and G. Assanto, "All-optical switching and logic gating with spatial solitons in liquid crystals," Appl. Phys. Lett. **81**, 3335–3337 (2002).

[5] K. I. Pushkarov, D. I. Pushkarov, and I. V. Tomov, "Self-action of light beams in nonlinear media: soliton solutions," Opt. Quantum Electron **11**, 471–478 (1979).

[6] S. Cowan, R. H. Enns, S. S. Ranganekar, and S. S. Sanghera, "Quasi-soliton and other behaviour of the nonlinear cubic-quintic schrödinger equation," Can. J. Phys. **64**, 311–315 (1986).

[7] B. L. Lawence, M. Cha, J. U. Kang, W. Torruellas, G. Stegeman, G. Baker, and S. E. J. Meth, "Large purely refractive nonlinear index of single crystal p-toluene sulphonate(PTS) at 1600nm," Electron. Lett. **30**, 447–448 (1994).

[8] F. Smektala, C. Quemard, V. Couderc, and A. Barthélémy, "Non-linear optical properties of chalcogenide glasses measured by Z-scan," J. Non-Cryst. Solids **274**, 232–237 (2000).

[9] P. Roussignol, D. Ricard, J. Lukasik, and C. Flytzanis, "New results on optical phase conjugation in semiconductor-doped glasses," J. Opt. Soc. Am. B. **4**, 5–11 (1987).

[10] L. H. Acioli, A. S. L. Gomes, J. M. Hickmann, and C. B. D. Araujo, "Femtosecond dynamics of semiconductor-doped glasses using a new source of incoherent light," Appl. Phys. Lett. **56**, 2279–2281 (1990).

[11] F. Lederer and W. Biehlig, "Bright solitons and light bullets in semiconductor waveguides," Electron. Lett. **30**, 1871–1872 (1994).

[12] K. Dimitrevski, E. Reimhult, E. Svensson, A. hgren, D. Anderson, A. Berntson, M. Lisak, and M. L. Quiroga-Teixeiro, "Analysis of stable self-trapping of laser beams in cubic-quintic nonlinear media," Phys. Lett. A **248**, 369–376 (1998).

[13] D. Pushkarov and S. Tanev, "Bright and dark solitary wave propagation and bistability in the anomalous dispersion region of optical waveguides with third- and fifth-order nonlinearities," Opt. Commun. **124**, 354–364 (1996).

[14] H. Michinel, J. Campo-Taboas, M. L. Quiroga-Teixeiro, J. R. Salgueiro, and R. Garcia-Fernandez, "Excitation of stable vortex solitons in nonlinear cubic-quintic materials," J. Opt. B: Quantum Semiclass. Opt **3**, 314–317 (2001).

[15] M. Mlejnek, M. Kolesik, J. V. Moloney, and E. M. Wright, "Optically turbulent femtosecond light guide in air," Phys. Rev. Lett. **83**, 2938–2941 (1999).

[16] N. Akozbek, C. M. Bowden, A. Talebpour, and S. L. Chin, "Femtosecond pulse propagation in air: Variational analysis," Phys. Rev. E **61**, 4540–4549 (2000).

[17] Y. S. Kivshar and G. P. Agrawal, *Optical Solitons - From Fibers to Phtonic Crystals* (Academic Press, San Diego, California, 2003).

[18] S. Henz and J. Herrmann, "Two-dimensional spatial optical solitons in bulk kerr media stabilized by self-induced multiphoton ionization: Variational approach," Phys. Rev. E **53**, 4092–4097 (1996).

[19] A. Couairon, "Dynamics of femtosecond filamentation from saturation of self-focusing laser pulses," Phys. Rev. A **68**, 15801 (2003).

[20] A. Couairona and A. Mysyrowicz, "Femtosecond filamentation in transparent media," Phys. Rep. **441**, 47–189 (2007).

[21] Y. Silberberg, "Collapse of optical pulses," Opt. Lett. **15**, 1282–1284 (1990).

[22] B. A. Malomed, D. Mihalache, F. Wise, and L. Torner, "Spatiotemporal optical solitons," J. Opt. B **7**, R53–R72 (2005).

[23] L. Berge, "Wave collapse in physics: principles and applications to light and plasma waves," Phys. Rep. **303**, 259–370 (1998).

[24] D. E. Edmundson, "Unstable higher modes of a three-dimensional nonlinear schrdinger equation," Phys. Rev. E **55**, 7636–7644 (1997).

[25] K. Hayata and M. Koshiba, "Multidimensional solitons in quadratic nonlinear media," Phys. Rev. Lett. **71**, 3275–3278 (1993).

[26] D. Mihalache, D. Mazilu, J. Dorring, and L. Torner, "Elliptical light bullets," Opt. Commun. **159**, 129–138 (1999).

[27] D. Mihalache, D. Mazilu, B. A. Malomed, and L. Torner, "Walking light bullets," Opt. Commun. **169**, 341–356 (1999).

[28] S. Raghavan and G. P. Agrawal, "Spatiotemporal solitons in inhomogeneous nonlinear media," Opt. Commun. **180**, 377–382 (2000).

[29] M. Blaauboer, B. A. Malomed, and G. Kurizki, "Spatiotemporally localized multidimensional solitons in self-induced transparency media," Phys. Rev. Lett. **84**, 1906–1909 (2000).

[30] I. V. Melnikov, D. Mihalache, and N.-C. Panoiu, "Localized multidimensional femtosecond optical pulses in an off-resonance two-level medium," Opt. Commun. **181**, 345–351 (2000).

[31] L. Torner, S. Carrasco, J. P. Torres, L.-C. Crasovan, and D. Mihalache, "Tandem light bullets," Opt. Commun. **199**, 277–281 (2001).

[32] X. Liu, L. J. Qian, and F. W. Wise, "Generation of optical spatiotemporal solitons," Phys. Rev. Lett. **82**, 4631–4634 (1999).

[33] I. Towers, A. V. Buryak, R. A. Sammut, and B. A. Malomed, "Stable localized vortex solitons," Phys. Rev. E **63**, 055601 (2001).

[34] A. Desyatnikov, A. Maimistov, and B. A. Malomed, "Three-dimensional spinning solitons in dispersive media with the cubic-quintic nonlinearity," Phys. Rev. E **61**, 3107–3113 (2000).

[35] D. Anderson, "Variational approach to nonlinear pulse propagation in optical fibers," Phys. Rev. A **27**, 3135–3145 (1983).

[36] R. Scarmozzino, A. Gopinath, R. Pregla, and S. Helfert, "Numerical techniques for modeling guided-wave photonic devices," IEEE J. Sel. Top. Quantum Electrons **6**, 150–162 (2000).

[37] A. Gourdin and M. Boumahrat, *Applied Numerical Methods* (Prentice Hall, New Delhi, 1996).

[38] S. Saltiel, S. Tanev, and A. D. Boardman, "High-order nonlinear phase shift caused by cascaded third-order processes," Opt. Lett. **22**, 148–150 (1997).

[39] D. Mihalache, D. Mazilu, L. C. Crasovan, B. A. Malomed, and F. Lederer, "Three-dimensional spinning solitons in the cubic-quintic nonlinear medium," Phys. Rev. E **61**, 7142–7145 (2000).

3

Solitons in Photorefractive Polymers

3.1 Introduction

CHAPTER 2 deals with the existence of solitons in a cubic-quintic nonlinear medium. In this chapter, we discuss with the photorefractive nonlinearity. The Photorefractive (PR) effect was discovered in the 1960's[1] and it was originally considered undesirable, since it led to scattering and deformation of collimated light beams. But soon photorefractivity was accepted as a novel nonlinear phenomenon with application in holography, optical phase conjugation and optical signal processing.[2] The PR effect refers to the spatial modulation of the index of refraction in an electro-optic material that is non-uniformly illuminated. We study modulational instability and beam propagation in a photorefractive polymer in the presence of absorption losses. The one dimensional beam propagation through the nonlinear media is studied using variational and numerical methods. Stable soliton propagation is observed both analytically and numerically. The concept of photorefractivity and the band transport model is introduced in section 3.1.1. The PR solitons is discussed in section 3.1.2. In section 3.2, the model for beam propagation through a PR polymer with loss effects is introduced. The propagation of broad optical beam through such a system is analyzed in section 3.3 and we calculate the steady state solutions and derive a dispersion relation for MI. Section 3.4 deals with the analytical analysis of the existence of spatial solitons in the PR polymer. Numerical studies on the system is discussed in section 3.5 and section 3.6 gives the conclusions.

49

3.1.1 Band transport model

The physics of the PR effect has been explained using a band transport model due to Kukhtarev et al.[3,4] The model assumes the existence of the donor and trapping centers located inside the energy band gap. In a photorefractive medium with an external bias electric field oriented along one of the transverse axes, an optical beam propagating along the z axis changes the refractive index due to the generation of free charge carriers and the subsequent creation of a space charge field by the light-matter interaction inside the material. Because the optically induced space charge field screens the externally applied electric field, the effective refractive index in a photorefractive crystal becomes a nonlinear function of the light intensity I, of the type that is analogous to a saturable nonlinearity. The physical mechanism behind the PR effect can be explained by a two step process. First the crystal has to be photoconductive implying that free charge carriers can be generated when light is illuminated upon it. Supposing that the electrons are the majority charge carriers, upon light illumination electrons can be excited from the crystal's conduction band to its valence band. These excited electrons move either by means of diffusion and/or drift due to external or internal electric field and might either be captured by the ionized donors or they move towards non-illuminated regions where they can be trapped by acceptor atoms. In the steady state, this process leads to charge separation inside the crystal (trapped electrons leave behind ionized donors) and a resulting space charge electric field. Since the crystal is electro-optic, the presence of the nonuniform electric field results in a modulation of its refractive index. The strength of this effect (i.e., refractive index change) is independent of the light intensity and is determined only by material parameters such as the electro-optic coefficients and the concentration of donor and acceptor centers.

To describe the PR effect, we start with the model equations presented by Kukhtarev et al. in 1979.[3] For the sake of simplicity, we assume that all the donor impurities are identical and have exactly the same energy state somewhere in the middle of the band gap as shown in Fig. 3.1.
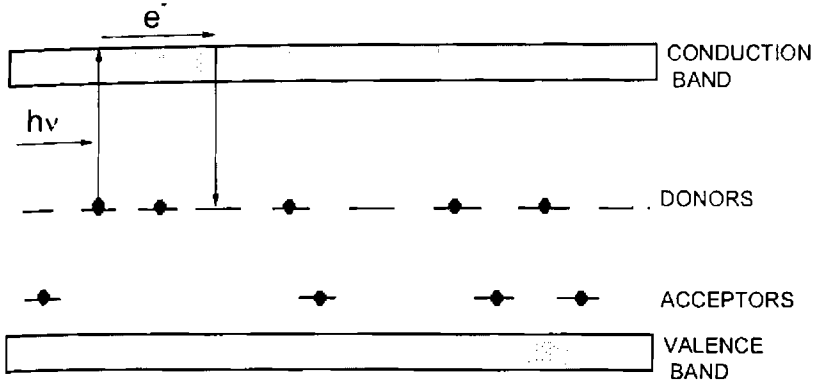
Figure 3.1: Band transport model for the photorefractive effect.

If N_d^+ is the density of ionized donor atoms and N_d is the density of donor impurities, the rate equation is

$$\frac{\partial N_d^+}{\partial t} = (sI + \beta_{dark})(N_d - N_d^+) - \gamma_r n_e N_d^+, \qquad (3.1)$$

where s is the photoionization cross section, β_{dark} is the dark generation rate, γ_r is the recombination rate coefficient, n_e is the density of free electrons and I is the intensity of light. In the steady state, the rate of generation of free charge carriers equals the recombination rate

$$(sI + \beta_{dark})(N_d - N_d^+) - \gamma_r n_e N_d^+ = 0. \qquad (3.2)$$

The current density j and the net charge density ρ are connected through the continuity equation

$$\frac{\partial \rho}{\partial t} = -\nabla \cdot \mathbf{j} = 0, \qquad (3.3)$$

and is equal to zero when the system is in steady state. The rate of generation of electrons is the same as that of the ionized impurities except that the electrons are mobile whereas the impurities are stationery. This is important for PR effect. The transport of electrons affect the electron density and the rate equation for the electron density can be written as

$$\frac{\partial n_e}{\partial t} - \frac{\partial N_d^+}{\partial t} = \frac{1}{e}\nabla \cdot \mathbf{j}, \qquad (3.4)$$

where e is the electronic charge (1.602×10^{-19}C). If we neglect the photovoltaic effect and assume that the contribution to current density $\mathbf{j}$ is due to only two process, the drift of charge carriers due to the electric field and the diffusion due to the gradient of carrier density, then we can express current density in terms of the static space-charge field $\mathbf{E_{sc}}$ and the electron density as

$$\mathbf{j} = e\mu_e n_e \mathbf{E_{sc}} + \mu_e k_B T \nabla n_e. \tag{3.5}$$

Here μ_e is the electron mobility, k_B is the Boltzman's constant and T is the absolute temperature. The Poisson's equation for the space-charge field can be written as

$$\nabla . \mathbf{E_{sc}} + (e/\epsilon_s)(n_e + N_A - N_d^+) = 0, \tag{3.6}$$

where ϵ_s is the low frequency dielectric constant and N_A is the number density of negatively charged acceptor atoms that compensate for the ionized donors. The refractive index is modulated via the space charge field through the electro-optic effect

$$\triangle n(E_{sc}) = -\frac{1}{2}n_b^3 r_{eff} E_{sc}, \tag{3.7}$$

where n_b is the unperturbed refractive index and r_{eff} is the effective electro-optic coefficient which depends on the specific light polarization and the crystal's geometry. The Helmholtz equation that describes the propagation of the light beam in $(1+1)$ D has the form

$$\left(\frac{\partial^2}{\partial x^2} + \frac{\partial^2}{\partial z^2}\right)E_{opt} + (k_0 n)^2 E_{opt} = 0. \tag{3.8}$$

In 1990, the PR phenomenon was first reported for a nonlinear organic crystal 2-cyclooctylamino-5-nitropyridine doped with 7,7,8,8- tetra-cyanoquinodimethane[5] and in 1991 for polymeric composites.[6] It is composed of an optically nonlinear epoxy polymer bisphenol-A-diglycidylether 4-nitro-1,2-phenylenediamine (bisA-NDPA), which was made photoconductive by doping with 30 wt% of the hole transport agent diethylaminobenzaldehydediphenylhydrazone (DEH). This material provided a proof-of-principle that the simultaneous requirements of optical nonlinearity, charge generation, transport, trapping, and absence of interfering photochromic effects can be combined in one material to produce photorefractivity. There are many reasons for pursuing the development of photorefractive polymers.[7-9] Polymers are easily processable into thin films of high optical

quality, can be modified easily by chemical doping, and are compatible with integrated circuit processing techniques, making them potentially useful in integrated optical device applications. Polymer PR systems can yield larger refractive index changes for equal densities of grating forming trapped charges when compared with inorganic crystals. This is because inorganic PR crystals with large electro-optic coefficients also have large dc dielectric constants. A large dielectric constant screens the Coulomb field produced by trapped charges thus reducing the internal space charge field. For organic nonlinear materials, the nonlinearity is a molecular property arising from the asymmetry of the electronic charge distributions in the ground and excited states of the individual molecules. For this reason large electro-optic coefficients are not accompanied by large dielectric constants and a potential improvement in performance of up to a factor of ten is possible. Polymeric systems are also of considerable interest because their spectral properties can be smoothly varied by changing the structure of polymers and polymeric composites. There is a great potential of doping such systems; in addition, they are cheap, readily processable and allow fabrication of parts of any shape and size which are compatible with modern microelectronic and optoelectronic devices, etc.

3.1.2 Photorefractive solitons

There has been tremendous growth in the field of optical spatial solitons since the first observation of self-trapping of light.[10] When an optical beam propagates in a suitable nonlinear medium, solitons can be formed and can be propagated without any diffraction effect. Spatial solitons with various dimensionality have been observed in various nonlinear media. The study of spatial solitons is considered to be important because of its possible applications in optical switching and routing. Segev et al. proposed a new kind of spatial soliton, the photorefractive soliton in the year 1992.[11] When illuminated, a space-charge field is formed in the photorefractive material which induces a nonlinear change in the refractive index of the material by the electro-optic (Pockels) effect. This change in refractive index can counter the effect of beam diffraction forming a PR soliton. The light beam effectively traps itself in a self-written waveguide. As compared to the Kerr-type solitons, these solitons exist in two dimensions and can be generated at low power levels of the order of several microwatts. The PR soliton has been investigated extensively by various groups as it has potential applications in all-optical switching, beam steering, optical interconnects etc. At present, three different kinds of PR solitons have

been proposed: quasi-steady state solitons,[11] screening solitons[12,13] and screening photovoltaic solitons.[14] The screening PR solitons are one of the most extensively studied solitons. They are possible in steady state when an external bias voltage is applied to a non-photovoltaic PR crystal. This field is partially screened by space charges induced by the soliton beam. The combined effect of the balance between the beam diffraction and the PR focusing effect results in the formation of a screening soliton.
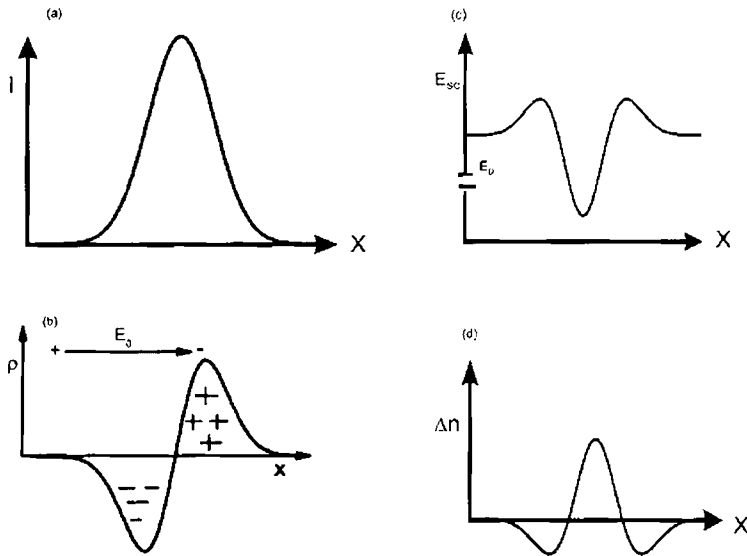

Figure 3.2: Sketch of drift dominated charge carrier transport process using a Gaussian intensity (a) and its effect on charge density (b), space charge field (c) and refractive index modulation (d).

Fig.3.2 shows the effect of a drift dominated charge transport process. The Gaussian light intensity pattern induces a positive refractive index modulation giving a focusing structure. The effect of a diffusion dominated charge transport process is depicted in Fig. 3.3. The resulting space charge field is asymmetric and the net refractive index change represents an asymmetric and deflecting structure as compared to the drift dominated process. Therefore, to obtain a focusing refractive index structure, the charge carrier transport process has to be drift dominated. Therefore, the crystal has to be biased by a dc-electric field in typical experimental setups for the generation of photorefractive screening solitons. However,

the diffusion process is always present, and the net refractive index change consists of contributions from both the drift and the diffusion effect.
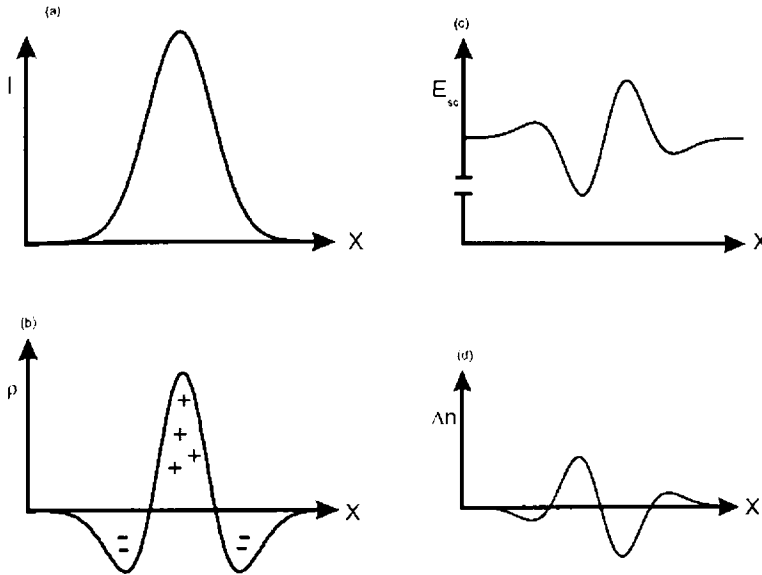

Figure 3.3: Sketch of diffusion dominated charge carrier transport process using a Gaussian intensity (a) and its effect on charge density (b), space charge field (c) and refractive index modulation (d).

Recently, a new kind of PR soliton, the photorefractive polymeric soliton, has been proposed[15] and observed[16] in a photorefractive polymer (made from a mixture of two dicyanomethylenedihydrofuran (DCDHF) chromophores (DCDHF-6 and DCDHF-6-C7M) at a 1:1 weight ratio sensitized with 0.5 wt.% of the charge generator buckminster fullerene(C_{60})). The PR polymer was discovered in 1991.[17] Since then it has attracted much research interest owing to the possibility of using them as highly efficient active optical elements for data transmission and controlling coherent radiation in various electro-optical and optical communication devices when compared to PR crystals.

A unique feature of the PR nonlinearity is its ability to exhibit either self-focusing or self-defocusing in the same crystal by a simple reversal of the polarity of the biasing field. Hence, the same crystal can be used to study either bright or dark solitons. But in a PR polymer, the reversal of polarity does not bring about a change in the sign of the nonlinear-

ity. This is achieved by changing the polarization of the incident light. Another feature of the PR nonlinearity is that this effect is wavelength sensitive. Hence it is possible to generate solitons using one wavelength (and low optical power) and then use the soliton-supported channels to guide another, much stronger optical beam of a different wavelength.

3.2   Model equation

We consider an optical beam propagating along the z axis of a nonlinear medium with the scalar electric field $E_{opt}(x,z) = \phi(x,z)\exp[ik_0 n_b z]\sqrt{I_b} +$ cc. Substituting in Eq. (3.8) we get

$$i\frac{\partial\phi}{\partial z} + \frac{1}{2k}\Big(\frac{\partial^2\phi}{\partial x^2} + \frac{\partial^2\phi}{\partial z^2}\Big) + \frac{1}{2k}k_0^2 \triangle(n^2)\phi = 0, \qquad (3.9)$$

where $\triangle(n^2) = n^2 - n_b^2$, $k = k_0 n_b$, $k_0 = 2\pi/\lambda$, λ is the free space wavelength of the beam and n_b is the unperturbed refractive index of the material.

The change in refractive index for x polarized light is governed by[15]

$$\triangle(n^2)_x = 4\pi N_{ch}\triangle\alpha(<\cos^2\theta - 1/3>), \qquad (3.10)$$

and that for y polarized light is governed by

$$\triangle(n^2)_y = -\triangle(n^2)_x/2. \qquad (3.11)$$

For most of the PR guest-host polymers

$$<\cos^2\theta - 1/3> = 0.043\Big(\frac{\mu_d E_{sc}}{k_b T_a}\Big)^2. \qquad (3.12)$$

Hence Eq. (3.9) can be simplified as

$$i\frac{\partial\phi}{\partial z} + \frac{1}{2k}\frac{\partial^2\phi}{\partial x^2} + \frac{1}{2k}k_0^2 C_{x,y}E_{sc}^2\phi = 0, \qquad (3.13)$$

where

$$C_x = 0.54 N_{ch}\triangle\alpha\Big(\frac{\mu_d}{k_b T_a}\Big)^2, \qquad (3.14)$$

and

$$C_y = -C_x/2,$$

for x- and y-polarized light, respectively. In Eq. (3.14), N_{ch} is the density of chromophores, μ_d is the permanent dipole moment of the chromophores,

k_B is the Boltzmann constant and T_a is the ambient temperature. $\triangle \alpha = \alpha_\| - \alpha_\perp$, where $\alpha_\|$ and $\alpha_\perp$ denotes the polarizabilities of chromophores parallel and perpendicular to its dipole moment, respectively. The space-charge field is obtained as

$$E_{sc}^{m+1} = E_0^{m+1} \frac{I_0 + I_b}{I + I_b}, \tag{3.15}$$

where E_0 and I_0 are, respectively, electric field E_{sc} and soliton intensity I, far away from the soliton center, m is a material parameter and its value ranges from less than one to greater than three.[18]

Simplifying, the envelope equation for the propagation of a light beam, with amplitude ϕ, through a photorefractive polymer with loss effect is then obtained as

$$i\phi_z + \frac{1}{2k}\phi_{xx} + \frac{k_0^2}{2k}C_{x,y}E_0^2\left(\frac{1+\gamma}{1+|\phi|^2}\right)^{\frac{2}{m+1}}\phi + \frac{i}{2}\alpha_0\phi = 0, \tag{3.16}$$

where $\gamma = I_0/I_b$ is the intensity ratio for dark solitons and is equal to zero for bright solitons. The absorption loss is given by the last term in Eq. (3.16) where α_0 is the absorption coefficient of the material.

Using the dimensionless variables $\zeta = z/2kx_0^2$, $\xi = x/x_0$, where x_0 is an arbitrary spatial width, Eq. (3.16) can be normalized as

$$i\phi_\zeta + \phi_{\xi\xi} + \beta\left(\frac{1+\gamma}{1+|\phi|^2}\right)^{\frac{2}{m+1}}\phi + i\alpha\phi = 0, \tag{3.17}$$

with $\beta = \beta_{x,y} = k_o^2 x_0^2 C_{x,y} E_0^2$ and $\alpha = k_o^2 x_0^2 \alpha_0$. For the case $m = 1$, Eq. (3.17) becomes

$$i\phi_\zeta + \phi_{\xi\xi} + \beta\left(\frac{1+\gamma}{1+|\phi|^2}\right)\phi + i\alpha\phi = 0. \tag{3.18}$$

This represents the normalized equation for the slowly varying beam envelope ϕ in a PR crystal.

3.3   Nonlinear plane waves and their modulational instability

Modulational instability (MI) is one of the most fundamental effects associated with wave propagation in nonlinear media. It causes the initially

uniform beam profile to breakup into a periodic pattern and, eventually, into periodically-spaced filaments. The instability can be intuitively described as the amplification of small amplitude noise superimposed to the input beam. The MI phenomenon has been previously observed in various media like Kerr media,[19] electrical circuits,[20] plasmas,[21] parametric band gap systems,[22] quasi-phase-matching gratings[23] and discrete dissipative systems.[24] The transverse instability of counter-propagating waves in PR media is studied by Saffman et al.[25]

For studying the modulational instability, we first use a transformation of the form, $\phi = Q(\zeta) \exp[-\alpha\zeta]$, which reduces Eq. (3.17) to

$$iQ_\zeta + Q_{\xi\xi} + \beta \Big(\frac{1 + \gamma}{1 + |Q|^2 e^{-2\alpha\zeta}} \Big)^{\frac{2}{m+1}} Q = 0. \tag{3.19}$$

The next step is to find the steady state solution of the governing Eq. (3.19) which is obtained as

$$Q(\zeta, \xi) = \sqrt{P} \exp[i\Phi(\zeta)], \tag{3.20}$$

where P is the input power and

$$\Phi(\zeta) = \beta(1 + \gamma)^{\frac{2}{m+1}}(1 + m)(e^{2\alpha\zeta}/P)^{2/m+1} H$$

is the nonlinear phase shift and $H[\frac{2}{m+1}, \frac{2}{m+1}, \frac{3+m}{m+1}, \frac{-e^{2\alpha\zeta}}{P}]$ is the hypergeometric function.

The linear stability of the steady state is studied by perturbing the steady state solution as

$$Q(\zeta, \xi) = (\sqrt{P} + a(\zeta, \xi)) \exp[i\Phi(\zeta)]. \tag{3.21}$$

Substituting this in Eq. (3.19) and linearizing around the solution we get

$$\begin{aligned} ia_\zeta \;+\; & a_{\xi\xi} - \beta(1 + \gamma)^{2/m+1} \Big(\frac{1}{(1 + Pe^{-2\alpha\zeta})^{2/m+1}} - \frac{1}{(1 + Pe^{-2\alpha\zeta})^{4/m+1}} \Big) a \\ -\; & \beta(1 + \gamma)^{2/m+1} \frac{2}{1 + m} \frac{Pe^{-2\alpha\zeta}}{(1 + Pe^{-2\alpha\zeta})^{4/m+1}} a^* = 0. \end{aligned} \tag{3.22}$$

It is important to note that the above equation reduces to the equation governing the perturbation in a photorefractive crystal[26] for $m = 1$ and $\alpha = 0$.

Now, we assume that the spatial perturbation $a(\zeta,\xi)$ is composed of two side band plane waves, i.e,

$$a(\zeta,\xi) = U(\zeta)\exp[i\kappa\xi] + V(\zeta)\exp[-i\kappa\xi]. \tag{3.23}$$

Substituting Eq. (3.23) in Eq. (3.22) gives two coupled equations as follows

$$U_\zeta = -i(\kappa^2 + A)U - iBV^*, \tag{3.24}$$
$$V_\zeta^* = iBU + i(\kappa^2 + A)V^*. \tag{3.25}$$

The above coupled equations can be written in the compact matrix form as

$$\partial_z \underline{X} = \mathbf{M}\underline{X},$$

where $\mathbf{M}$ is a 2x2 matrix given by

$$\mathbf{M} = \begin{pmatrix} a_{11} & a_{22} \\ a_{33} & a_{44} \end{pmatrix}, \tag{3.26}$$

and

$$a_{11} = -i(\kappa^2 + A),$$
$$a_{22} = -iB,$$
$$a_{33} = iB,$$
$$a_{44} = i(\kappa^2 + A),$$

with

$$A = \beta(1+\gamma)^{2/m+1}\left(\frac{1}{(1+Pe^{-2\alpha\zeta})^{2/m+1}} - \frac{1}{(1+Pe^{-2\alpha\zeta})^{4/m+1}}\right),$$

and

$$B = \beta(1+\gamma)^{2/m+1}\frac{2}{1+m}\frac{Pe^{-2\alpha\zeta}}{(1+Pe^{-2\alpha\zeta})^{4/m+1}}.$$

This equation has a nontrivial solution only if the determinant of the matrix vanishes. The real part of the eigenvalues of the stability matrix in Eq. (3.26) gives the gain associated with the system.[27] The eigenvalues are given by the following relation

$$\Lambda_\pm = \pm(B^2 - A^2 - 2A\kappa^2 - \kappa^4)^{1/2}. \tag{3.27}$$

For $\Lambda > 0$, the perturbation grows exponentially during propagation with the growth rate or gain given by $Re[\Lambda]$, indicating MI. For $m = 1$, $A = B$ and the eigenvalue reduces to that in a PR crystal.[26]
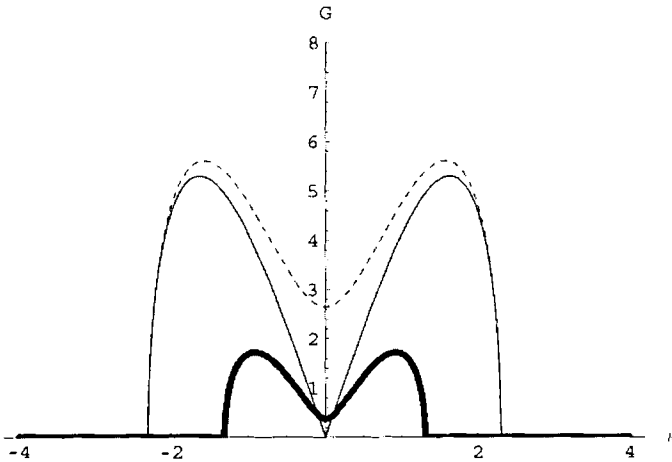

Figure 3.4: Normalized growth rate as a function of normalized spatial frequency κ for PR crystal (line), PR polymer with no loss (dotted line) and PR polymer with loss (thick line).

The growth rate for the three cases: $m = 1$ and $\alpha = 0$ (photorefractive crystal), $m = 2$ and $\alpha = 0$ (photorefractive polymer with no loss), and $m = 2$ and $\alpha \neq 0$ is plotted in Fig. 3.4. We can see that for the same parameters, the gain for the PR crystal (line) and the PR polymer (dotted line) is almost same but there is a finite gain value even for $\kappa = 0$ for the PR polymer. The effect of the absorption term is to reduce the gain (thick line).

The growth rate as a function of input power P is plotted in Fig. 3.5. The MI gain increases with the input power. When there is no loss, the MI gain increases with power and saturates (Fig. 3.6). This is in contrast with that of a PR crystal. Here the MI gain decreases with power[28] (see Fig. 3.7).
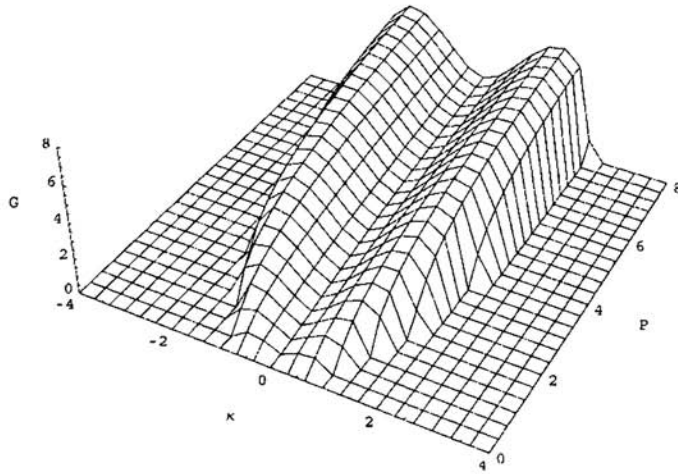
Figure 3.5: Normalized gain G versus normalized spatial frequency κ and normalized input power P for PR polymer with loss.
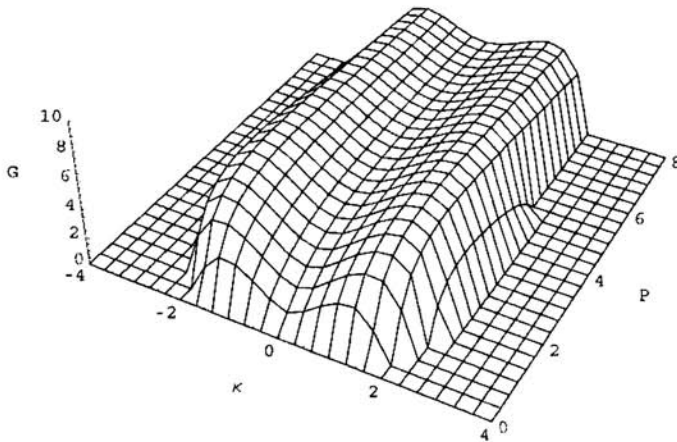

Figure 3.6: Normalized gain G versus normalized spatial frequency κ and normalized input power P for PR polymer with no loss.
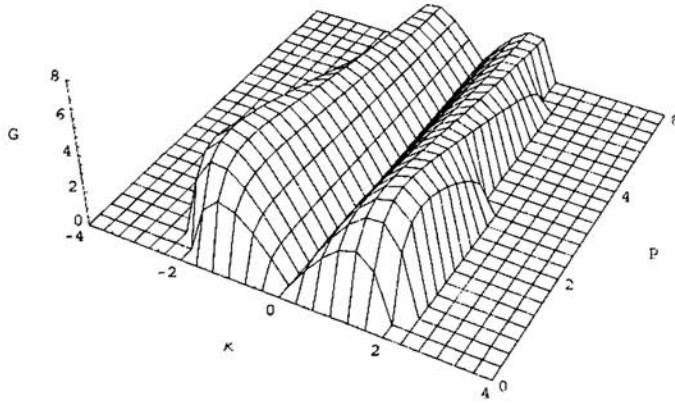
Figure 3.7: Normalized gain G versus normalized spatial frequency κ and normalized input power P for PR crystal.

3.4 Variational analysis for the beam propagation

In this section, we study the propagation of a one dimensional spatial soliton through the PR polymer. Since Eq. (3.17) is in general non-integrable, for our further analysis, we use the variational method for studying the dynamics of a light beam propagating through a photorefractive polymer. The Lagrangian associated with the system can be written as

$$L = \left(\frac{i}{2}(\phi\phi_\zeta^* - \phi^*\phi_\zeta) + |\phi_\xi|^2 + \beta(1+\gamma)\frac{1+m}{1-m}\left(\frac{1+\gamma}{1+|\phi|^2}\right)^{\frac{1-m}{1+m}} \right) e^{2\alpha\zeta}. \quad (3.28)$$

To proceed, a trial solution of the form

$$\phi(\zeta,\xi) = A(\zeta)\exp\left[-\frac{\xi^2}{2a\zeta^2} + ib(\zeta)\xi^2 \right], \quad (3.29)$$

is assumed.

Substituting Eq. (3.29) in the Lagrangian and then defining the re-

duced Lagrangian as $\langle L \rangle = \int_0^\infty L dx$ we get,

$$
\begin{aligned}
\langle L \rangle &= e^{2\alpha\zeta}\{i(\Lambda\Lambda_\zeta^* - A^*A_\zeta)a\frac{\sqrt{\pi}}{4} + 2b_\zeta|A|^2a^3\frac{\sqrt{\pi}}{4} \\
&+ (\frac{1}{a^4} + 4b^2)|\Lambda|^2a^3\frac{\sqrt{\pi}}{4} - (1+\gamma)^{\frac{2}{1+m}}\beta|A|^2a\frac{\sqrt{\pi}}{2} \\
&+ (1+\gamma)^{\frac{2}{1+m}}\beta|A|^4\frac{a}{2(1+m)}\sqrt{\frac{\pi}{4}} + C\},
\end{aligned}
\tag{3.30}
$$

where $C = \beta l\frac{1+m}{1-m}(1+\gamma)^{\frac{2}{1+m}}$ and l is a constant. The variational equations are obtained from the variational principle

$$
\frac{\partial}{\partial z}\Big(\frac{\partial\langle L\rangle}{\partial q_z}\Big) - \frac{\partial\langle L\rangle}{\partial q} = 0,
\tag{3.31}
$$

where q represents the various variational parameters. Finding the variation of the reduced Lagrangian with various variational parameters, we get the following set of equations:

$$
\begin{aligned}
\Lambda\frac{\partial\langle L\rangle}{\partial A} &= e^{2\alpha\zeta}\{i\Lambda\Lambda_\zeta^*a\frac{\sqrt{\pi}}{4} + 2b_\zeta|\Lambda|^2a^3\frac{\sqrt{\pi}}{4} \\
&+ |A|^2(\frac{1}{a^4} + 4b^2)a^3\frac{\sqrt{\pi}}{4} - (1+\gamma)^{\frac{2}{1+m}}\beta|A|^2a\frac{\sqrt{\pi}}{2} \\
&+ (1+\gamma)^{\frac{2}{1+m}}\beta|A|^4a\frac{\sqrt{\pi}}{\sqrt{2}(m+1)}\},
\end{aligned}
\tag{3.32}
$$

$$
\begin{aligned}
A^*\frac{\partial\langle L\rangle}{\partial A^*} &= e^{2\alpha\zeta}\{iA^*A_\zeta a\frac{\sqrt{\pi}}{4} + 2b_\zeta|A|^2a^3\frac{\sqrt{\pi}}{4} \\
&+ |A|^2(\frac{1}{a^4} + 4b^2)a^3\frac{\sqrt{\pi}}{4} - (1+\gamma)^{\frac{2}{1+m}}\beta|A|^2a\frac{\sqrt{\pi}}{2} \\
&+ (1+\gamma)^{\frac{2}{1+m}}\beta|\Lambda|^4a\frac{\sqrt{\pi}}{\sqrt{2}(m+1)}\},
\end{aligned}
\tag{3.33}
$$

$$
\begin{aligned}
\frac{\partial\langle L\rangle}{\partial a} &= e^{2\alpha\zeta}\{i(\Lambda\Lambda_\zeta^* - \Lambda^*\Lambda_\zeta)\frac{\sqrt{\pi}}{4} + 6b_\zeta|A|^2a^2\frac{\sqrt{\pi}}{4} \\
&+ |A|^2(12b^2 - \frac{1}{a^4})a^2\frac{\sqrt{\pi}}{4} - (1+\gamma)^{\frac{2}{1+m}}\beta|A|^2\frac{\sqrt{\pi}}{2} \\
&+ (1+\gamma)^{\frac{2}{1+m}}\beta|A|^4\frac{\sqrt{\pi}}{\sqrt{2}(m+1)}\},
\end{aligned}
\tag{3.34}
$$

$$a(\zeta)|A(\zeta)|^2 e^{2\alpha\zeta} = a_0|A_0|^2 = E_0, \qquad (3.35)$$

$$b = \frac{1}{2a}\frac{da}{d\zeta}, \qquad (3.36)$$

$$\frac{d^2a}{d\zeta^2} = \frac{3}{a^3} - \beta(1+\gamma)^{\frac{2}{1+m}}\frac{2}{a} + 3\sqrt{2}E_0\beta(1+\gamma)^{\frac{2}{1+m}}\frac{1}{a^2 e^{2\alpha\zeta}}. \qquad (3.37)$$

The evolution of the beam in a PR polymeric medium is determined by the competition between two factors: diffraction (given by the first term on the right-hand side of (3.37)) and the nonlinear self-focusing (net effect of the second and third term).

Integrating Eq (3.37) and introducing the normalization $a(\zeta)/a_0 = y(\zeta)$, we get an equation describing the motion of a particle in a potential well

$$\frac{1}{2}\left(\frac{dy}{d\zeta}\right)^2 + \Pi(y) = 0. \qquad (3.38)$$

The potential function is given by

$$\Pi(y) = \mu/y^2 + \nu\log[y] - \eta/y + K, \qquad (3.39)$$

where

$$\mu = 3/2a_0^4,$$

$$\nu = 2\beta\log(a_0)/a_0^2,$$

and

$$\eta = 3\beta e^{-2\alpha\zeta}/\sqrt{2}a_0^3.$$

Here we have used the fact that $\gamma = 0$ for the case of bright solitons.

Assuming that the beam at $z = 0$ has width $a(0) = a_0$ and using the boundary condition, $[da(z)/dz]_{z=0} = 0$, we get, $K = -(\mu - \eta)$. When only the diffraction effect is present, that is in the absence of any nonlinear effects, the potential function takes the form

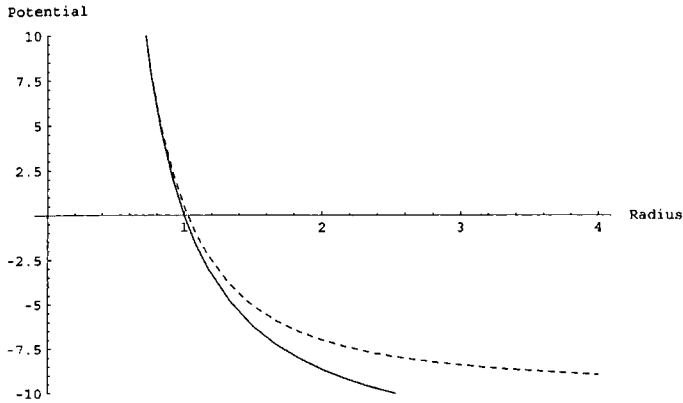$$\Pi(y) = \mu/y^2 - (\mu - \eta). \qquad (3.40)$$

Figure 3.8: Qualitative plot of the normalized potential function vs normalized width when β is positive. Dotted line gives the linear case.
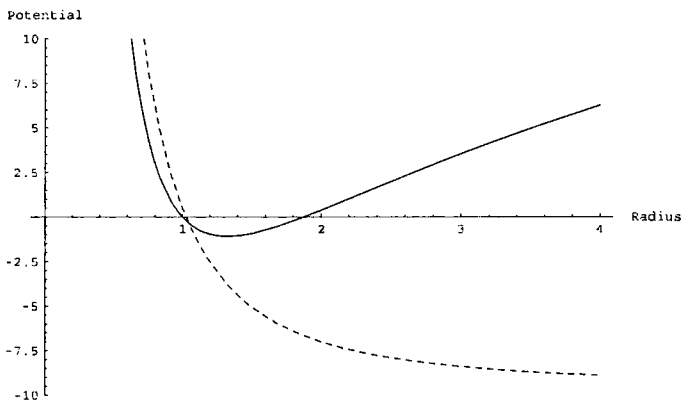

Figure 3.9: Qualitative plot of the normalized potential function vs normalized width when β is negative (intermediately high nonlinearity). Dotted line gives the linear case.
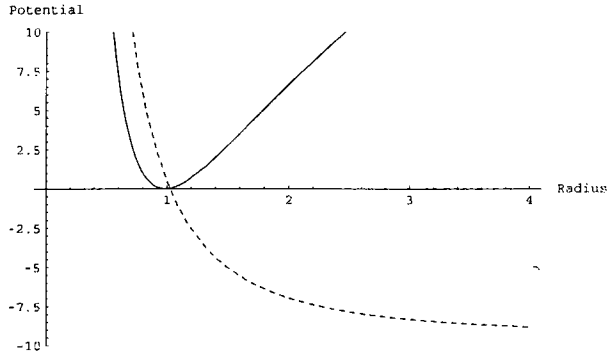
Figure 3.10: Qualitative plot of the normalized potential function vs normalized width showing trapping of the beam. Dotted line gives the linear case.

The potential function is plotted for different nonlinearity regimes. When the nonlinearity is of defocusing nature, i.e., when the value of β is positive, the beam diffracts even more than that of the linear case (Fig. 3.8). Now, for intermediately high focusing nonlinearity (β negative), a potential well is formed (Fig. 3.9). When the nonlinearity is sufficiently high, the potential well degenerates into a single point as in Fig. 3.10. In all these cases dissipation is considered to be very low. For the case $\alpha = 0$, our variational results reproduce the earlier result obtained by Shih et al.[15]

3.5   Numerical Analysis

In this section, we confirm our analytical solutions by numerical simulations. The system represented by Eq. (3.17) was studied numerically using the finite difference beam propagation method. A 10 μm beam is propagated through different PR polymers with a wide range of absorption coefficients. The polymers with their absorption coefficients are given in table 3.1.[9] The material parameters of the polymers are chosen as $m = 2$, $N_{ch} = 1.27 \times 10^{21} cm^{-3}$, $\mu_d = 1.83 \times 10^{-29} cm$, $\triangle \alpha = 3.9 \times 10^{-23}$, $T_a = 300K$ and $E_0 = 70V/\mu m$. The propagation of the beam does not change even when the absorption coefficient is as high as $200 cm^{-1}$ (Fig. 3.11). The beam maintains its shape and thus propagates as a stable soliton. The beam propagates a distance of 10 ζ in the normalized coordinates. This corresponds to 3 cm (10 diffraction length) of propagation through the PR polymer in the normal units.
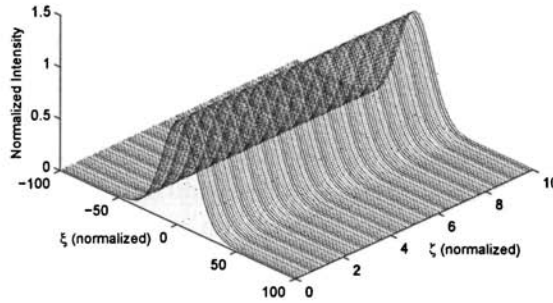
Figure 3.11: Soliton propagation through the PR polymer 1. The soliton propagates 3 cm through the material which corresponds to 10 diffraction length.

Sl. No	Name	wavelength (nm)	$\alpha_0(cm^{-1})$
NLO			
polymers	BisA-NAS:		
1	29DEH	650	200
Inert			
polymer host	PMMA:33		
2	DTNBI:0.2C60	676	20
3	PC:20NPP:30		
	TTA:0.25C60	633	0.4
4	PMMA:30DPDCP:		
	15TPD:0.3C60	676	2

Table 3.1: Absorption coefficient of some photorefractive polymers

3.6 Conclusions

We studied the propagation of laser beam through a photorefractive polymer in the presence of linear absorption loss. A spatial instability is shown to occur in this medium. Linear stability analysis was carried out to study the modulational instability of plane waves propagating through the medium. A comparison with the gain spectrum of PR crystal and PR

polymer with no loss is made. Variational method is used to derive a set of ordinary differential equations which describes the propagation of low power laser beam through the PR polymer. The system is then studied numerically. The beam propagates without any shape change for over 10 diffraction length, even when the loss is as high as 200 cm^{-1}. The variational and numerical analysis show the existence of stable solitons in the medium. The fact that PR polymers are relatively inexpensive and are compact enough to meet manufacturing requirements makes them ideal candidates for widespread applications. Additionally, these polymers are compatible with semiconductor laser diode wavelengths (680 nm) which keeps the manufacturing costs of devices lower than previously proposed systems. All applications predicted with the solitons in organic crystals can be realized in a PR polymer.

References

[1] A. Ashkin, G. D. Boyd, J. M. Dziedzic, R. G. Smith, A. A. Ballman, J. J. Levinstein, and K. Nassau, "Optially induced refractive index inhomogenities in linbo3 and litao3," Appl. Phys. Lett. **9**, 72–72 (1966).

[2] L. Solymar, D. J. Webb, and A. Grunnet-Jepsen, *The Physics and Applications of Photorefractive Materials* (Oxford University Press, New York, 1996).

[3] N. V. Kukhtarev, V. B. Markov, S. . G. Odulov, M. S. Soskin, and V. L. Vinetskii, "Holographic storage in electrooptic crystals. i. steady state," Ferroelectrics **22**, 949–960 (1979).

[4] N. V. Kukhtarev, V. B. Markov, S. . G. Odulov, M. S. Soskin, and V. L. Vinetskii, "Holographic storage in electrooptic crystals. ii. beam coupling - light amplification," Ferroelectrics **22**, 961–964 (1979).

[5] K. Sutter, J. Hulliger, and P. Günter, "Photorefractive effects observed in the organic crystal 2-cyclooctylamino-5-nitropyridine doped with 7,7,8,8-tetracyanoquinodimethane," Solid State Commun **74**, 867–870 (1990).

[6] S. Ducharme, J. C. Scott, R. J. Twieg, and W. E. Moerner, "Observation of the photorefractive effect in a polymer," Phys. Rev. Lett **66**, 1846–1849 (1991).

[7] W. Moerner and S. Silence, "Polymeric photorefractive materials," Chem. Rev. **94**, 127–155 (1994).

[8] A. V. Vannikov and A. D. Grishina, "The photorefractive effect in polymeric systems," Russian Chemical Reviews **72**, 471–488 (2003).

[9] W. E. Moerner, A. Grunnet-Jepsen, and C. L. Thompson, "Photorefractive polymers," Annu. Rev. Mater. Sci. **27**, 585–623 (1997).

[10] R. Y. Chiao, E. Garmire, and C. H. Townes, "Self-trapping of optical beams," Phys. Rev. Lett. **13**, 479–482 (1964).

[11] M. Segev, B. Crosignani, A. Yariv, and B. Fischer, "Spatial solitons in photorefractive media," Phys. Rev. Lett. **68**, 923–926 (1992).

[12] M. Segev, G. C. Valley, B. Crosignani, P. DiPorto, and A. Yariv, "Steady-state spatial screening solitons in photorefractive materials with external applied field," Phys. Rev. Lett. **73**, 3211–3214 (1994).

[13] D. N. Christodoulides and M. J. Carvalho, "Bright, dark, and gray spatial soliton states in photorefractive media," J. Opt. Soc. Am. B **12**, 1628–1633 (1995).

[14] G. C. Valley, M. Segev, B. Crosignani, A. Yariv, M. M. Fejer, and M. C. Bashaw, "Dark and bright photovoltaic spatial solitons," Phys. Rev. A **50**, R4457–R4460 (1994).

[15] M.-F. Shih and F.-W. Sheu, "Photorefractive polymeric optical spatial solitons," Opt. Lett **24**, 1853–1855 (1999).

[16] Z. Chen, M. Asaro, O. Ostroverkhova, W. E. Moerner, M. He, and R. J. Twieg, "Self-trapping of light in an organic photorefractive glass," Opt. Lett **28**, 2509–2511 (2003).

[17] S. Ducharme, J. C. Scott, R. J. Twieg, and W. E. Moerner, "Observation of the photorefractive effect in a polymer," Phys. Rev. Lett **66**, 1846–1849 (1991).

[18] P. J. Melz, "Photogeneration in trinitrofluorenone-poly(n-vinylcarbazole)," J. Chem. Phys. **57**, 1694–1699 (1972).

[19] Y. R. Shen, *The Principles of Nonlinear Optics* (Wiley, New York, 2002).

[20] J. M. Bilbaut, P. Marquié, and B. Michaux, "Modulational instability of two counterpropagating waves in an experimental transmission line," Phys. Rev. E **51**, 817–820 (1995).

[21] A. Hasegawa, *Plasma Instabilities and Nonlinear Effects* (Springer, Heidelberg, 1975).

[22] H. He, A. Arraf, C. M. de Sterke, P. D. Drummond, and B. A. Malomed, "Theory of modulational instability in bragg gratings with quadratic nonlinearity," Phys. Rev. E **59**, 6064–6078 (1999).

[23] J. F. Corney and O. Bang, "Complete modulational-instability gain spectrum of nonlinear quasi-phase-matching gratings," J. Opt. Soc. Am. B **21**, 617 621 (2004).

[24] A. Mohamadou and T. C. Kofané, "Modulational instability and pattern formation in discrete dissipative systems," Phys. Rev. E **73**, 046607 (2006).

[25] M. Saffman, D. Montgomery, A. A. Zozulya, K. Kuroda, and D. Z. Anderson, "Transverse instabilty of counterpropagating waves in photorefractive media," Phys. Rev. A **48**, 3209–3215 (1993).

[26] M. I. Carvalho, S. R. Singh, and D. Christodoulides, "Modulational instability of quasi-plane-wave optical beams biased in photorefractive crystals," Opt. Comm. **126**, 167–174 (1996).

[27] R. Boyd, *Nonlinear Optics* (Wiley, New York, 1998), 3rd ed.

[28] N. Zhu, R. Guo, S. Liu, Z. Liu, and T. Song, "Spatial modulation instability in self-defocusing photorefractive crystal LiNbO$_3$:Fe," J. Opt. A: Pure Appl. Opt. **8**, 149154 (2006).

4

Modulational Instability in Photorefractive Crystals in the Presence of Wave Mixing

4.1 Introduction

MODULATIONAL instability (MI) in a photorefractive medium is studied in the presence of two wave mixing. We then propose and derive a model for forward four wave mixing in the photorefractive medium and investigate the modulational instability induced by four wave mixing effects. By using the standard linear stability analysis the instability gain is obtained. This chapter is organized as follows. Section 4.2 gives a general introduction to Holographic solitons. The basic propagation equation for the two wave mixing (TWM) geometry is presented in Section 4.3 and the modulational instability in this geometry is studied. In section 4.4 the governing equations for the forward four wave mixing geometry is presented. The system is studied without using the undepleted pump beam approximation. The standard linear stability analysis for the coupled equations is carried out and the gain spectrum is obtained. Section 4.5 concludes the chapter giving the main observations.

Modulational instability is a universal process in which tiny phase and amplitude perturbations that are always present in a wide input beam grow exponentially during propagation under the interplay between diffraction (in spatial domain) or dispersion (in temporal domain) and nonlinearity. Instabilities and chaos can occur in many types of nonlinear physical systems. Optical instabilities can be classified as temporal and spatial instabilities depending on whether the electromagnetic wave is modulated temporally or spatially after it passes through the medium. Temporal instability has been studied by various authors[1-3] and the first experimental

observation of MI in a dielectric material was in 1986.[4] The temporal MI occurs as an interplay between self-phase modulation and group velocity dispersion. In the spatial domain, diffraction plays the role of dispersion. When both diffraction and dispersion are present simultaneously, it results in spatio-temporal MI.[5] Recently, Wen et al.[6] investigated MI in negative refractive index materials. In a rather loose context, MI can be considered as a precursor of self-trapped beam formation.

In the spatial domain, MI manifests itself as filamentation of a broad optical beam through the spontaneous growth of spatial-frequency sidebands. The MI is a destabilization mechanism for plane waves. It leads to delocalization in momentum space and, in turn, to localization in position space and the formation of self-trapped structures. During MI, small amplitude and phase perturbations tend to grow exponentially as a result of the combined effects of nonlinearity and diffraction. As a result of MI in the spatial domain, a large-diameter optical beam tends to disintegrate during propagation. Castillo et al.[7] have provided experimental evidence of such induced MI in a photorefractive bismuth titanium oxide crystal. Saffman et al.[8] study theoretically and experimentally the modulational instability of broad optical beams in photorefractive media. The MI phenomena has been previously observed in various media like Kerr media,[9] electrical circuits,[10] plasmas,[11] parametric band gap systems,[1] quasi-phase-matching gratings[12] and discrete dissipative systems.[13] The transverse instability of counterpropagating waves in PR media is studied by Saffman et al.[14] From the above investigations, it is clear that the study of MI in a medium is both of fundamental as well as of technological importance.

To introduce the concept of MI, we consider the $(1 + 1)$D nonlinear Schrödinger (NLS) equation and show that this equation exhibits an instability and leads to spatial or temporal modulation of a constant-intensity plane wave. The NLS equation has the form

$$iu_z + \frac{1}{2}u_{xx} \pm |u|^2 u = 0, \qquad (4.1)$$

where u is the amplitude of the beam. The sign of third term is positive for a focusing type of nonlinearity and negative for defocusing nonlinearity.

Equation 4.1 admits plane wave solutions of the form

$$u(z, x) = u_0 \exp[i\phi(z)], \qquad (4.2)$$

where u_0 is a constant and corresponds to the input intensity. Substituting Eq. (4.2) in Eq. (4.1), we get

$$\phi(z) = \pm u_0^2 z. \qquad (4.3)$$

Hence the plane wave solution can be written as

$$u(z, x) = u_0 \exp[\pm i u_0^2 z]. \tag{4.4}$$

Such a solution shows that the plane wave of amplitude u_0 propagates through the nonlinear medium without any change except for acquiring an intensity dependent phase shift. Now, we need to study the stability of these plane waves against small perturbations. For this we use the standard linear stability analysis method, which is an important technique to study the stability of solutions. The method proceeds by first perturbing the plane wave solution in the form

$$u(z, x) = (u_0 + a) \exp[\pm i u_0^2 z], \tag{4.5}$$

where a is a small complex perturbation. Substituting this in Eq. (4.1) and linearizing in a, we get

$$i a_z + \frac{1}{2} a_{xx} \pm (a + a^*) u_0^2 = 0. \tag{4.6}$$

Considering that the perturbation consists of two side bands, we can write

$$a(x, z) = u_1(z) \exp[iKx] + v_1(z) \exp[-iKx]. \tag{4.7}$$

This gives a system of two coupled equations in u_1 and u_2 as

$$u_{1z} = i\left(-\frac{1}{2} K^2 \pm u_0^2 \right) u_1 \pm i u_0^2 v_1^*, \tag{4.8}$$

$$v_{1z}^* = \mp i u_0^2 u_1 + i\left(\frac{1}{2} K^2 \mp u_0^2 \right) v_1^*. \tag{4.9}$$

The above coupled equations can be written in the compact matrix form as

$$\partial_z \underline{X} = \mathbf{M} \underline{X}, \tag{4.10}$$

where $\mathbf{M}$ is a 2x2 matrix given by

$$\mathbf{M} = \begin{pmatrix} a_{11} & a_{22} \\ a_{33} & a_{44} \end{pmatrix}, \tag{4.11}$$

and

$$a_{11} = i\left(-\frac{1}{2} K^2 \pm u_0^2 \right), \tag{4.12}$$

$$a_{22} = \pm i u_0^2, \tag{4.13}$$

$$a_{33} = \mp i u_0^2, \tag{4.14}$$

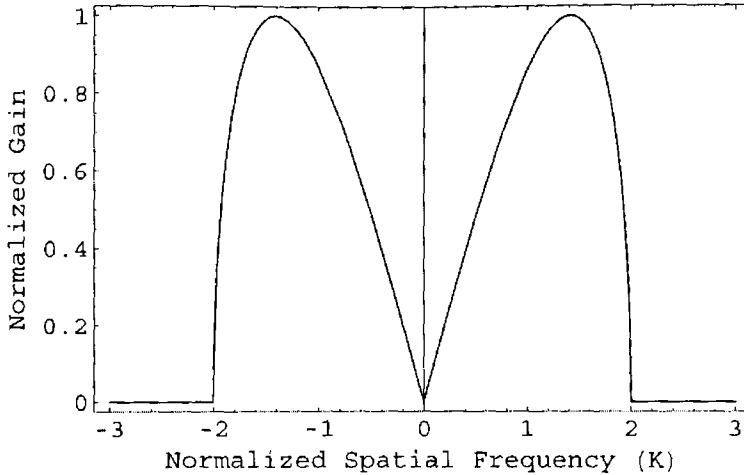$$a_{44} = i\left(\frac{1}{2} K^2 \mp u_0^2 \right). \tag{4.15}$$

Figure 4.1: Gain spectrum for $u_0 = 1$ for a focusing nonlinearity.

This equation has a nontrivial solution only if the determinant of the matrix vanishes. The real part of the eigenvalues of the stability matrix in Eq. (4.11) gives the gain associated with the system.[15] The eigenvalues are given by the following relation

$$\Lambda_{\pm} = \pm \frac{1}{2}(-K^4 \pm 4K^2 u_0^2)^{1/2}. \qquad (4.16)$$

For $\Lambda > 0$, the perturbation grows exponentially during propagation with the growth rate or gain given by $Re[\Lambda]$, indicating MI. Equation 4.16 shows that the continuous wave solution is absolutely stable only in the case of a self-defocusing nonlinearity. The solution is unstable in the case of self-focusing nonlinearity. The gain spectrum of modulational instability in the case of focusing nonlinearity is shown in Fig. 4.1 for $u_0 = 1$.

Four wave mixing in the phase conjugate geometry is widely used in photorefractive materials for various applications. It can be used to implement several different computing functions,[16] optical interconnects,[17] matrix addition,[18] and optical correlator.[19] Nonlinear solutions for photorefractive vectorial two-beam coupling and for forward phase conjugation in photorefractive crystals has been found in.[20] Recently Jia et al.[21] experimentally demonstrated degenerate, forward four-wave mixing effects in a self-defocusing PR medium, in both one and two transverse dimensions. They observed the nonlinear evolution of new modes as a function

of propagation distance, in both the near-field and far-field (Fourier space) regions.

4.2   Holographic solitons

Recently, a new kind of spatial solitons, holographic (HL) solitons was proposed by Cohen et al.[22] They are formed when the broadening tendency of diffraction is balanced by phase modulation that is due to Bragg diffraction from the induced grating. Holographic solitons are solely supported by cross-phase modulation arising from the induced grating, not involving self-phase modulation at all. In 2006,[23] they showed that the nonlinearity in periodically poled photovoltaic photorefractives can be solely of the cross phase modulation type. The effects of self-phase modulation and asymmetric energy exchange, which exist in homogeneously poled photovoltaic photorefractives, can be considerably suppressed by the periodic poling. They demonstrated numerically that periodically poled photovoltaic photorefractives can support Thirring-type (solitons which exist only by virtue of cross phase modulation) (holographic) solitons. HL solitons in PR dissipative medium was studied by Liu.[24] Existence of HL solitons in a grating mediated waveguide was studied by Freedman et al.[25]

A spatial soliton is formed in a nonlinear medium when the optical beam modifies the refractive index of the medium in such a way that it induces a positive lens. As a result, the change in refractive index at the center of the beam is greater than that at its margins. The refractive index structure resembles that of a graded index waveguide. The beam then gets self-trapped and thus forms a spatial soliton. The mechanism responsible for this is the self-focusing effect. Another mechanism that can support spatial solitons arises from the nonlinear phase coupling that results from symmetric energy exchange between two or more mutually coherent beams.

One such example is the quadratic solitons. Quadratic solitons form by the mutual trapping and locking of multiple-frequency waves. The light does not change the refractive index in the case of quadratic nonlinearity of a noncentrosymmetric media. The nonlinear effects are observed when the fundamental frequency becomes phase matched with one of its harmonics. The simplest case corresponds to the process of second harmonic generation (SHG) or optical parametric generation (OPG), where a fundamental frequency wave and its second-harmonic generate each other.
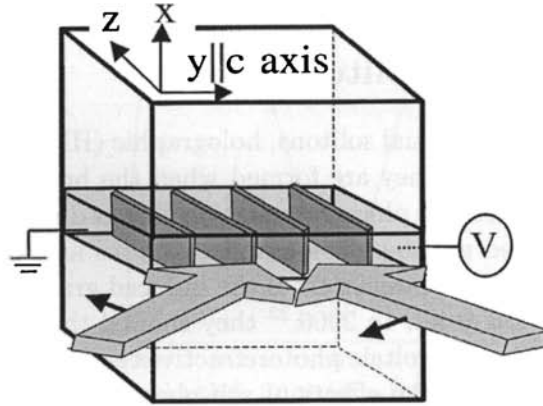
Figure 4.2: Schematic of a HL soliton in a PR medium[22]

The resulting soliton contains both the fundamental and harmonic fields, which in the simplest case exhibit a classical bell-shape. Solitons form when the material and light propagation conditions inside the quadratic nonlinear crystal are set so that the diffraction and dispersion lengths that measure the spreading of the beams and pulses, and the nonlinear length that measures the strength of the frequency conversion process, are comparable. Each beam continuously loses some of its energy and regains the same amount, such that the net power in each beam is conserved. In this interaction, the field that constitutes the acquired energy (to each of the beams) is phase retarded relative to the primary field of each beam. Thus, as the acquired field is added to the primary field, it effectively slows the phase velocity of the beam. Hence, if the interaction occurs in such a way that the effect is more intense at the center of the beam (or for the lowest spatial frequencies of the beam), then it reduces or eliminates the broadening effects of diffraction.

Such a phase coupling between two mutually coherent beams can be induced through a grating in the refractive index produced by the interference of the two beams. This is the case in HL solitons. Fig. 4.2 shows the schematic representation of the configuration for the existence of HL solitons.[22] Such a soliton is created in the absence of the self-action effect, solely due to the beam cross-coupling through the induced Bragg reflection. Salgueiro et al.[26] studied the composite spatial solitons supported by

mutual beam focusing in a Kerr-like nonlinear medium in the absence of the self-action effects. They predicted the existence of continuous families of single and two-hump composite solitons, and studied their stability and interaction. In 2007, two-dimensional holographic photovoltaic bright spatial solitons were observed in a $Cu:K_{0.25}Na_{0.75}Sr_{1.5}Ba_{0.54}Nb_5O_{15}$ crystal in which two coherent laser beams, a signal beam, as well as a strong and uniform pump beam at 532 nm are coupled to each other via two-wave mixing.[27]

In the case of a HL dissipative soliton, one beam acts as a pump beam to supply energy for the other beam, which behaves as the signal beam. In such a system the two beam coupling results in an asymmetric energy exchange between the two beams such that energy is transferred from the pump beam into the signal beam. There is a double balance occurring here: diffraction is balanced by nonlinearity and loss is balanced by the gain due to the asymmetric energy transfer. But only the signal beam can propagate as a soliton. Both the bright and dark HL dissipative solitons[28] have been studied.

4.3 Two wave mixing geometry

The periodic variation of intensity due to interference of two beams of coherent electromagnetic radiation inside a PR material results in the formation of a volume index grating. The presence of this grating affects the propagation of these two beams. Due to perfectly phase-matched Bragg scatterings, the two beams are strongly diffracted by the index grating. Fig. 4.3 shows the Bragg scattering of the two beams due to the volume index grating. Beam 1 is scattered by the grating and it propagates along the direction of beam 2. Similarly beam 2 is scattered and it propagates along the direction of beam 1.

In this section, we present the derivation of the model equation for the TWM geometry[29,30] and study the MI in it. Consider the interaction of two laser beams inside a photorefractive medium (see Fig. 4.3). A stationary interference pattern is formed, if the two beams are of the same frequency.
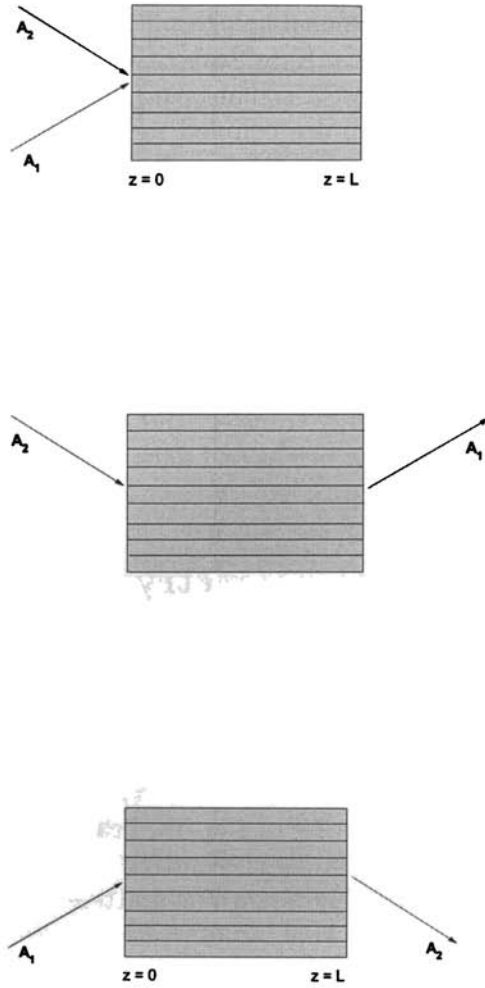
Figure 4.3: Bragg scattering from the gratings formed in PR media. Grating induced by the pair of beams (top). Beam A_2 is diffracted by the grating producing beam A_1 (middle). Beam A_1 is diffracted by the grating producing beam A_2 (bottom).

Let the electric field of the two beams be written as

$$E_j = A_j \exp[i(\omega t - \mathbf{k}_j.\mathbf{r})], \text{ for } j = 1, 2. \tag{4.17}$$

Here, A_1 and A_2 are the amplitudes, ω is the angular frequency, and $\mathbf{k}_1$ and $\mathbf{k}_2$ are the wave vectors.

The medium is assumed to be isotropic and both beams are polarized perpendicular to the plane of incidence. The total intensity of the beams is

$$I = |E|^2 = |E_1 + E_2|^2, \tag{4.18}$$

which can be expressed as

$$I = |A_1|^2 + |A_2|^2 + A_1 A_2^* \exp[i\mathbf{K}.\mathbf{r}] + A_2 A_1^* \exp[-i\mathbf{K}.\mathbf{r}], \tag{4.19}$$

where

$$\mathbf{K} = \mathbf{k}_2 - \mathbf{k}_1.$$

The magnitude of the vector $\mathbf{K}$ is $2\pi/\Lambda$ where Λ is the period of the fringe pattern.

Eq. 4.19 represents a spatial variation of optical energy in the photorefractive medium. Such an intensity pattern will generate and redistribute charge carriers. As a result, a space charge field is created in the medium. This field induces an index volume grating via the Pockels effect. In general, the index grating will have a spatial phase shift relative to the interface pattern.

The index of refraction including the fundamental component of the intensity-induced gratings can be written as

$$n = n_0 + \left[\frac{n_1 A_1^* A_2}{2I_0} \exp[i\phi] \exp[-i\mathbf{K}.\mathbf{r}] + \text{cc} \right], \tag{4.20}$$

where n_0 is the index of refraction when no light is present, ϕ is real and n_1 is a real and positive number. The wave equation reduces to the Helmholtz equation for highly monochromatic waves like laser beams which can be viewed as a superposition of many monochromatic plane waves with almost identical wave vectors

$$\nabla^2 E + \omega^2 n^2 E/c^2 = 0, \tag{4.21}$$

where $E = E_1 + E_2$.

Now let

$$E_j = A_j(x, y, z) \exp[i\omega t - i\beta_j z].$$

Here $A(x, y, z)$ is the complex amplitude that depends on position, β_1 and β_2 are the z component of the wave vectors $\mathbf{k}_1$ and $\mathbf{k}_2$ inside the medium respectively and z is measured along the central direction of propagation. We solve for the steady state so that A_j is taken to be time independent.

$$\left(\frac{\partial^2}{\partial x^2} + \frac{\partial^2}{\partial y^2} + \frac{\partial^2}{\partial z^2} + \omega^2 n^2/c^2\right) E = 0. \tag{4.22}$$

Substituting Eq. (4.20) and solving by neglecting the second order term n_1^2 and using the fact that for highly directional monochromatic waves with $a >> \lambda$, $\partial^2 A/\partial z^2$ can be neglected and we get

$$2i\beta_1 \frac{\partial A_1}{\partial z} = \nabla_\perp^2 A_1 + \frac{\omega^2 n_0 n_1}{c^2 I_0} e^{-i\phi} A_2^* A_2 A_1, \tag{4.23}$$

and

$$2i\beta_2 \frac{\partial A_2}{\partial z} = \nabla_\perp^2 A_2 + \frac{\omega^2 n_0 n_1}{c^2 I_0} e^{-i\phi} A_1^* A_1 A_2. \tag{4.24}$$

Now for the case when the two laser beams enter the medium from the same side at $z = 0$

$$\beta_1 = \beta_2 = k \cos\theta = \frac{2\pi}{\lambda} n_0 \cos\theta.$$

Here, 2θ is the angle between the beams inside the medium. Simplifying we obtain

$$i\frac{\partial A_1}{dz} = \frac{1}{2k\cos\theta} \nabla_\perp^2 A_1 + \frac{\Gamma}{2I_0} A_1 |A_2|^2, \tag{4.25a}$$

$$i\frac{\partial A_2}{dz} = \frac{1}{2k\cos\theta} \nabla_\perp^2 A_2 + \frac{\Gamma}{2I_0} A_2 |A_1|^2, \tag{4.25b}$$

where

$$\Gamma = \frac{2\pi n_1}{\lambda \cos\theta} e^{-i\phi}, \tag{4.26}$$

is the complex coupling coefficient. A similar model was used to study the existence of Holographic solitons.[22]

A prerequisite for obtaining Holographic focusing is that the induced grating be in phase with the intensity grating. If it is shifted by π, then the grating leads to holographic defocusing. If it is $\pm\pi/2$ phase shifted with respect to the intensity grating, then the interaction will yield an asymmetric energy exchange between the two beams beacuse of the two

beam coupling property of the photorefractive material. Therefore, $\phi = 0$ for the existence of bright solitons. This gives the coupling constant as

$$\Gamma = \frac{2\pi n_1}{\lambda \cos\theta}. \tag{4.27}$$

The next step is to study the propagation of a broad optical beam through the PR medium. We study MI of a one dimensional broad optical beam. Hence the y dependent term in the transverse Laplacian in Eq. (4.25) can be neglected. For a broad optical beam, the diffraction term in Eq. (4.25) can be set to zero giving the steady state solutions as

$$A_j = \sqrt{P} \exp\left[-i\frac{\Gamma P}{2I_0}z\right], \tag{4.28}$$

for $j = 1, 2$.

To study MI, we consider small perturbations of the steady state solutions as

$$A_j = (\sqrt{P} + a_j)\exp\left[-i\frac{\Gamma P}{2I_0}z\right]. \tag{4.29}$$

Substituting in Eq. (4.25) and neglecting the quadratic and higher order terms in a_j, the perturbations a_1 and a_2 are found to satisfy the following linearized set of two coupled equations :

$$i\frac{\partial a_1}{\partial z} = \frac{1}{2k\cos\theta}\frac{\partial^2 a_1}{\partial x^2} + \frac{\Gamma P}{2I_0}(a_2 + a_2^*), \tag{4.30}$$

$$i\frac{\partial a_2}{\partial z} = \frac{1}{2k\cos\theta}\frac{\partial^2 a_2}{\partial x^2} + \frac{\Gamma P}{2I_0}(a_1 + a_1^*). \tag{4.31}$$

It is important to note that the evolution of the perturbations depend solely on the cross phase modulation. To solve Eq. (4.30) and Eq. (4.31), we assume that the perturbations be composed of two side bands :

$$a_j(x, z) = U_j(z)\exp[i\kappa x] + V_j(z)\exp[-i\kappa x]. \tag{4.32}$$

The substitution of Eq. (4.32) in Eqs. (4.30) and Eq. (4.31) results in a set of four homogeneous equations in U_1, U_2, V_1 and V_2 as

$$\frac{\partial U_1}{\partial z} = i\frac{\kappa^2}{2k\cos\theta}U_1 - i\frac{\Gamma P}{2I_0}(U_2 + V_2^*), \tag{4.33}$$

$$\frac{\partial V_1^*}{\partial z} = -i\frac{\kappa^2}{2k\cos\theta}V_1^* + i\frac{\Gamma P}{2I_0}(U_2 + V_2^*), \tag{4.34}$$

$$\frac{\partial U_2}{\partial z} = i\frac{\kappa^2}{2k\cos\theta}U_2 - i\frac{\Gamma P}{2I_0}(U_1 + V_1^*), \tag{4.35}$$

$$\frac{\partial V_2^*}{\partial z} = -i\frac{\kappa^2}{2k\cos\theta}U_1 + i\frac{\Gamma P}{2I_0}(U_1 + V_1^*). \tag{4.36}$$
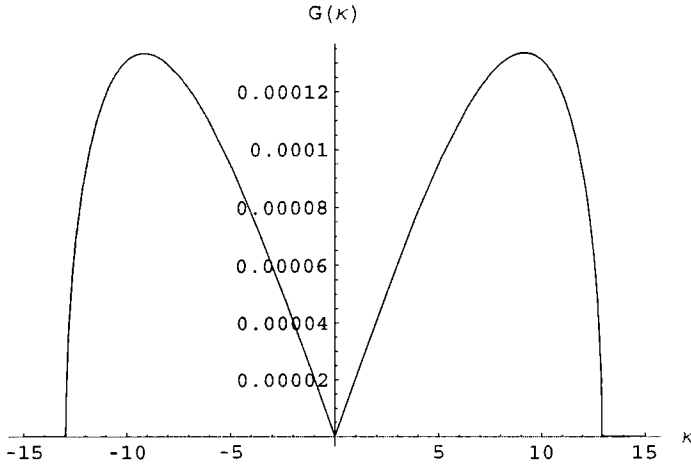
Figure 4.4: Growth rate as a function of spatial frequency for the two wave mixing geometry.

This set has a nontrivial solution only if the determinant of the coefficient matrix vanishes. The eigenvalues of the system are obtained as

$$\Lambda 1_{\pm} = \pm \frac{1}{2A} \left(\frac{-I_0 \kappa^4 - 2A\Gamma P \kappa^2}{I_0} \right)^{1/2}, \tag{4.37}$$

$$\Lambda 2_{\pm} = \pm \frac{1}{2A} \left(\frac{-I_0 \kappa^4 + 2A\Gamma P \kappa^2}{I_0} \right)^{1/2}, \tag{4.38}$$

where $A = k \cos \theta$. The plane wave solution is stable if perturbations at any wave number κ do not grow with propagation. This is the case as long as κ is imaginary. MI gain will exist only when $Re[\Lambda] > 0$. This condition is satisfied only by the second set of eigenvalues. The gain associated with the system is given by

$$\mathbf{G} = |\Re(\Lambda_{\pm})|. \tag{4.39}$$

A typical plot of the gain spectrum is given in Fig. 4.4. We consider the case of BaTiO$_3$ crystal with a space charge field of 10^4V/m, electro-optic coefficient $r_{42} = 1640 \times 10^{-12}$m/V and refractive index $n = 2.4$ which gives a coupling constant $\Gamma = 20$ cm^{-1}. Fig. 4.5 gives the variation of gain with the angle θ. The gain increases with decrease in angle.
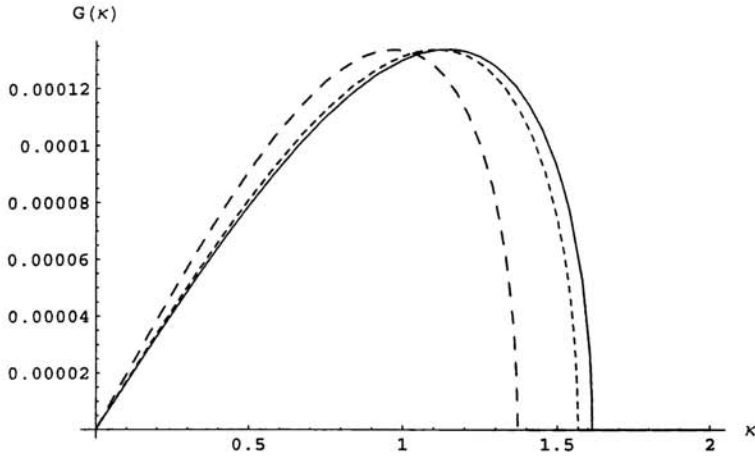
Figure 4.5: Variation of gain with respect to the angle between the two beams. The lowermost curve is for $\theta = \pi/4$, the dotted curve is for $\pi/8$ and the topmost curve is for $\pi/16$.
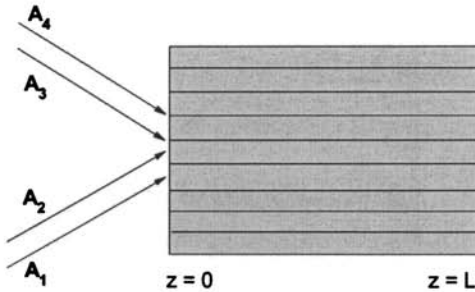

Figure 4.6: Forward four wave mixing in photorefractive media in the transmission geometry.

4.4   Forward four wave mixing geometry

In the two wave mixing case, two coherent beams interfere inside a photorefractive medium and produce a volume index grating. In the case of optical phase conjugation, using four-wave mixing, a third beam is incident at the Bragg angle from the opposite side and a fourth beam is generated. Now we consider the situation in which the third beam is incident from the front at the Bragg angle and a diffracted beam is generated. That is we consider the interaction of four beams in a PR medium in the forward geometry. We assume that all the beams have the same frequency ω. We propose a model for the observation of MI in a PR medium induced by four wave mixing. The method proceeds by first writing the four coupled equations for the present geometry. Of the four beams, let beams A_2 and A_3 be the pump beam, A_1 be the signal beam and A_4 be the generated beam. Beam A_1 is coherent with beam A_2 and beam A_3 is coherent with beam A_4. Thus the index grating consists of two contributions : $A_1^* A_2$ and $A_3^* A_4$. The index of refraction including the fundamental component of the intensity-induced gratings can thus be written as

$$n = n_0 + \left[\frac{n_1 (A_1^* A_2 + A_3^* A_4)}{2I_0} \exp[i\phi] \exp[-i\mathbf{K}.\mathbf{r}] + \text{cc} \right], \qquad (4.40)$$

where $\mathbf{k}_2 - \mathbf{k}_1 = \mathbf{k}_4 - \mathbf{k}_3 = \mathbf{K}$.
    We have

$$E = \sum_{j=1}^{4} E_j, \qquad (4.41)$$

and

$$n^2 = \frac{n_0 n_1 (A_1^* A_2 + A_3^* A_4)}{I_0} \exp[i\phi] \exp[-i\mathbf{K}.\mathbf{r}] + \text{cc}. \qquad (4.42)$$

This gives

$$\nabla^2 E = \sum_{j=1}^{4} \left(\frac{\partial^2 A_j}{\partial z^2} - 2i\beta_j \frac{\partial A_j}{\partial z} - A_j \beta_j^2 + \frac{\partial^2 A_j}{\partial x^2} \right) \exp[i(\omega t - \beta_j.r)]. \quad (4.43)$$

Substituting the above equations in Eq. (4.21) gives

$$
\frac{\partial^2 A_1}{\partial x^2} \exp[-i\beta_1 z] + \frac{\partial^2 A_2}{\partial x^2} \exp[-i\beta_2 z] + \frac{\partial^2 A_3}{\partial x^2} \exp[-i\beta_3 z]
$$

$$
+ \quad \frac{\partial^2 A_4}{\partial x^2} \exp[-i\beta_4 z] - 2i\beta_1 \frac{\partial A_1}{\partial z} \exp[-i\beta_1 z] - 2i\beta_2 \frac{\partial A_2}{\partial z} \exp[-i\beta_2 z]
$$

$$
- \quad 2i\beta_3 \frac{\partial A_3}{\partial z} \exp[-i\beta_3 z] - 2i\beta_4 \frac{\partial A_4}{\partial z} \exp[-i\beta_4 z]
$$

$$
= \quad -\frac{\omega^2 n_0 n_1}{c^2 I_0}\{(A_1^* A_2 + A_3^* A_4)\exp[i\phi]\exp[-i\mathbf{K.r}] + c.c\}. \qquad (4.44)
$$

Multiplying Eq. (4.44) with $\exp[i\beta_2 z]$ and equating the coefficients, we get the following four coupled equations for the present geometry:

$$
i\frac{\partial A_1}{dz} = \frac{1}{2k\cos\theta}\nabla_\perp^2 A_1 + \frac{\Gamma}{2I_0}(A_1 A_2^* + A_3 A_4^*)A_2, \qquad (4.45a)
$$

$$
i\frac{\partial A_2}{dz} = \frac{1}{2k\cos\theta}\nabla_\perp^2 A_2 + \frac{\Gamma}{2I_0}(A_1^* A_2 + A_3^* A_4)A_1, \qquad (4.45b)
$$

$$
i\frac{\partial A_3}{dz} = \frac{1}{2k\cos\theta}\nabla_\perp^2 A_1 + \frac{\Gamma}{2I_0}(A_1 A_2^* + A_3 A_4^*)A_4, \qquad (4.45c)
$$

$$
i\frac{\partial A_4}{dz} = \frac{1}{2k\cos\theta}\nabla_\perp^2 A_2 + \frac{\Gamma}{2I_0}(A_1^* A_2 + A_3^* A_4)A_3, \qquad (4.45d)
$$

where $I_0 = I_1 + I_2 + I_3 + I_4$ and $\beta_1 = \beta_2 = \beta_3 = \beta_4 = k\cos[\theta]$.

The model permits plane wave solutions of the form $A_j(x,z) = \sqrt{P}\exp[-i\frac{\Gamma P}{2I_0}z]$. The next step is to carry out a linear stability analysis of the plane wave solutions. For this the plane wave solution is perturbed as

$$
A_j = (\sqrt{P} + a_j(x,z))\exp\left[-i\frac{\Gamma P}{2I_0}z\right], \qquad (4.46)
$$

where a_j is a small complex perturbation. Inserting this into the coupled Eq. (4.45) and linearizing around the solution yields the equations for the perturbations:

$$
i\frac{\partial a_1}{\partial z} = -\frac{\Gamma P}{2I_0}a_1 + \frac{1}{2k\cos\theta}\frac{\partial^2 a_1}{\partial x^2} + \frac{\Gamma P}{2I_0}(2a_2 + a_2^* + a_3 + a_4), \qquad (4.47)
$$

$$
i\frac{\partial a_2}{\partial z} = -\frac{\Gamma P}{2I_0}a_2 + \frac{1}{2k\cos\theta}\frac{\partial^2 a_2}{\partial x^2} + \frac{\Gamma P}{2I_0}(2a_1 + a_1^* + a_3^* + a_4), \qquad (4.48)
$$

$$
i\frac{\partial a_3}{\partial z} = -\frac{\Gamma P}{2I_0}a_3 + \frac{1}{2k\cos\theta}\frac{\partial^2 a_3}{\partial x^2} + \frac{\Gamma P}{2I_0}(a_1 + a_2^* + 2a_4 + a_4^*), \qquad (4.49)
$$

$$i\frac{\partial a_4}{\partial z} = -\frac{\Gamma P}{2I_0}a_4 + \frac{1}{2k\cos\theta}\frac{\partial^2 a_4}{\partial x^2} + \frac{\Gamma P}{2I_0}(a_1^* + a_2 + 2a_3 + a_3^*). \qquad (4.50)$$

Now, we assume that the spatial perturbation $a(x,z)$ is composed of two side band plane waves, i.e

$$a_j(x,z) = U_j(z)\exp[i\kappa x] + V_j(z)\exp[-i\kappa x]. \qquad (4.51)$$

Substituting we get eight homogeneous equations as

$$\frac{\partial U_1}{\partial z} = -i(-\frac{\Gamma P}{2I_0} - \frac{\kappa^2}{2k\cos\theta})U_1 - i\frac{\Gamma P}{2I_0}(2U_2 + V_2^* + U_3 + V_4^*) \qquad (4.52a)$$

$$\frac{\partial U_2}{\partial z} = -i(-\frac{\Gamma P}{2I_0} - \frac{\kappa^2}{2k\cos\theta})U_2 - i\frac{\Gamma P}{2I_0}(2U_1 + V_1^* + V_3^* + U_4) \qquad (4.52b)$$

$$\frac{\partial U_3}{\partial z} = -i(-\frac{\Gamma P}{2I_0} - \frac{\kappa^2}{2k\cos\theta})U_3 - i\frac{\Gamma P}{2I_0}(U_1 + V_2^* + 2U_4 + V_4^*) \qquad (4.52c)$$

$$\frac{\partial U_4}{\partial z} = -i(-\frac{\Gamma P}{2I_0} - \frac{\kappa^2}{2k\cos\theta})U_4 - i\frac{\Gamma P}{2I_0}(V_1^* + U_2 + 2U_3 + V_3^*) \qquad (4.52d)$$

$$\frac{\partial V_1^*}{\partial z} = i(-\frac{\Gamma P}{2I_0} - \frac{\kappa^2}{2k\cos\theta})V_1^* + i\frac{\Gamma P}{2I_0}(2V_2^* + U_2 + V_3^* + U_4), \qquad (4.52e)$$

$$\frac{\partial V_2^*}{\partial z} = i(-\frac{\Gamma P}{2I_0} - \frac{\kappa^2}{2k\cos\theta})V_2^* + i\frac{\Gamma P}{2I_0}(2V_1^* + U_1 + U_3 + V_4^*), \qquad (4.52f)$$

$$\frac{\partial V_3^*}{\partial z} = i(-\frac{\Gamma P}{2I_0} + \frac{\kappa^2}{2k\cos\theta})V_3^* + i\frac{\Gamma P}{2I_0}(V_1^* + U_2 + 2V_4^* + U_4), \qquad (4.52g)$$

$$\frac{\partial V_4^*}{\partial z} = i(-\frac{\Gamma P}{2I_0} - \frac{\kappa^2}{2k\cos\theta})V_4^* + i\frac{\Gamma P}{2I_0}(U_1 + V_2^* + 2V_3^* + U_3). \qquad (4.52h)$$

The eight coupled equations obtained above can be written in a compact matrix form as, $\partial_z \underline{X} = \mathbf{M}\underline{X}$, where $\mathbf{M}$ is an 8x8 matrix with $\underline{X} = [U_1\ U_2\ U_3\ U_4\ V_1^*\ V_2^*\ V_3^*\ V_4^*]^T$.

This system has a nontrivial solution only if the determinant of the matrix vanishes. The real part of the eigenvalues of the stability matrix of Eq. (4.52) gives the gain associated with the system.[15] Out of the eight roots of the system, only the root with maximum positive value contributes to the MI gain. Here only the eigenvalue given by

$$\Lambda 2_\pm = \pm\frac{1}{2A}\left(\frac{-I_0\kappa^4 + 4A\Gamma P\kappa^2}{I_0}\right)^{1/2}, \qquad (4.53)$$

contributes to the MI of the system.

We note that the gain vanishes for all values of κ greater than $\kappa_{max}^2 = 4A\Gamma P/I_0$. Defining $\gamma = \Gamma P/I_0$, we can rewrite the gain as

$$\frac{G}{\gamma} = \sqrt{4\left(\frac{\kappa}{\kappa_{max}}\right)^2\left(1 - \left(\frac{\kappa}{\kappa_{max}}\right)^2\right)}. \qquad (4.54)$$
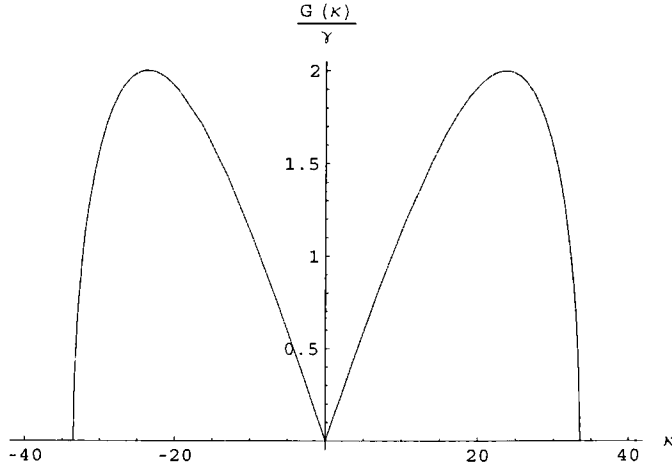

Figure 4.7: A typical plot showing the gain spectrum of the system in the forward four wave mixing process with respect to the spatial perturbation κ.

The variation of the gain coefficient in the forward four wave mixing process with respect to the spatial perturbation is plotted in Fig. 4.7. Such instabilities are useful for pattern formation. A transverse modulation instability of a single beam or counterpropagating beams is a general mechanism that leads to pattern formation in nonlinear optics.[31,32] We expect that similar results will be obtained using the present geometry.

4.5   Conclusions

We first studied MI occurring in a PR medium in the two wave mixing geometry and further modeled the forward four wave mixing occurring in a PR medium and studied MI in this geometry. In both the cases, the geometry is such that the nonlinear effect is manifested through holographic focusing. MI does not rely on self-phase-modulation self-focusing

but results only by virtue of the competition between induced periodic modulation of the refractive index and diffraction of the beam. The MI gain spectrum is obtained for both two wave mixing and forward four wave mixing geometry. Such instabilities will be useful for pattern formation. Photorefractive materials are attractive for the studies of pattern formation as their slow time constant gives the possibility of observing the spatiotemporal dynamics of the system in real time. This also reduces the demands on experimental equipment where speed is often a crucial parameter. Another advantage of photorefractive pattern formation is that patterns can be observed using optical powers of tens of mW. In contrast, pattern formation using other nonlinearities require optical powers in the order of 1W.

References

[1] H. He, A. Arraf, C. M. de Sterke, P. D. Drummond, and B. A. Malomed, "Theory of modulational instability in bragg gratings with quadratic nonlinearity," Phys. Rev. E **59**, 6064-6078 (1999).

[2] G. P. Agrawal, P. L. Baldeck, and R. R. Alfano, "Modulational instability induced by cross-phase modulation in optical fibers," Phys. Rev. A **39**, 3406–3413 (1989).

[3] R. Ganapathy and V. C. Kuriakose, "Cross-phase modulational instability in an elliptical birefringent fiber with higher order nonlinearity and dispersion," Pramana J. Phys **58**, 669–684 (2002).

[4] K. Tai, A. Hasegawa, and A. Tomita, "Observation of modulational instability in optical fibers," Phys. Rev. Lett. **56**, 135–138 (1986).

[5] L. W. Liou, X. D. Cao, C. J. McKinstrie, and G. P. Agrawal, "Spatiotemporal instabilities in dispersive nonlinear media," Phys. Rev. A **46**, 4202–4208 (1992).

[6] S. Wen, Y. Wang, W. Su, Y. Xiang, X. Fu, and D. Fan, "Modulation instability in nonlinear negative-index material," Phys. Rev. E **73**, 036617 (2006).

[7] M. D. Iturbe-Castillo, M. Torres-Cisneros, J. J. Sanchez-Mondragon, S. Chavez-Cerda, S. I. Stepanov, V. A. Vysloukh, and G. E. Torres-Cisneros, "Experimental evidence of modulation instability in a photorefractive $Bi_{12}TiO_{20}$ crystal," Opt. Lett. **20**, 1853–1855 (1995).

[8] M. Saffman, G. McCarthy, and W. Królikowski, "Two-dimensional modulational instability in photorefractive media," J. Opt. B: Quantum Semiclass. Opt. **6**, S397–S403 (2004).

[9] Y. R. Shen, *The Principles of Nonlinear Optics* (Wiley, New York, 2002).

[10] J. M. Bilbaut, P. Marquié, and B. Michaux, "Modulational instability of two counterpropagating waves in an experimental transmission line," Phys. Rev. E **51**, 817–820 (1995).

[11] A. Hasegawa, *Plasma Instabilities and Nonlinear Effects* (Springer, Heidelberg, 1975).

[12] J. F. Corney and O. Bang, "Complete modulational-instability gain spectrum of nonlinear quasi-phase-matching gratings," J. Opt. Soc. Am. B **21**, 617–621 (2004).

[13] A. Mohamadou and T. C. Kofané, "Modulational instability and pattern formation in discrete dissipative systems," Phys. Rev. E **73**, 046607 (2006).

[14] M. Saffman, D. Montgomery, A. A. Zozulya, K. Kuroda, and D. Z. Anderson, "Transverse instabilty of counterpropagating waves in photorefractive media," Phys. Rev. A **48**, 3209–3215 (1993).

[15] R. Boyd, *Nonlinear Optics* (Wiley, New York, 1998), 3rd ed.

[16] P. Yeh and A. E. T. Chiou, "Optical matrix-vector multiplication through four-wave mixing in photorefractive media," Opt. Lett. **12**, 138–140 (1987).

[17] A. Chiou and P. Yeh, "Energy efficiency of optical interconnections using photorefractive holograms," Appl. Opt. **29**, 1111–1117 (1990).

[18] P. Yeh, S. Campbell, and S. Zhou, "Optical implementation of a multiwavelength half-adder," Opt. Lett. **18**, 903–905 (1993).

[19] C. Halvorson, B. Kraabel, A. J. Heeger, B. L. Volodin, K. Meerholz, Sandalphon, and N. Peyghambarian, "Optical computing by use of photorefractive polymers," Opt. Lett. **20**, 76–78 (1995).

[20] B. Fischer, J. . White, M. Cronin-Golomb, and A. Yariv, "Nonlinear vectorial two-beam coupling and forward four-wave mixing in photorefractive materials," Opt. Lett. **11**, 239–241 (1986).

[21] S. Jia, W. Wan, and J. W. Fleischer, "Forward four-wave mixing with defocusing nonlinearity," Opt. Lett. **32**, 1668–1670 (2007).

[22] O. Cohen, T. Carmon, M. Segev, and S. Odoulov, "Holographic solitons," Opt. Lett. **27**, 2031–2033 (2002).

[23] O. Cohen, M. M. Murnane, H. C. Kapteyn, and M. Segev, "Cross-phase-modulation nonlinearities and holographic solitons in periodically poled photovoltaic photorefractives," Opt. Lett. **31**, 954–956 (2006).

[24] J. Liu, "Holographic solitons in photorefractive dissipative systems," Opt. Lett. **28**, 2237–2239 (2003).

[25] B. Freedman, O. Cohen, O. Manela, M. Segev, J. W. Fleischer, and D. N. Christodoulides, "Grating-mediated wave guiding and holographic solitons," J. Opt. Soc. Am. B **22**, 1349–1355 (2005).

[26] J. R. Salgueiro, A. A. Sukhorukov, and Y. S. Kivshar, "Spatial optical solitons supported by mutual focusing," Opt. Lett. **28**, 1457–1459 (2003).

[27] J. Liu, S. Liu, G. Zhang, and C. Wang, "Observation of two-dimensional holographic photovoltaic bright solitons in a photorefractive-photovoltaic crystal," Appl. Phys. Lett. **91**, 111113 (2007).

[28] Z. Hui-Lan and L. Jin-Song, "Evolution and stability of dark holographic solitons in photorefractive dissipative systems," Chin. Phys. Lett. **23**, 2109–2112 (2006).

[29] P. Yeh, *Photorefractive Nonlinear Optics* (Wiley, New York, 1998), 3rd ed.

[30] T. Honda and P. Banerjee, "Threshold for spontaneous pattern formation in reflection-grating-dominated photorefractive media with mirror feedback," Opt. Lett. **21**, 779– (1996).

[31] M. Schwab, C. Denz, and M. Saffman, "Multiple-pattern stability in a photorefractive feedback system," Appl. Phys. B **69**, 429–433 (1999).

[32] O. Sandfuchs, F. Kaiser, and M. R. Belić, "Self-organization and Fourier selection of optical patterns in a nonlinear photorefractive feedback system," Phys. Rev A **64**, 063809 (2001).

5

Self-written waveguide in a methylene blue doped photopolymer

5.1 Introduction

THIS chapter deals with the observation of self-written waveguide inside a bulk Methylene Blue sensitized poly (Vinyl Alcohol)/Acrylamide photopolymer material. We first study the system analytically using the variational method and then demonstrate the formation of a self-wriiten waveguide experimentally. Light from a low power He-Ne laser is focused into the material and the evolution of the beam is monitored. The refractive index of the material is modulated in the region of high intensity due to photobleaching and photopolymerization effects occurring in the material. As a result, the beam propagates through the medium without any diffraction effects. The analytical study predicts stable propagation of two-dimensional laser beam through the material which is in agreement with the experimental observation. We briefly discuss photosensitivity in section 5.1.1. In section 5.1.2, we present the model equation for the beam propagation through the photopolymer and analyze it using the variational method in section 5.2. A potential well formulation is developed. In section 5.3, we present the experimental details. Section 5.4 gives the conclusions.

5.1.1 Photosensitivity

A laser beam when focussed on to the edge of a photosensitive material can write its own waveguide and then get guided by this waveguide.[1] In this process, the beam of light which initially diffracts, changes the refractive index of the medium. As time passes on, the beam dynamically creates

a channel that counteracts diffraction and guides the beam through the material.

Hill et al.,[2] in an experiment in 1977 using germanium-doped optical fiber observed *Hill gratings* which are self-written. These gratings were formed due to the photosensitivity of the glass core to the 488 nm light launched into the core. The refractive index of the glass is increased permanently by illuminating it with ultraviolet light at wavelengths near to 250 nm. This phenomenon is known as photosensitivity. Later, Lam et al.[3] showed that photosensitivity at 488 nm is a two-photon absorption process and it was suggested that self-writing may occur for one-photon wavelength of 244 nm, and this was demonstrated for a grating imprinted via photosensitivity.

Light induced or self-written waveguide formation is a recognized technology by which one can form an optical waveguide as a result of the self-trapping action of a laser beam passed through a converging lens or a single mode fiber. Self-writing is a relatively new and emerging area of research in optics. One of the first evidence of a self-writing process was reported in 1992 by Brocklesby et al.[4] who reported the experimental results on optically written waveguides in ion implanted $Bi_4Ge_3O_{12}$. Independently, Frisken in 1993[5] demonstrated the formation of permanent uptapers in a UV-cured epoxy by a self-induced waveguide, created by exposure to a continuous wave of wavelength 532 nm. Initially the material has a uniform refractive index and the light is confined in two dimensions. In the experiment, the beam of light self-writes the uptaper which guides it through the epoxy, and as the index changes are long-lasting, uptapers written in this way can subsequently be used at other wavelengths. Since then, the phenomenon of self-writing has been reported in a number of photosensitive optical materials including UV-cured epoxy, planar chalcogenide glass, germano-silicate glass[1]etc.

The physics of self-writing in all cases is very similar to the physics of spatial solitons[6] which occurs due to the balance between linear diffraction effect and nonlinear self-focusing effect. These waveguides have a number of advantages compared to other methods of fabricating waveguides such as epitaxial growth, diffusion methods and direct writing.

The self-written waveguides so formed are of particular interest as these waveguides can be formed at low power levels and the material response is wavelength sensitive; therefore a weak beam can guide an intense beam at a less photosensitive wavelength.
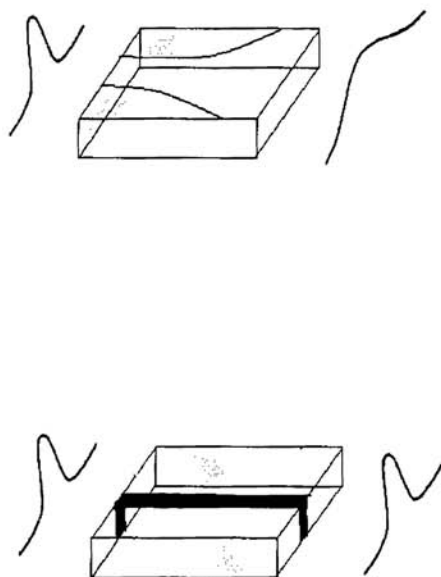
Figure 5.1: Initial diffraction of a beam incident on a photosensitive material (top). Formation of a self-written waveguide (bottom). The beam is guided in the waveguide it creates.

These waveguides evolve dynamically, and they experience minimal radiation losses due to the absence of sharp bends. Many processing steps are needed to form buried waveguides. But, if the buffer layer is transparent at the writing wavelength, self-writing can be used to form these buried waveguides.

Another application of self-written waveguides is in telecommunication. The major obstacles in the widespread use of single mode fibers in the telecommunication industry are the problems associated with effective low cost coupling of light into single mode optical fibers and the incorporation of bulk devices into optical fibers. A self-written waveguide structure induced by laser-light irradiation is considered as a candidate for

convenient coupling technique between the optical fiber and waveguide.[7-9]

Fig. 5.1 gives a schematic diagram of the self-writing process. When a Gaussian intensity is incident on a planar or bulk photosensitive medium, the beam initially diffracts. The refractive index of the medium changes in response to this illumination. A region of raised refractive index is formed along the propagation direction. This then reduces the diffraction of the beam and the beam is confined in the waveguide it creates. This is a self-written waveguide because the beam of light that creates the waveguide is subsequently guided by it.

Polymer optical waveguides have attracted considerable attention for their possible application as optical components in future optical communication systems; because fabricating waveguides from polymers is much easier than fabricating them from inorganic materials.[10-13] In recent years, experiments with photopolymerizable materials have produced promising results. Kewitsch and Yariv[14] demonstrated both experimentally and theoretically, self-trapping and self-focusing in photopolymerizable materials (a liquid diacrylate photopolymer). They observed these phenomena after an initial diffraction period lasting approximately 20s. Friedrich et al.[15] fabricated a directional coupler using a three-dimensional waveguide structure. Recently, Jaeyoun et al.[16] successfully fabricated artificial ommatidia (imaging unit of insect's compound eyes) by use of self-writing and polymer integrated optics. These biomimetic structures were obtained by configuring microlenses to play dual roles for self-writing of waveguides (during the fabrication) and collection of light (during the operation).

In this work, we study the observation of self-writing in a bulk photopolymer (Methylene Blue sensitized poly (Vinyl Alcohol)/Acrylamide (MBPVA/Acrylamide)). When the photopolymer is illuminated with light of appropriate wavelength (632.8 nm), the polymer chains begin to join. The length of these chains determines the density of these polymers. As a result the refractive index of the exposed part of the material changes. The change in refractive index occurs both due to photobleaching of methylene blue and the photopolymerization effect. Photobleaching[17] is a term that applies to techniques of exposing dye-doped materials to light whose wavelength lies within the spectral absorption bands of the composite dye-polymer system. The change in refractive index so produced is much larger than that of traditional nonlinear optical phenomena such as Kerr or photorefractive effects. However, the index change upon illumination is not instantaneous as compared to these two effects.

In recent years, many types of photopolymerizable systems have been developed as holographic recording media.[18-20] These materials have char-

acteristics such as good spectral sensitivity, high resolution, high diffraction efficiency, high signal to noise ratio, temporal stability and processing in real time, which make them suitable for recording holograms. Because of these properties, photopolymer materials are useful in applications such as optical memories, holographic displays, holographic optical elements, optical computing and holographic interferometry.[21,22] The most widely used photopolymer recording medium consists of acrylamide and poly(vinyl alcohol).[23,24] Owing to these properties and its use in holography, we chose MBPVA/Acrylamide for our studies.

5.1.2 Theoretical Model

The photosensitive process in both glasses and polymers occurs slowly relative to the transit time of light inside the material. Hence the evolution of the beam inside the photopolymerizable material can be described by a paraxial wave equation of the form[25]

$$ik_0 n_0 \frac{\partial \mathcal{E}}{\partial Z} + \frac{1}{2}\nabla_\perp^2 \mathcal{E} + k_0^2 n_0 \triangle n \mathcal{E} + \frac{i}{2} k_0 n_0 \alpha \mathcal{E} = 0, \tag{5.1}$$

where k_0 is the free space wave number, $\triangle n$ is the change in refractive index and is time dependent, n_0 is the initial refractive index and α accounts for the attenuation of the beam. The effect of photosensitive refractive index changes on light propagation is given by the third term and that of material loss by the fourth term of Eq. (5.1). For a bulk material, $\nabla_\perp^2 = \partial^2/\partial X^2 + \partial^2/\partial Y^2$ and $\mathcal{E}$ is the amplitude of the electric field.

Several phenomenological models have been proposed for the photosensitivity to account for the observation of refractive index modulation in various photosensitive materials. All the models assume that the refractive index increases upon illumination. Krug et al.[26] used a model of the form

$$\frac{\partial \triangle n}{\partial t} \propto I, \tag{5.2}$$

to describe photosensitivity at 244 nm and showed that it agrees well with the data. A simple model for the evolution of the refractive index is

$$\frac{\partial \triangle n}{\partial t} = A_p I^p, \tag{5.3}$$

which can be used when the index changes are relatively small.

Considering saturation effects in refractive index, it is observed that as the refractive index approaches the saturation value $\triangle n_s$, the increase

in $\triangle n$ slows exponentially. This model has been used for saturation in a photopolymer,[27] and it agrees with the experiments at 488 nm by Hand et al.[28] The phenomenological model for the evolution of refractive index now has the form[28]

$$\frac{\partial \triangle n}{\partial t} = A_p I^p \left(1 - \frac{\triangle n}{\triangle n_s} \right), \tag{5.4}$$

where, A_p is a real coefficient depending upon material properties, $I = \mathcal{E}\mathcal{E}^*$, t is the time, p is 1 or 2 depending upon one-photon or two-photon process and $\triangle n_s$ is the maximum refractive index change in the photopolymer. The input beam is assumed to be Gaussian. Solving this, we get an equation which has a soliton solution.[25]

For a wide range of acrylate photopolymers, the index response to an optical field is of the form[14]

$$\triangle n_1(x, y, z, t) = \triangle n_{10} \left\{ 1 - \exp \left[-\frac{1}{U_0} \int_0^{t-\tau} |\mathcal{E}(t')|^2 dt' \right] \right\}, \tag{5.5}$$

where τ is the monomer radical lifetime and U_0 is the critical exposure needed to induce polymerization. The expression for absorption photobleaching is approximately

$$\triangle n_2(x, y, z, t) = \triangle n_{20} \exp \left[-\frac{1}{U_0} \int_0^t |\mathcal{E}(t')|^2 dt' \right]. \tag{5.6}$$

Eq. 5.1 can be normalized using the dimensionless variables $z = Z/(k_0 n_0 a_0^2)$, $N = a_0^2 k_0^2 n_0 \triangle n$, $L = a_0^2 k_0^2 n_0 \alpha$ and defining $x = X/a_0$, $y = Y/a_0$ and $E = \mathcal{E}/\mathcal{E}_0$ as

$$i\frac{\partial E}{\partial z} + \frac{1}{2}\nabla_\perp^2 E + NE + \frac{i}{2}LE = 0, \tag{5.7}$$

where a_0 and $\mathcal{E}_0$ are the initial beam width and amplitude of electric field. For our analysis, we assume that the loss in the medium is negligible and hence, neglect the last term in Eq. (5.7) and proceed. Assuming a refractive index modulation of the form given in Eq. (5.5), the evolution Eq. (5.7) can be written as

$$i\frac{\partial E}{\partial z} + \frac{1}{2}\nabla_\perp^2 E + N_{10} \left\{ 1 - \exp \left[-\frac{1}{U_0} \int_0^{t-\tau} |E(t')|^2 dt' \right] \right\} E = 0. \tag{5.8}$$

At the beginning of the propagation, one can assume that the shape of the exciting beam has not changed, and hence can write

$$\int_0^{t-\tau} |E(t')|^2 dt' = |E(t')|^2 t. \tag{5.9}$$

Expanding the exponential gives

$$i\frac{\partial E}{\partial z} + \frac{1}{2}\nabla_\perp^2 E + N_{10}E - N_{10}\left\{1 - \frac{1}{U_0}|E|^2 t + \left(\frac{1}{U_0}|E|^2 t\right)^2\right\}E = 0, \tag{5.10}$$

and simplifying we get

$$i\frac{\partial E}{\partial z} + \frac{1}{2}\nabla_\perp^2 E + N_1|E|^2 E + N_2|E|^4 E = 0, \tag{5.11}$$

where

$$N_1 = N_{10}t/U_0,$$

$$N_2 = -N_{10}t^2/U_0^2,$$

and

$$N_{10} = a_0^2 k_0^2 n_0 \triangle n_{10}.$$

The equation now has the form of a cubic-quintic nonlinearity. Both the cubic and quintic terms contribute to the self-focusing of the beam.

5.2 Analysis using variational method

We analyze the system using the variational method. This is an approximate method and is widely used to get an insight into the nature of the solution in cases where it is difficult to get an exact analytical solution. We will take cylindrical coordinates for our analysis. Hence the Lagrangian corresponding to Eq. (5.11) can be written as

$$L = \frac{i}{2}r\left(E\frac{\partial E^*}{\partial z} - E^*\frac{\partial E}{\partial z}\right) + \frac{r}{2}\frac{\partial E}{\partial r}\frac{\partial E^*}{\partial r} - rN_1|E|^4 - rN_2|E|^6. \tag{5.12}$$

The method proceeds by assuming a suitable trial solution of the form,

$$E = A(z)\exp[-\frac{r^2}{2a(z)^2} + ib(z)r^2], \tag{5.13}$$

where $A(z)$ is the amplitude, $a(z)$ is the beam width and $b(z)$ is the curvature parameter. This gives

$$
\begin{aligned}
L &= \frac{i}{2} r \exp[-\frac{r^2}{a(z)^2}]\{AA_z^* - A^*A_z - 2ib_z r^2|A|^2\} \\
&+ \frac{r}{2}|A|^2 \exp[-\frac{r^2}{a(z)^2}]\{\frac{r^2}{a^4} + 4b^2 r^2\} \\
&- rN_1|A|^4 \exp[-\frac{2r^2}{a(z)^2}] - rN_2|A|^6 \exp[-\frac{3r^2}{a(z)^2}]. \quad (5.14)
\end{aligned}
$$

Now the reduced Lagrangian for the system can be written as

$$
\begin{aligned}
\langle L \rangle &= \int_0^\infty Lr\,dr \\
&= \frac{\sqrt{\pi}}{8}\Big[i(AA_z^* - A^*A_z)a^3 + 3b_z|A|^2 a^5 \\
&+ \frac{3}{2}|A|^2\left(\frac{1}{a^4} + 4b^2\right)a^5 - \frac{1}{\sqrt{2}}N_1|A|^4 a^3 - \frac{2}{3\sqrt{3}}N_2|A|^6 a^3\Big]
\end{aligned}
$$

The next step is to find the variation of $\langle L \rangle$ with respect to the various Gaussian parameters $A(z)$, $A(z)^*$, $a(z)$ and $b(z)$. The variation with $A(z)$ and $A(z)^*$ gives

$$
\begin{aligned}
A\frac{\partial\langle L\rangle}{\partial A} &= 0 \Rightarrow \frac{\partial}{\partial z}(-ia^3 A^*) \\
&= iAA_z^* a^3 + 3b_z|A|^2 a^5 + \frac{3}{2}|A|^2(\frac{1}{a^4} + 4b^2)a^5 \\
&- \frac{2}{\sqrt{2}}N_1|A|^4 a^3 - \frac{2}{\sqrt{3}}N_2|A|^6 a^3, \quad (5.15)
\end{aligned}
$$

$$
\begin{aligned}
A^*\frac{\partial\langle L\rangle}{\partial A^*} &= 0 \Rightarrow \frac{\partial}{\partial z}(ia^3 A) \\
&= -iA^*A_z a^3 + 3b_z|A|^2 a^5 + \frac{3}{2}|A|^2(\frac{1}{a^4} + 4b^2)a^5 \\
&- \frac{2}{\sqrt{2}}N_1|A|^4 a^3 - \frac{2}{\sqrt{3}}N_2|A|^6 a^3. \quad (5.16)
\end{aligned}
$$

Simplifying

$$
A\frac{\partial\langle L\rangle}{\partial A} - A^*\frac{\partial\langle L\rangle}{\partial A^*} = 0 \implies \frac{d}{dz}(a^2|A|^2) = 0. \quad (5.17)
$$

This gives

$$
a^2|A|^2 = E_0. \quad (5.18)
$$

The variation with a gives

$$\frac{\partial \langle L \rangle}{\partial a} = 3ia^2(AA_z^* - A^*A_z) + 15b_z|A|^2a^4$$
$$+\frac{3}{2}|A|^2 + 30b^2a^4 - \frac{3}{\sqrt{2}}N_1|A|^4a^2 - \frac{2}{\sqrt{3}}N_2|A|^6a^2 = 0. \qquad (5.19)$$

Similarly, after some algebra, we get the following equations:

$$b = \frac{1}{2a}\frac{da}{dz} \qquad (5.20)$$

$$\frac{d^2a}{dz^2} = -\frac{1}{2a^3} - \frac{N_1E_0}{2\sqrt{2}a^3} - \frac{2N_2E_0^2}{3\sqrt{3}a^4}. \qquad (5.21)$$

Integration of Eq. (5.21) and introducing the normalized variables, $a(z)/a_0 = y(z)$, gives an equation of the form

$$\frac{1}{2}\left(\frac{dy}{dz}\right)^2 + \Pi(y) = 0, \qquad (5.22)$$

where

$$\Pi(y) = \frac{\mu}{y^2} + \frac{\nu}{y^4} + K, \qquad (5.23)$$

with

$$\mu = \frac{1}{4a_0^4} - \frac{N_1E_0}{4\sqrt{2}a_0^4},$$

$$\nu = -\frac{N_2E_0^2}{6\sqrt{3}a_0^6},$$

$$K = \frac{c}{a_0^2},$$

and c is a constant of integration.

This represents a particle in a potential well. Fig. 5.2 gives the evolution of the potential function for different regimes of propagation depending upon the sign and magnitude of the nonlinearity. The bottommost curve (f1) gives the evolution of the potential when the nonlinearity is of negative sign. The beam diffracts even more than the linear case (represented by curve f4). This means that the incident beam results in a decrease in refractive index which causes the beam to diffract even more than the linear case. Such light induced decrease of refractive index results in the formation of dark spatial solitons.[30] Curve f2 gives the evolution
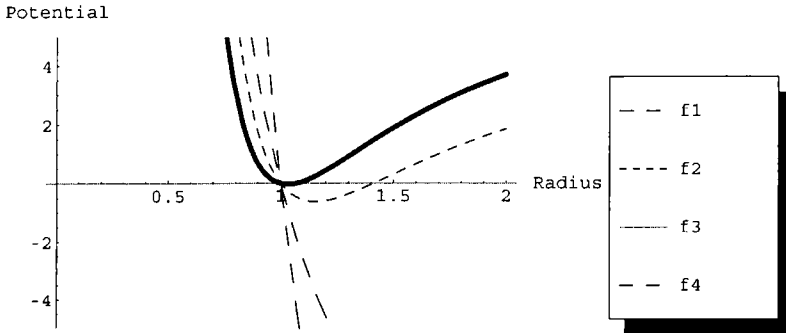
Figure 5.2: Qualitative plot of the evolution of the potential function for different magnitude and sign of nonlinearity.

for intermediately strong nonlinearity with positive sign. This represents a focusing nonlinearity and as a result the equivalent particle moves in a potential well and is confined in this well. A stable state is obtained when the diffraction of the beam is completely balanced by the refractive index change due to the self-writing process. This is the limit case (curve f3). Here the potential well has degenerated to a single point and the beam propagates without any shape change.

A similar analysis of Eq. (5.7) can be done. Here we proceed by assuming that the refractive index saturates after sometime[6] and hence do not consider the evolution of refractive index with time. Such an analysis does not show the effect of cancelation of diffraction. We will get a potential of the form given by Eq. (5.23) with the terms corresponding to N_1 and N_2 absent. This is the linear case and it shows that there is no confinement of the beam and the beam diffracts.

5.3   Experimental method

We will now describe the experiments performed, in our laboratory, to demonstrate the self-writing in the photopolymer.

5.3.1   Sample preparation and optical properties

Polymer materials are the most commonly used medium to fabricate optical devices of any kind. Components so fabricated will be quite inexpen-

sive. The incorporation of dyes into a polymer material results in a host of interesting optical phenomena. Photopolymer systems typically comprise of one or more monomers, a photo-initiation system and an inactive component often referred to as a binder. The MBPVA/Acrylamide solution is prepared by sensitizing the 10% polyvinyl alcohol (PVA) solution (molecular wt 1, 25,000 MERCK) with methylene blue (MB) (SD Fine) and triethanol amine (SD fine) and acrylamide (SRL). The concentration of each of the components in the prepared solution is: Methylene blue : 2.8×10^{-4} mol/liter, Triethanolamine (TEA) : 0.05 M and Acrylamide : 0.381 mol/liter.
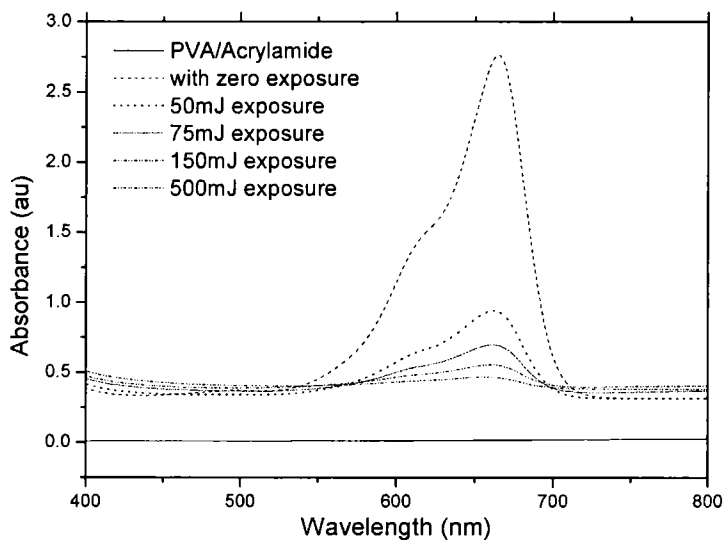
Figure 5.3: Change in absorbance as a function of exposure. The topmost curve is the spectrum of unexposed film. The lower most curve is that of PVA/Acrylamide film (prior to MB doping).

Poly Vinyl Alcohol (PVA) doped with acrylamide has excellent transparency across the visible spectrum. The absorption peak of MBPVA/Acrylamide is at 632.8 nm. The polymer films of MBPVA/Acrylamide can be bleached to almost complete transparency in the visible on exposure. The absorption spectra of 2 mm thick films of the photopolymer at different levels of exposure taken using a JASCO spectrophotometer (Model

V-570) are shown in Fig 5.3. The film is exposed to $0, 50, 75, 150$ and 500 mJ of energy. The topmost curve is the absorption of unexposed film. The lowermost curve is the absorption spectrum of pure PVA doped with acrylamide. The film bleached to complete transparency after an exposure of 500 mJ. The refractive index before and after exposure is measured using an Atago DR-M2 refractometer. The initial refractive index of the MBPVA/Acrylamide photopolymer is 1.5167. After the film is completely bleached, the change in refractive index is measured to be of the order of 10^{-3}. The refractive index modulation saturates in about 1.5 sec.
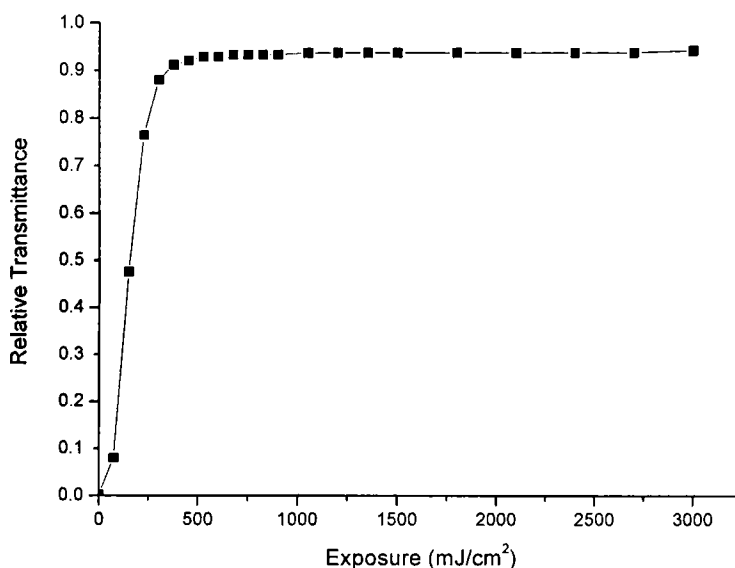
Figure 5.4: Relative transmittance vs. exposure for an incident intensity of 5mW /cm^2.

The real time relative transmittance of the film for an incident intensity of 5 mW/cm^2 for 10 minutes is shown in Fig 5.4. From this also we can see that the film bleached to complete transparency after 500 mJ of energy. The maximum change in refractive index occurs at this point. This gradient in refractive index between the exposed and unexposed region results in the formation of a waveguide and the writing beam gets self-trapped in this self-induced waveguide.
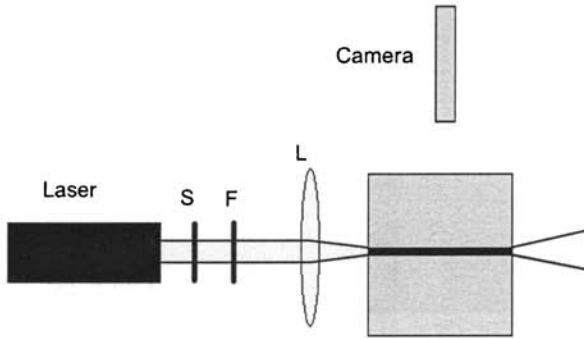
Figure 5.5: Experimental setup for the observation of self-writing of a low power He-Ne beam in a liquid photopolymer. S:Shutter, F:ND Filter and L:Lens.

5.3.2   Self-trapping experiment

For the self-trapping experiment, freshly prepared solution of MBPVA/ Acrylamide is taken in a cuvette of dimension 1cm x 1cm x 5cm. Gaussian beam from a low power He-Ne laser (5 mW, 632.8 nm, Melles Griot) is focused to a spot size of 70 μm and allowed to pass through the material. The experimental setup for the observation of self-writing is shown in Fig. 5.5.

   The beam propagates through the liquid photopolymer without any diffraction effects (Fig. 5.6). The observation of self-trapping in this system is of particular interest because MBPVA/Acrylamide photopolymer can be easily prepared. The guides induced in this material are of permanent nature. So it can be used for the fabrication of new organic optical devices, photonic crystals[31] etc. We could prepare 1 cm long waveguide as compared to the 1 mm guide created inside a bulk photopolymerizable resin by Dorkenoo et al.[32] using 5 μW power. For an increase in power they observed chaotic behavior. The irradiation power in our experiments is comparable to the power used by Yamashita et al.[9] in an another ex-
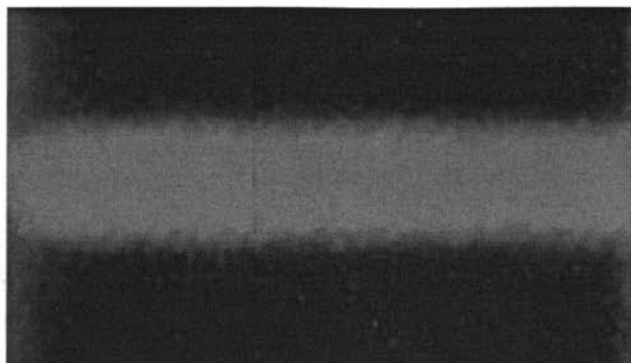
Figure 5.6: Propagation of the beam through the medium without any diffraction effects.

periment where the exposure time of around 5 min is required for the formation of the waveguide. To create a 1 cm long waveguide, it takes around 15-20 seconds. The current experiments have been done using liquid MBPVA/Acrylamide system, which results in a solid core and a liquid cladding waveguide. But its possible to observe self-writing in this system in an all solid form by allowing the solution to solidify. The suggested material has been originally developed for holographic applications and is quite inexpensive with a high diffraction efficiency. It has a low shrinkage during writing and can be cast into thickness of greater than 1 mm and has a very high sensitivity to the writing beam. These additional properties can be utilized for successful fabrication of devices in this material.

5.4   Conclusions

We have shown the stable propagation of a low power He-Ne laser beam through a liquid MBPVA/Acrylamide photopolymer material. The beam propagated through the medium over a distance of 1 cm without any diffraction effects. The propagation of the beam can be described by the previously studied theoretical models. We have also studied the beam propagation using the variational method and both the analytical and experimental results match well. The guides induced in this material are of particular interest owing to the fact that MBPVA/Acrylamide can be easily prepared and has low cost as compared to the materials used by previous researchers. The proposed material was originally proposed as a recording material in holography with suggested application in optical

memories, holographic displays, holographic optical elements and optical computing. The additional use of this material as a medium for writing waveguides which can be used to guide another light and which behaves as spatial solitons can realize all-optical applications. We strongly believe that these guides can be used for the fabrication of integrated optical devices.

References

[1] T. M. Monro, D. Moss, M. Bazylenko, C. M. de Sterke, and L. Poladian, "Observation of self-trapping of light in a selfwritten channel in photosensitive glass," Phys. Rev. Lett. **80**, 4072–4075 (1998).

[2] K. O. Hill, Y. Fujii, D. C. Johnson, and B. S. Kawasaki, Appl. Phys. Lett. **32**, 647–649 (1978).

[3] D. K. W. Lam and B. K. Garside, "Characterization of single-mode optical fiber filters," Appl. Opt. **20**, 440–445 (1981).

[4] W. S. Brocklesby, S. J. Field, D. C. Hanna, A. C. Large, J. R. Lincoln, D. P. Shepherd, and A. C. Tropper, "Optically written waveguides in ion implanted $Bi_4Ge_3O_{12}$," Opt. Mater. **1**, 177–184 (1992).

[5] S. J. Frisken, "Light-induced optical waveguide uptapers," Opt. Lett. **18**, 1035–1037 (1993).

[6] Y. S. Kivshar and G. P. Agrawal, *Optical Solitons - From Fibers to Phtonic Crystals* (Academic Press, San Diego, California, 2003).

[7] T. Yamashita, M. Kagami, and H. Ito, "Waveguide shape control and loss properties of light-induced self-written (LISW) optical waveguides," J. Lightwave Technol. **20**, 1556–1562 (2002).

[8] T. Yamashita and M. Kagami, "Fabrication of light-induced self-written waveguides with a w-shaped refractive index profile," J. Lightwave Technol. **23**, 2542–2548 (2005).

[9] K. Yamashita, T. Kuro, K. Oe, K. Mune, T. Hikita, and A. Mochizuki, "Self-written waveguide structure in photosensitive polyimide resin fabricated by exposure and thermosetting process," IEEE Photon. Technol. Lett. **16**, 801–803 (2004).

[10] H. Ma, A. K.-Y. Jen, and L. R. Dalton, "Polymer-based optical waveguides: Materials, processing, and devices," Adv. Mater. **14**, 1339–1365 (2002).

[11] L. Eldada and L. W. Shacklette, "Advances in polymer integrated optics," IEEE J. Sel. Top. Quantum Electron **6**, 54–68 (2000).

[12] J.-W. Kang, J.-J. Kim, and E. Kim, "All-optical Mach-Zehnder modulator using a photochromic dye-doped polymer," Appl. Phys. Lett. **80**, 1710–1712 (2002).

[13] J.-W. Kang, M.-J. Kim, J.-P. Kim, S.-J. Yoo, J.-S. Lee, D. Y. Kim, and J.-J. Kim, "Polymeric wavelength filters fabricated using holographic surface relief gratings on azobenzene-containing polymer films," Appl. Phys. Lett. **82**, 3823–3825 (2003).

[14] A. S. Kewitsch and A. Yariv, "Self-focusing and self-trapping of optical beams upon photopolymerization," Opt. Lett. **21**, 24–26 (1996).

[15] L. Friedrich, P. Dannberg, C. Wkhter, T. Hennig, A. Brker, and W. Karthe, "Directional coupler device using a three-dimensional waveguide structure," Opt. Commun. **137**, 239–243 (1997).

[16] J. Kim, K.-H. Jeong, and L. P. Lee, "Artificial ommatidia by self-aligned microlenses and waveguides," Opt. Lett. **30**, 5–7 (2005).

[17] D. T. A. R. Mickelson, "Photobleaching for waveguide formation in a guesthost polyimide," Appl. Opt. **38**, 3893–3903 (1999).

[18] B. M. John, U. M, K. Sreekumar, R. Joseph, and C. S. Kartha, "Enhancement of diffraction efficiency and storage life of poly (vinyl chloride) based optical recording medium with the incorporation of an electron donor," Appl. Opt. **46**, 346–350 (2007).

[19] M. Ushamani, K. Sreekumar, C. S. Kartha, and R. Joseph, "Fabrication and characterization of methylene-blue-doped polyvinyl alcohol-polyacrylic acid blend for holographic recording," Appl. Opt. **43**, 3697–3703 (2004).

[20] B. M. John, M. Ushamani, K. Sreekumar, R. Joseph, and C. S. Kartha, "Reusable recording medium based on MBPVA and vinyl acetate," J. Mod. Opt. **53**, 343–355 (2006).

[21] C. Garca, I. Pascual, and A. Fimia, "Diffraction efficiency and signal-to-noise ratio of diffuse-object holograms in real time in polyvinyl alcohol photopolymers," Appl. Opt. **38**, 5548–5551 (1999).

[22] S. Blaya, R. M. L. Carretero and, A. Fimia, and R. F. Madrigal, "Holography as a technique for the study of photopolymerization kinetics in dry polymeric films with a nonlinear response," Appl. Opt. **38**, 955–962 (1999).

[23] C. Garcia, I. Pascual, A. Costela, I. Garcia-Moreno, C. Gomez, A. Fimia, and R. Sastre, "Hologram recording in polyvinyl alcohol /acrylamide photopolymers by means of pulsed laser exposure," Appl. Opt. **41**, 2613–2620 (2002).

[24] S. Gallego, M. Ortuño, C. Neipp, A. Márquez, A. Beléndez, and I. Pascual, "Characterization of polyvinyl alcohol/acrylamide holographic memories with a first-harmonic diffusion model," Appl. Opt. **44**, 6205–6210 (2005).

[25] T. M. Monro, C. M. de Sterke, and L. Poladian, "Catching light in its own trap," J. Mod. Opt. **48**, 191–238 (2001).

[26] P. A. Krug, R. Stolte, and R. Ulrich, "Measurement of index modulation along an optical fiber bragg grating," Opt. Lett. **20**, 1767–1769 (1995).

[27] A. S. Kewitsch and A. Yariv, "Nonlinear optical properties of photoresists for projection lithography," Appl. Phys. Lett. **68**, 455–457 (1996).

[28] D. P. Hand and P. S. Russell, "Photoinduced refractive-index changes in germanosilicate fibers," Opt. Lett. **15**, 102–104 (1990).

[29] D. Anderson, "Variational approach to nonlinear pulse propagation in optical fibers," Phys. Rev. A **27**, 3135–3145 (1983).

[30] S. Sarkisov, M. Curley, A. Wilkosz, and V. Grymalsky, "Optical channel waveguides formed by upconverted photobleaching of dye-doped polymer film in regime of dark spatial soliton," Opt. Commun. **161**, 132–140 (1999).

[31] S. Shoji, H.-B. Sun, and S. Kawata, "Photofabrication of wood-pile three-dimensional photonic crystals using four-beam laser interference," Appl. Phys. Lett. **83**, 608–610 (2003).

[32] K. Dorkenoo, O. Crégut, L. Mager, F. Gillot, C. Carre, and A. Fort, "Quasi-solitonic behavior of self-written waveguides created by photopolymerization," Opt. Lett. **27**, 1782–1784 (2002).

6

Dynamics of a light induced self-written waveguide directional coupler in a photopolymer

6.1 Introduction

WE propose and study, using the variational approximation as well as numerical simulation, the evolution of a probe beam through a directional coupler formed in a photopolymer system. Both the results compare well. An analytical expression is derived for describing the dynamics of the coupler. The expression compares well with that of the standard linear coupler. The two waveguides of the coupler are self-written by photopolymerization. Such a coupler can be formed by direct self-writing using low power beams with wavelength corresponding to the sensitivity of the material. In section 6.2 the model equations are introduced and the variational formalism is developed. An analytic solution is derived for the system and the result is compared with the numerical results. The dynamics of the coupler is explained using a potential well formulation as well. Finally the results obtained are compared with that from the direct numerical simulation of the original coupled partial differential equation. Section 6.3 concludes the chapter.

The phenomenon of optical tunneling can be used not only to couple energy from a fiber or a beam to a waveguide, but also to couple one waveguide to another. Couplers of this type are usually called directional couplers (DC) because energy is transferred in a coherent fashion so that the direction of propagation is maintained. Directional couplers are the basis of several guided wave devices and are mainly used for optical switching networks. It is a passive device which couples part of the transmission power by a known amount through two transmission lines which are very
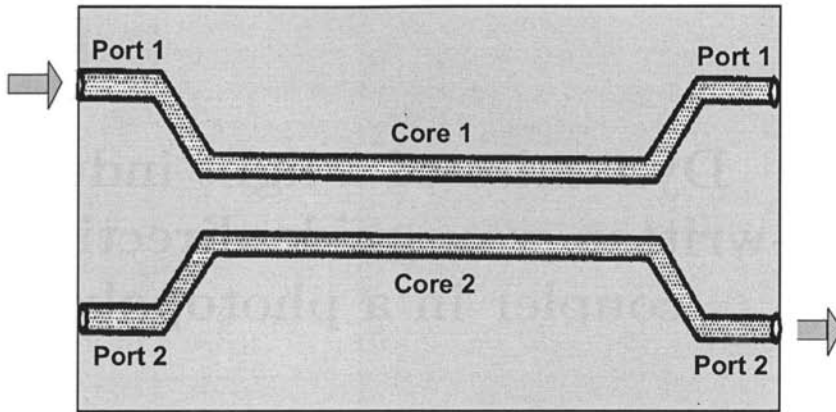
Figure 6.1: Schematic illustration of a directional coupler.

close to each other such that energy passing through one is coupled to the other.[1] The separation between the waveguides determines the coupling efficiency. The schematic diagram of a DC is shown in Fig. 6.1.

In an optical waveguide directional coupler where two identical single mode waveguides are close to each other with a gap only of the order of several wavelengths, 100 percent optical power is transferred, in principle, from one waveguide to the other Therefore, electro-optic modulation and switching with high extinction ratio (the ratio of the maximum and the minimum output levels) are possible.[2] This energy is transferred by a process of synchronous coherent coupling between the overlapping evanescent tails of the modes guided in each waveguide. If one were to measure the optical energy density while moving in the z direction along one channel of a DC, a sinusoidal variation with distance would be observed. For a coupler to transfer any given fraction of the energy, it is necessary only to bend away the secondary channel at the proper point. In this way either a 10 dB coupler for measurement padding, a 3 dB coupler for beam splitting, or a 100% coupler for beam switching can be made. The coupling length L_c is determined by the propagation constant difference between the even and odd modes. Coupler fabrication is generally accomplished by using techniques such as photoresist masking, thin film deposition and epitaxial growth. Certain specialized methods such as, holographic exposure of

photoresist to make grating couplers, are also used.

As discussed in Chapter 5, light induced or self-written waveguide formation can be used for the formation of an optical waveguide as a result of the self-trapping action of a laser beam passed through a converging lens or a single mode fiber.[3] The waveguides thus formed are of particular interest as these waveguides can be formed at low power levels and the material response is wavelength sensitive; therefore a weak beam can guide an intense beam at a less photosensitive wavelength.[4] Materials which show change in refractive index with optical intensity has application in integrated optics.[5,6] Kewitsch and Yariv demonstrated both experimentally and theoretically, self-trapping and self-focusing phenomena to occur in photopolymerizable materials (a liquid diacrylate photopolymer).[7] A photosensitive material experiences long-lasting refractive index changes in response to illumination at specific wavelengths, and the larger changes in the refractive index occur in the regions with higher intensity of light. This results in creation of a waveguide-type structure which can reduce or even completely suppress the beam diffraction. A possible application of these permanent light-induced waveguides is in networks of optical interconnects between linear arrays of optical transmitters and receivers.

The directional couplers have been studied both experimentally and theoretically. Lan et al.[8]studied waveguides and directional couplers induced by two mutually incoherent photorefractive solitons propagating in parallel at close proximity and Lu et al.[9] by using incoherent white light. The nonlinear directional coupler was first discussed by Jensen.[10] Switching properties of such a device have been studied both theoretically[11–13] and experimentally.[14] First experiments were reported in 1987.[15] The effect of extra terms, such as gain or loss, in the standard coupler equations were considered by Wilson and Stegeman.[16] We study theoretically the coupling of light beam in a directional coupler formed in a photopolymer. Here the two waveguides are formed in a photopolymerizable material using self-writing.

6.2 Model equation and analysis using analytical and numerical methods

A laser beam when focused on to the edge of a photosensitive material can write its own waveguide and then get guided by this waveguide.[17] In this process, the beam of light which initially diffracts, changes the refractive index of the medium and dynamically creates a channel that counteracts

diffraction and guides the beam through the material. The physics of self-writing is very similar to the physics of spatial soliton formation[18] and is based on the self-action of light.

An electric field $A(r, t)$ in a dielectric medium satisfies Maxwell's equation of the form

$$\nabla^2 A - \frac{1}{c^2}\frac{\partial^2 D}{\partial t^2} = \nabla(\nabla.A), \tag{6.1}$$

where $D = \epsilon A$ is the displacement vector in the dielectric medium, with ϵ being the dielectric constant relative to vacuum and it is approximately equal to n^2; n being the refractive index. D can be written as, $D = (n_0 + \triangle n)^2 A$ where, $A = \frac{1}{2}[E(r, t)\exp i(wt - kz) + c.c]$. Using this we can reduce the Maxwell's equation to

$$ik_0 n_0 \frac{\partial E}{\partial Z} + \frac{1}{2}\nabla_\perp^2 E + k_0^2 n_0 \triangle n E = 0, \tag{6.2}$$

where $k_0 = 2\pi/\lambda$ is the free space wave number, n_0 is the initial refractive index, $\triangle n$ is the change in refractive index and E is the electric field envelope in the waveguide.

This is the paraxial equation governing the wave propagation in a lossless photosensitive material.[19] This can be written in the dimensionless form by defining, $z = Z/(k_0 n_0 a_0^2)$, $x = X/a_0, y = Y/a_0$ and $N = a_0^2 k_0^2 n_0 \triangle n$.

A series expansion technique for analyzing the waveguides which can be self-written in photosensitive materials and photopolymers have been studied by Monro et al.[19] The model is also studied using group theoretical methods in[20] and using symmetry analysis.[21] The details of the refractive index modulation and the various phenomenological models for describing the evolution of refractive index have been discussed in Chapter 5. Here we consider only the permanent waveguides created by the self-writing process. Such permanent waveguides can be used for guiding another signal light or two such waveguides created very close to each other can be used as a directional coupler.

The DC under study consists of two waveguides formed using self-writing. The advantage of such waveguides is that the waveguide remains permanent even after the writing beam is switched off. The two cores of the coupler are formed very close to each other such that there is no interaction between the two waveguides, except the evanescent wave coupling between the two waveguides. Beam propagation through such a coupler can be described in terms of two linearly coupled equations in the dimensionless

form as

$$i\frac{\partial E_j}{\partial z} + \frac{1}{2}\nabla_\perp^2 E_j + NE_j + k_c E_{3-j} = 0. \tag{6.3}$$

E_j with $j = 1, 2$ is the electric field envelope in the two waveguides and k_c is the coupling constant. Here we are interested in the one dimensional case, that is propagation along the z axis and diffraction along x axis.

6.2.1   Lagrangian formalism

The coupled Eq. (6.3) is studied analytically using the variational method. The analysis is based on the Lagrangian associated with Eq. (6.3). The analysis proceeds by first assuming a suitable trial solution and then finding the reduced Lagrangian associated with the problem. The reduced Lagrangian has the form

$$\langle L \rangle = \int_0^\infty L \, dx, \tag{6.4}$$

where L is the Lagrangian of the system. The Lagrangian for our system is

$$L = L_j + L_{12}, \tag{6.5}$$

with

$$L_j = \frac{i}{2}\left[E_j\frac{\partial E_j^*}{\partial z} - E_j^*\frac{\partial E_j}{\partial z}\right] + \frac{1}{2}\left|\frac{\partial E_j^2}{\partial x^2}\right|^2$$
$$- N|E_j|^2, \tag{6.6}$$

and

$$L_{12} = k_c\left(E_1^* E_2 + E_2^* E_1\right), \tag{6.7}$$

where L_j for $j = 1, 2$ corresponds to the single Lagrangian and L_{12} represents the interaction Lagrangian.

For the solution of the problem, a simple trial function of the form

$$\psi_j(x, z) = F_j(z)\exp(\rho x^2)\exp[i\theta_j(z)],$$

is assumed, where F_j, the amplitude of the field in the core and the phase θ_j depend only on z variable and ρ is a constant. Substituting this in Eq. (6.5), we find the reduced Lagrangian

$$\langle L \rangle = F_j^2\frac{\partial\theta_j}{\partial z}\frac{\sqrt{\pi/2}}{2\sqrt{\rho}} + \frac{\rho F_j^2}{4} - NF_j^2\frac{\sqrt{\pi/2}}{2\sqrt{\rho}}$$
$$+ 4k_c F_1 F_2\cos(\theta_1 - \theta_2)\frac{\sqrt{\pi/2}}{2\sqrt{\rho}}, \tag{6.8}$$

Now, varying the effective Lagrangian with respect to the variational parameters F_j and θ_j results in a set of four coupled nonlinear equations of the form

$$\frac{d\theta_j}{dz} = -\frac{1}{\sqrt{\pi}} + 2N - \frac{4k_c F_{3-j}}{F_j} \cos(\theta_1 - \theta_2), \qquad (6.9)$$

$$\frac{dF_j}{dz} = (-1)^j 2k_c F_{3-j} \sin(\theta_1 - \theta_2). \qquad (6.10)$$

To proceed further, we define the functions

$$\theta(z) = \theta_1(z) - \theta_2(z),$$

which is the new phase variable

$$U(z) = F_1^2(z) - F_2^2(z),$$

variable for energy difference and

$$F_1^2 + F_2^2 = N = constant,$$

which gives the total energy. Using this, the set of four coupled nonlinear equations can be reduced to a set of two coupled ordinary differential equations:

$$\frac{d\theta_1}{dz} - \frac{d\theta_2}{dz} = -4k_c \cos(\theta_1 - \theta_2)\left(\frac{F_2}{F_1} - \frac{F_1}{F_2}\right), \qquad (6.11)$$

which gives

$$\frac{d\theta}{dz} = \frac{4k_c U \cos(\theta)}{(N^2 - U^2)^{1/2}}, \qquad (6.12)$$

and

$$\frac{dU}{dz} = 2F_1 \frac{dF_1}{dz} - 2F_2 \frac{dF_2}{dz}, \qquad (6.13)$$

which gives

$$\frac{dU}{dz} = -4k_c(N^2 - U^2)^{1/2} \sin(\theta). \qquad (6.14)$$

Eqs. (6.12) and (6.14) are solved numerically. Figs. 6.2 and 6.3 show the numerical result. Here the normalized energy difference in the two cores is plotted for different coupling constant values. The values of the parameter used are $N = 10$ and 100 which is the normalized total energy. At $z = 0$ the intensity in the first core is maximum. As the beam propagates through the first core, part of its energy is coupled into the second waveguide and finally at $z = 50$, the energy is completely coupled into
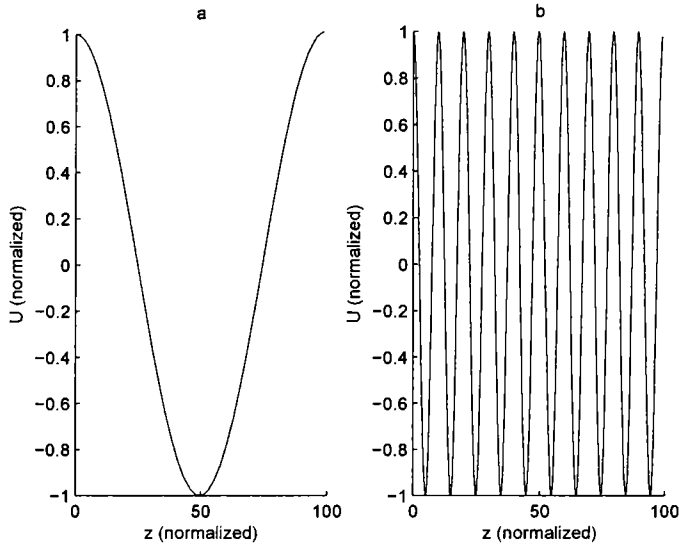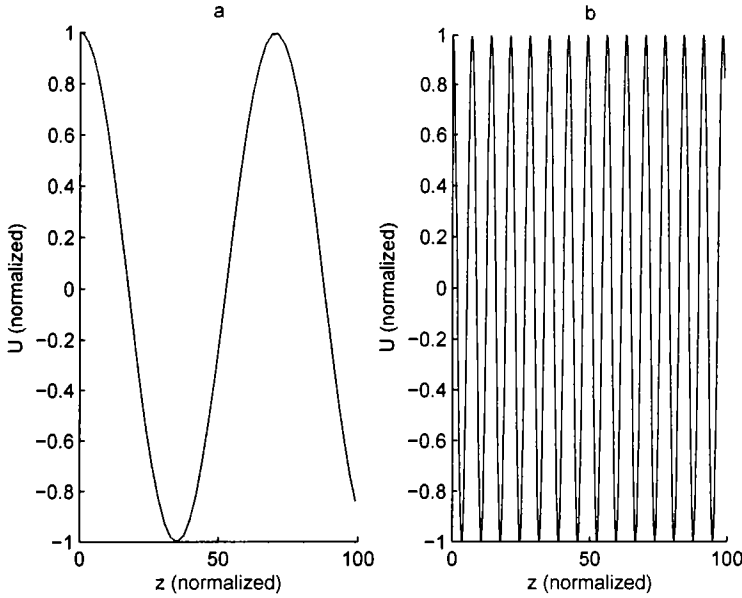
Figure 6.2: Qualitative plot of evolution of difference in energy in the two waveguides with respect to distance z for $N = 10$ with coupling constant a) $k_c = 0.016$ b) $k_c = 0.15$.

the second waveguide (Fig.6.2a). This coupling of energy between the two waveguides occurs in a periodic manner and depends upon the coupling coefficient. The coupling coefficient is related to the distance between the two waveguides. If the distance is large the coupling is low (see Figs. 6.2a and 6.3a). When the distance between the two waveguides is less, the coupling efficiency increases (see Figs. 6.2b and 6.3b). Increasing the energy has no effect on the dynamics of the coupler (Fig.6.4). The coupler studied here is a linear coupler with no nonlinear effects. As a result we do not observe nonlinear switching at high intensities.

6.2.2 Analytic solution

We now derive an analytic solution for the dynamics of the coupler. For this, the system of Eqs. (6.12) and (6.14) is recast into a single equation by first finding out a constant of motion for this coupled system. As the Lagrangian (Eq. (6.5)) does not contain θ_j, we can obtain the constant of motion from Eq. (6.12) as

$$G = -4k_c(N^2 - U^2)^{1/2} \cos(\theta). \tag{6.15}$$
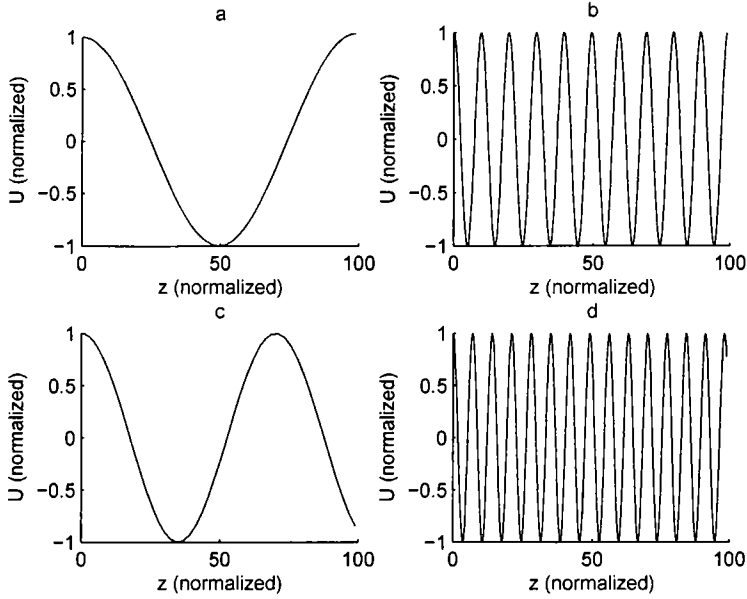
Figure 6.3: Qualitative plot of evolution of difference in energy in the two waveguides with respect to distance z for $N = 10$ with coupling constant a) $k_c = 0.02$ b) $k_c = 0.2$.

Using this we can write a single equation for U as

$$\frac{dU}{dz} = - \left((4k_c)^2 (N^2 - U^2) - G^2 \right)^{1/2} . \tag{6.16}$$

Eq. 6.16 can be solved exactly to obtain $U(z)$ as

$$U(z) = \sqrt{N^2 - g^2} \cos(2k_c z), \tag{6.17}$$

where

$$g^2 = G^2 / (4k_c)^2.$$

This is the exact solution for the linear coupler describing the sinusoidal variation of energy in each core.[22] Increasing the power has no effect on the dynamics of the coupler. Changing the coupling constant modifies the period of switching. The same result is obtained numerically (see Figs. (6.2 and 6.3)).

Figure 6.4: Qualitative plot of evolution of difference in intensity in the two waveguides with respect to distance z for $N = 100$ with a) $k_c = 0.016$ b) $k_c = 0.15$ c) $k_c = 0.02$ d) $k_c = 0.2$. There is no change in the coupler behavior with increase in energy.

6.2.3 Particle in a well description

To get a physical insight into the process of coupling, we follow the method of Anderson[23] to describe the dynamics of the coupler in terms of a particle moving in a potential well. The equation describing a particle moving in a potential well has the form

$$\frac{1}{2}\left(\frac{dU}{dz}\right)^2 + \Pi(U) = 0, \tag{6.18}$$

where $\Pi(U)$ is the potential.

Simplifying Eq. (6.16) gives

$$\frac{d^2U}{dz^2} = -\left((4k_c)^2(N^2 - U^2) - G^2\right)^{-1/2}(4k_c)^2U\frac{dU}{dz}. \tag{6.19}$$

That is,

$$\frac{d^2U}{dz^2} = -(4k_c)^2U. \tag{6.20}$$
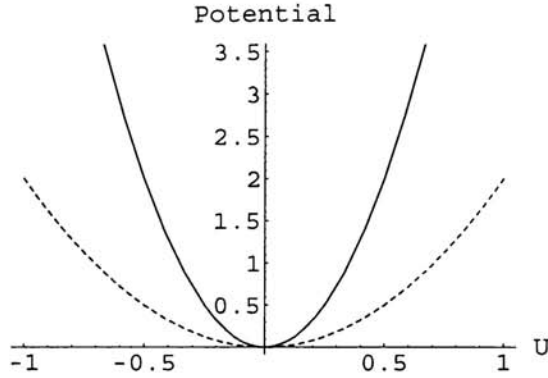
Figure 6.5: Plot of the potential well for $k_c = 0.05$ and $k_c = 0.5$. The
equivalent particle is initially at rest at $U = +1$

Integrating Eq. (6.20) gives

$$\frac{1}{2}\left(\frac{dU}{dz}\right)^2 = -8k_c^2 U^2, \tag{6.21}$$

where

$$\Pi(U) = 8k_c^2 U^2, \tag{6.22}$$

is the potential.

Let the equivalent particle be subjected to the following initial conditions:

$$U(z = 0) = +1,$$
$$\left.\frac{dU}{dz}\right|_{U=0} = 0$$

and the potential function is such that,

$$\Pi(U = 0) = 0$$
$$\left.\frac{d\Pi}{dU}\right|_{U=0} = 0$$
$$\Pi(\pm 1) = 8k_c^2$$
$$\left.\frac{d\Pi}{dU}\right|_{U=\pm 1} = \pm 16k_c^2.$$

Since it is a linear coupler, there is no effect when the input energy
is increased. The particle is initially at rest at $U = +1$. Complete en-
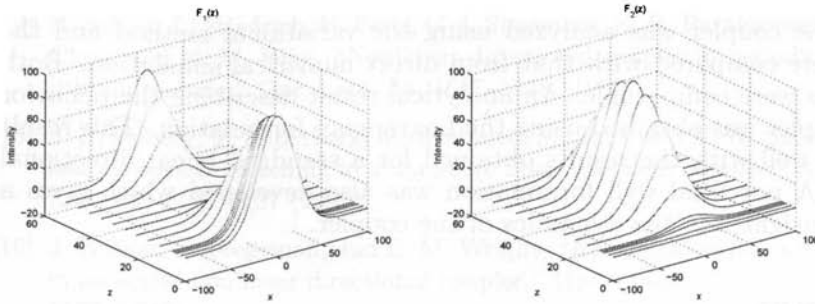ergy transfer occurs when the particle reaches $U = -1$. For a particular

Figure 6.6: Plot of direct numerical evolution of intensity in the two waveguides with respect to distance z.

coupling constant, a complete and periodic energy transfer is predicted in agreement with Eq. (6.17). Now, when the coupling constant is lowered, the initial height of the well is lowered and the well is flattened. The particle takes longer time to reach $U = -1$, which means that the period is increased. The two cases are plotted in Fig. 6.5. We find that the particle takes longer time to reach $U = -1$ when the coupling constant is changed from $k_c = 0.5$ to $k_c = 0.05$. This is in agreement with the numerical results of Figs. 6.2 and 6.3.

6.2.4   Direct simulation

Fig. 6.6 gives the result of direct numerical simulation of the coupled partial differential Eq. (6.3) for the same parameters as that used in the variational method. Both the results are comparable. $F_1(z)$ gives the intensity in the first core and $F_2(z)$ that in the second core. The periodic switching behavior is clearly observed. The coupling length increases when the coupling constant is reduced. There is no change in the dynamics of the coupler when the energy of the input beam is increased.

6.3   Conclusions

We have proposed and studied the dynamics of a directional coupler formed in a photopolymer system. The two waveguides of the coupler are formed by direct self-writing. The waveguides so formed are permanent and can be used to guide light. We could show that probe beam launched into one of the core can efficiently couple into the other core and the efficiency of coupling increases with the reduction of distance between the two waveg-

uides. The coupler was analyzed using the variational method and the results were compared with that from direct numerical simulation. Both the results were comparable. An analytical result describing the behavior of the coupler was obtained using the Lagrangian formulation. This result compares well with the results obtained for a standard linear directional coupler. A potential well formulation was also developed which gives a physical insight into the dynamics of the coupler.

References

[1] R. Syms and J. Cozens, *Optical Guided Waves and Devices* (McGraw-Hill International Ltd., 1992).

[2] R. V. Schmidt and L. L. Buhl, "Experimental 4x4 optical switching network," Electron. Lett. **12**, 575–577 (1976).

[3] M. Kagami, T. Yamashita, and H. Ito, "Light-induced self-written three-dimensional optical waveguide," Appl. Phys. Lett. **79**, 1079 (2001).

[4] K. D. Dorkenoo, S. Klein, J.-P. Bombenger, A. Barsella, L. Mager, and A. Fort, Mol. Cryst. Liq. Cryst. **446**, 446 (2006).

[5] M. Asaro, M. Sheldon, Z. Chen, O. Ostroverkhova, and W. Moerner, "Soliton-induced waveguides in an organic photorefractive glass," Opt. Lett. **30**, 519–521 (2005).

[6] S. Shoji, S. Kawata, A. A. Sukhorukov, and Y. S. Kivshar, "Self-written waveguides in photopolymerizable resins," Opt. Lett. **27**, 185–187 (2002).

[7] A. S. Kewitsch and A. Yariv, "Self-focusing and self-trapping of optical beams upon photopolymerization," Opt. Lett. **21**, 24–26 (1996).

[8] S. Lan, E. DelRe, Z. Chen, M. feng Shih, and M. Segev, "Directional coupler with soliton-induced waveguides," Opt. Lett. **24**, 475–477 (1999).

[9] Y. Lu, S. Liu, G. Zhang, R. Guo, N. Zhu, and L. Yang, "Waveguides and directional coupler induced by white-light photovoltaic dark spatial solitons," J. Opt. Soc. Am. B **21**, 1674–1678 (2004).

[10] S. M. Jensen, "Nonlinear coherent coupler," IEEE J. Quantum Electron. **18**, 1580–1583 (1981).

[11] P. L. Chu, G. D. Peng, and B. A. Malomed, "Analytical solution to soliton switching in nonlinear twin-core fibers," Opt. Lett. **18**, 328–330 (1993).

[12] P. L. Chu, B. A. Malomed, G. D. Peng, and I. M. Skinner, "Soliton dynamics in periodically modulated directional couplers," Phys. Rev. E **49**, 5763–5767 (1994).

[13] Y. S. Kivshar and B. A. Malomed, "Interaction of solitons in tunnel-coupled optical fibers," Opt. Lett. **14**, 1365–1367 (1989).

[14] R. Schiek, L. Friedrich, H. Fang, G. I. Stegeman, K. R. Parameswaran, M.-H. Chou, and M. M. Fejer, "Nonlinear directional coupler in periodically poled lithium niobate," Opt. Lett. **24**, 1617–1619 (1999).

[15] S. R. Friberg, Y. Silberberg, M. Andrejco, M. Saifi, and E. W. Smith, "Ultrafast all-optical switching in a dual-core fiber nonlinear coupler," Appl. Phys. Lett. **51**, 1135–1137 (1987).

[16] J. Wilson, G. Stegeman, and E. M. Wright, "All-optical switching of solitons in an active nonlinear directional coupler," Opt. Quant. Electron. **24**, 1325–1336 (1992).

[17] T. M. Monro, D. Moss, M. Bazylenko, C. M. de Sterke, and L. Poladian, "Observation of self-trapping of light in a selfwritten channel in photosensitive glass," Phys. Rev. Lett. **80**, 4072–4075 (1998).

[18] A. A. Sukhorukov, S. Shoji, and Y. S. Kivshar, "Self-written waveguides in photosensitive materials," J Nonlinear Opt Phys **11**, 391–407 (2002).

[19] T. M. Monro, L. Poladian, and C. M. de Sterke, "Analysis of self-written waveguides in photopolymers and photosensitive materials," Phys. Rev. E **57**, 1104–1113 (1998).

[20] M. Senthilvelan, L. Poladian, and C. M. de Sterke, "Symmetries and invariant solutions of the planar paraxial wave equation in photosensitive media," Phys. Rev. E **65**, 066607 (2002).

[21] L. Poladian, M. Senthilvelan, J. A. Besley, and C. M. de Sterke, "Symmetry analysis of self-written waveguides in bulk photosensitive media," Phys. Rev. E **69**, 016608 (2004).

[22] C. Paré and M. Florjańczyk, "Approximate model of soliton dynamics in all-optical couplers," Phys. Rev. A **41**, 6287–6295 (1990).

[23] D. Anderson, "Variational approach to nonlinear pulse propagation in optical fibers," Phys. Rev. A **27**, 3135–3145 (1983).

What we call the beginning is often the end. And to make an end is to make a beginning. The end is where we start from.

T. S. Eliot (1888-1965)

Results and Conclusion

THE study of spatial solitons and its realization is an active area of research. Such self-trapped states can attract and guide beams and can be considered as inducing optical waveguides that can guide another beam of a different wavelength or polarization through the effect of induced cross-phase modulation. Many such waveguides can create a self-reconfigurable waveguide network of virtual circuitry giving greater versatility over more conventional waveguides and devices. The variety of nonlinearity accessible is far broader and the physical phenomenon are much richer in the case of spatial solitons as compared to their temporal counterpart. Following are the main conclusions of this thesis.

- We studied **spatial solitons** in a cubic-quintic medium stabilized by multiphoton ionization. Analytical analysis, using variational method, and numerical analysis is carried out for studying the propagation of a high power laser beam through such a nonlinear medium. In order to apply the variational method to problems which involves physical effects such as plasma defocusing and the delayed Kerr effect that cannot, in principle, enter in the Lagrangian, we made an assumption that the test function has separable variables. It is then possible to derive the evolution equation for the beam width and other variational parameters. The system is analyzed numerically and the existence of two dimensional spatial solitons is established.

- We further explored the existence of spatio-temporal solitons in such a medium. The existence of **light bullets** is established both analytically and numerically. Such effect is beneficial for many applications, since it helps increasing the length of the interaction between laser and medium. This is crucial, for example, in laser-driven particle acceleration, laser-fusion schemes and high harmonic generation.

- We then studied the existence of spatial solitons and modulational

instability in media exhibiting photorefractive nonlinearity. We have predicted the existence of **photorefractive polymeric solitons** in a photorefractive polymer with absorption and study the modulational instability occurring in it.

- We derived the model equations describing the propagation of laser beams through a photorefractive material in the presence of two wave mixing and forward four wave mixing geometry. We then studied modulational instability in a photorefractive crystal in the presence of these two effects and showed the **existence of modulational instability**. Such instabilities are useful for pattern formation.

- We then focused our attention on light beam propagation through a photopolymer material. We have demonstrated the **practical realization of self-trapped states in the photopolymer system**. Formation of self-written waveguides in a photosensitive material is also analyzed using variational method.

- The same system is considered again and the formation of a **directional coupler** in such a system is predicted theoretically.

Future prospects

There are many frontiers still to be explored in optical soliton physics. The temporal solitons in fibers is well studied and is being used for practical applications in modern wavelength-division-multiplexing fiber systems. There are many open problems in the field of spatial solitons. One needs a suitable medium with proper nonlinearity that can sustain spatial solitons. Also, the medium should be such that we require only low power lasers for generating solitons.

1. The model equations derived for the study of MI in the two wave and forward four wave mixing geometry in Chapter 4 can be used for studying the existence of Holographic solitons in a PR medium. Such solitons exist only by virtue of the cross-phase modulation effects.

2. The directional coupler formed in a photopolymer material, studied in this thesis can be realized practically in the laboratory and its characteristics can be studied. Such a coupler can be created easily using low cost materials. The photopolymer material discussed in Chapter 5 becomes more important when nano-particles are doped

into the photopolymerizable material. In such a case the refractive index modulation is much more permanent in nature. Suitable equations can be derived to describe the propagation of light through such a medium. This equation can be analyzed using analytical and numerical techniques for possible existence of solitons.

3. The model equations can be further extended to include the effect of coupling as a result of two closely written soliton induced waveguides. Based on the results obtained theoretically, a nonlinear directional coupler can be fabricated.

" Karmani ave adhikars te
ma phalesu kadachana
ma karmaphal hetur bhoo
ma sangostu akramani"
— Bhagavad Gita

you have the power to act only
you do not have the power to influence the result
therefore you must act without the anticipation of the result
without succumbing to inaction

List of Symbols

n_b unperturbed refractive index

α loss in the material

β_{dark} dark generation rate

χ^1 linear susceptibility

χ^2 second order nonlinear susceptibility

χ^3 third order nonlinear susceptibility

ϵ dielectric constant relative to vacuum

ϵ_0 vacuum permittivity

γ_r recombination rate coefficient

λ wavelength of light

μ_e electron mobility

ω_0, ω frequency of light

c velocity of light

D displacement vector

k_B Boltzman's constant

k_c coupling constant

$n_0(\omega), n$ linear refractive index

N_A number density of negatively charged acceptor atoms

N_d density of donor impurities

N_d^+ density of ionized donor atoms

N_e number density of free electrons

n_e density of free electrons

N_{cr} critical plasma density

r_{eff} effective electro-optic coefficient

Index